COORDINATION OF REPLICATION-COUPLED PROTEIN DESTRUCTION AND ORIGIN LICENSING CONTROL DURING CELL CYCLE TRANSITIONS

Kate Elizabeth Coleman

A dissertation submitted to the faculty of the University of North Carolina at Chapel Hill in partial fulfillment of the requirements for the degree of Doctor of Philosophy in the Curriculum of Genetics and Molecular Biology.

Chapel Hill
2015

Approved by:

Jeanette Gowen Cook

Cyrus Vaziri

M. Ben Major

Dale Ramsden

W. Kimryn Rathmell

ABSTRACT

Kate Elizabeth Coleman: Coordination of Replication-Coupled Protein Destruction and Origin Licensing Control During Cell Cycle Transitions.
(Under the direction of Jeanette Gowen Cook)

Timely ubiquitin-mediated protein degradation is fundamental to cell cycle control, but the precise degradation order at each cell cycle phase transition is still unclear. In this work, we investigated the degradation order of targets of a single human E3 ubiquitin ligase important for S-phase proteolysis, known as $CRL4^{Cdt2}$. We showed that in both synchronized cells and asynchronously proliferating cells, $CRL4^{Cdt2}$-mediated degradation of the cell cycle proteins Cdt1, p21, and PR-Set7 occurs in a consistent order during both the G1/S transition and during DNA repair synthesis. We additionally showed that these different rates of degradation are determined by the $CRL4^{Cdt2}$ targeting motif called a PCNA interacting peptide (PIP) degron, which allows for substrate binding to DNA-bound proliferating cell nuclear antigen (PCNA) and recognition by $CRL4^{Cdt2}$. Manipulating the degradation order such that p21 was degraded prematurely promoted stalled replication in mid-S phase and sensitivity to replication arrest. Collectively, these results establish for the first time that ordered degradation at the G1/S transition, facilitated by the $CRL4^{Cdt2}$ E3 ligase, is important to avoid replication stress and genome instability.

Another process that is tightly controlled at cell cycle transitions is replication origin licensing, in which replication initiation sites, or origins, are rendered competent for replication by the DNA loading of the replicative helicase, the Mini-Chromosome Maintenance (MCM) complex. Through the collective action of ORC, Cdc6, and Cdt1 proteins, MCM complexes are

loaded onto DNA exclusively in G1 phase in an inactive form, and become activated by protein kinases during S phase. MCM loading is strictly inhibited beyond the G1/S transition and during cellular quiescence (G_0 phase), although at the time of this study, mechanisms contributing to this licensing block specifically during G_0 phase were poorly understood. To identify novel protein mediators of quiescence establishment and maintenance, we performed a mass spectrometry screen designed to identify differential MCM binding partners in quiescent vs. proliferating cells. We prioritized several novel MCM interactions uncovered from this initial screen for further validation experiments, including three with previously characterized roles in the control of cell proliferation/quiescence: Sam68 (KHDRBS1), Nme1, and Host Cell Factor C1 (HCFC1). Future work will be needed to improve the initial screening approach and to establish a role for these new MCM interactions in cell cycle control and/or MCM loading regulation.

ACKNOWLEDGEMENTS

First and foremost, I would like to especially thank my mentor, Dr. Jean Cook, for all of her guidance throughout the graduate school process. Whenever prospective students/postdocs interview for a position in our lab, I always tell them that very few PIs compare to Jean in terms of her ability to foster professional development. I have grown tremendously in the past five years as an independent scientist, and she has always challenged me to become a daring experimentalist and creative thinker. Even though I have had my share of challenges in the lab, she has always been supportive of me from the beginning, and I cannot thank her enough for the very broad skillset I have developed under her guidance. She is remarkably talented.

I would also like to acknowledge my committee members, Drs. Cyrus Vaziri, Ben Major, Kim Rathmell, and Dale Ramsden. Every committee meeting since the very beginning has been extremely productive and informative. Thank you for always being engaged, and for your help in guiding me through troubleshooting and prioritizing experiments.

Thank you to the members of the Cook lab, both past and present, who have helped me throughout this journey. Karen Lane, Sri Chandrasekaran, Kim Raiford, and Lindsay Rizzardi were especially influential during my training in the beginning years and served as excellent models to follow throughout the process. Gavin Grant, Dileep Varma, Kristen Brantley, and Ben Workman each made substantial contributions to our *Genes & Development* paper, and it all would not have been possible without their experiments. Jacob Matson, Daniel Tesfu, and Seeun Oh have each assisted me technically on various projects when I was feeling

overwhelmed, and I am very grateful for their help. Also, aside from just the benchwork, every member of the lab has contributed somehow to both the scientific and social framework of the lab, and I owe it to each of them for a great work environment. You have been outstanding friends and colleagues and I will miss every one of you.

Special thanks to our collaborators Ray Haggerty and Jeremy Purvis, as well as Etsuko Shibata and Anindya Dutta. Their contributions helped bring our *Genes & Development* paper to a whole new level. I am excited to see how the Purvis lab/Cook lab collaboration will develop in the future!

During my time in graduate school, I have made so many wonderful friendships that it would be impossible for me to mention them all in a short paragraph. This period of my life has been an emotional roller coaster to say the least, and my friends have been there through every twist and turn. Thank you all for making sure I had so many fun and new experiences, and for helping me through the hard times. Aside from that, a number of my friends have also enhanced my scientific development, and I would like to particularly thank Crystal Waters, Tiki Hayes, and Kathleen Mulvaney for all their advice. Also, thanks to some of you for keeping me in shape and getting me into running as a hobby (Talia Hatkevich especially), and for all the great dinners and social outings throughout the years! I will always be nostalgic for my time in Chapel Hill because of you.

And lastly I would like to express my sincerest gratitude to my family: Jim, Sylvia, and Jimmy Coleman. There is absolutely no way my PhD would have been possible without your love and support during both the good and bad times. My family may not always fully understand my struggles and what motivates me to do this, but they have always been very encouraging of my decision to pursue my degree and proud of my accomplishments. I am eternally grateful to have that safety net around me and I love you more than words can say.

TABLE OF CONTENTS

LIST OF TABLES

LIST OF FIGURES

LIST OF ABBREVIATIONS AND SYMBOLS

Δ -- deletion

APC/C –- Anaphase Promoting Complex/Cyclosome

ATM -- Ataxia Telangiectasia Mutated

ATP -- adenosine triphosphate

ATR -- Ataxia Telangiectasia and Rad3 related

BER – Base Excision Repair

BrdU -- Bromodeoxyuridine

Cdc6 – Cell division cycle 6

CDK – Cyclin dependent kinase

Cdt1 – Cdc10 dependent transcript 1

Cdt2 – Cdc10 dependent transcript 2

CFP – cyan fluorescent protein

CKI – cyclin dependent kinase inhibitor

CMG -- Cdc45-GINS-MCM2-7 complex

CRL – Cullin RING E3 ubiquitin ligase

CSN -- COP9-signalosome

DDK – Dbf4 dependent kinase

DMEM – Dulbecco’s Modified Eagle Medium

DNA – Deoxyribonucleic acid

dNTP -- deoxyribonucleotide triphosphate

FASP -- filter-aided sample preparation

FBS – Fetal bovine serum

Fen1 – flap structure specific endonuclease 1

GAPDH – glyceraldehyde-3-phosphate dehydrogenase

GO – Gene ontology

GST – Glutathione-S-transferase

HBO1 – histone acetyltransferase binding to Orc1

HCFC1 – Host Cell Factor C1

HECT -- Homologous to E6-AP C-terminus

HU – hydroxyurea

IP -- Immunoprecipitation

JNK -- c-Jun N-terminal kinase

LC-MS/MS – Liquid chromatography-tandem mass spectrometry

MAPK – Mitogen-activated protein kinase

MCM – Minichromosome maintenance complex

MOI – Multiplicity of Infection

NEDD8 – Neural precursor cell expressed developmentally down-regulated protein 8

NLS -- Nuclear localization signal

NSAF – Normalized Spectral Abundance Factor

ORC – Origin Recognition Complex

ORF – Open reading frame

PCNA – Proliferating Cell Nuclear Antigen

PI – Propidium Iodide

PIP – PCNA interacting protein motif

pre-RC – Pre-replication complex

PTM – Post-translational modification

RFC – Replication factor C

RING -- Really Interesting New Gene

RNR – Ribonucleotide reductase

SAC – Spindle Assembly Checkpoint

SCF – Skp, Cullin, F-box containing complex

siRNA – Small interfereing RNA

Skp2 – S phase kinase-associated protein 2

SRF -- substrate recognition factor

TDG – Thymine DNA glycosylase

TLS – Trans-lesion synthesis

TRIM39 -- Tripartite Motif 39

UBC -- ubiquitin-conjugating enzymes

UV – ultraviolet radiation

WT – wild-type

XPG -- xeroderma pigmentosum group G

YFP -- yellow fluorescent protein

Chapter 1: Introduction

An overview of the eukaryotic cell cycle

The eukaryotic cell cycle is a highly regulated process that directs accurate cell growth, duplication, and division to produce two identical daughter cells. Events during the cell cycle are described in terms of four distinct phases **(Figure 1.1)**. During G1 (Gap 1) phase, the cell senses extracellular cues and if conditions are appropriate for cell division, expresses components necessary for deoxyribonucleic acid (DNA) replication. If conditions are unfavorable for division, the cell can also at this point exit to become quiescent; during quiescence (also G_0 phase) cells are still metabolically active, but express low levels of cell cycle promoting factors and do not proliferate. When cells have committed to undergo cell division (termed the "restriction point" in late G1; (Pardee 1974) they progress into S phase, when they duplicate the entire genome. Completion of DNA duplication in S phase gives rise to a second gap phase, G2, in which the cell makes preparations for mitosis. Finally, during mitosis, the newly replicated chromosomes are segregated to separate nuclei and subsequent cell division produces two new daughter cells. Mitosis is divided into four distinct stages: prophase, metaphase, anaphase, and telophase (reviewed in (Schafer 1998).

Transitions between cell cycle phases are controlled in large part by the activity of cyclin-dependent kinases (CDKs), which are a family of enzymes that phosphorylate various protein substrates involved in cell cycle progression. As their name suggests, CDKs require the presence of proteins called cyclins; cyclins have no enzymatic activity on their own but

activate CDKs upon binding to them. Cyclin levels oscillate during the cell cycle, owing to changes in synthesis (controlled by transcription and translation) as well as their destruction via ubiquitin-mediated proteolysis, which will be discussed in the next section. These oscillations allow different cyclin-CDK complexes to form at different times to trigger events specific to a given cell cycle phase (reviewed in (Morgan 1997; Schafer 1998). Cyclin activity is also negatively regulated by cyclin-dependent kinase inhibitors (CKIs). There are two main families of CKIs; the INK4 family, which includes $p16^{INK4}$, and the CIP family typified by $p21^{CIP1/WAF1}$, $p27^{Kip1}$, and $p57^{Kip2}$. The abundance of these proteins is tightly controlled during cell cycle progression (reviewed in (Sherr and Roberts 1999; Sheaff 1996). A list of cyclin-CDK complexes and CKIs in mammalian cells is detailed in **Figure 1.1**.

The precise order with which events occur in each of these cell cycle phases is crucial, and many types of human cancers arise as a consequence of inappropriate cell cycle transitions. While the ordering of cell cycle events have been studied extensively in terms of this four-stage model, the cell cycle likely also consists of "subphases" at key transitions to ensure orderly progression from one phase to the next. The sequence of events occurring at these critical transition phases, however, has not been as well studied and is the focus of this dissertation. *Chapter 2 will look at the ordered degradation of proteins at the G1/S transition and its importance to S phase progression. Chapter 3 will examine how replication inhibition is established as cells transition from the active cell cycle to cellular quiescence.*

The ubiquitin-proteasome pathway drives cell cycle transitions

As mentioned above, by causing the orderly destruction of cyclins and other important cell cycle regulators, the ubiquitin-proteasome pathway is also central to coordinating cell cycle transitions. In the process, a small 76-amino-acid peptide called

Figure 1.1.

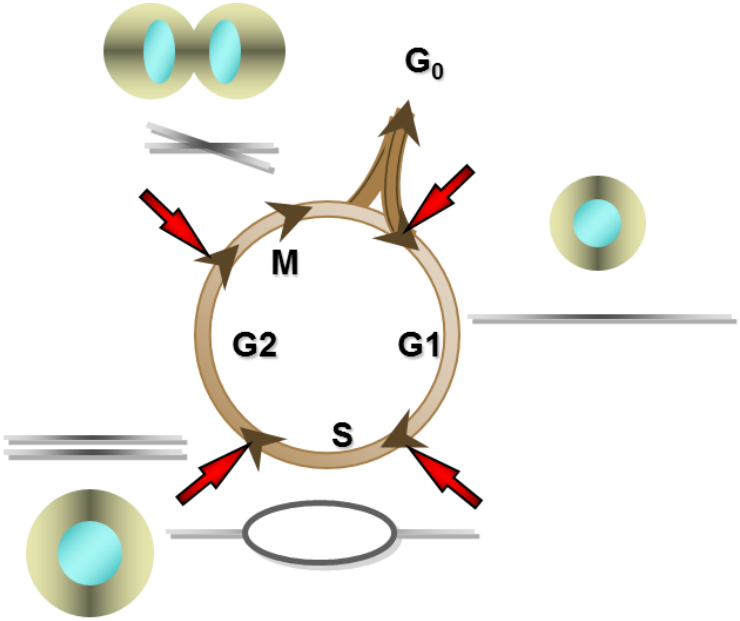

Cdk	Cyclin	function
Cdk1	Cyclin B	mitosis
Cdk2	Cyclin A	S phase completion
Cdk2	Cyclin E	G1-S transition
Cdk4	Cyclin D	G1 progression
Cdk6	Cyclin D	G1 progression

CKI	Interacts with…
p16	Cdk4,6
p18	Cdk4,6
p21	CyclinE1/Cdk2
p27	Cyclin D3/Cdk4, CyclinE1/Cdk2
p57	CyclinE1/Cdk2

Figure 1.1. An overview of eukaryotic cell cycle regulation. Events occurring during different phases of the eukaryotic cell cycle are highlighted. This dissertation emphasizes the ordering of events specifically at transitions between phases, marked by red arrows. Cell cycle transitions are positively regulated by cyclin-CDKs specific to each phase (left table) and negatively regulated by interactions of CDKs with CKIs (right table).

ubiquitin is attached to proteins via an isopeptide bond between the C-terminal glycine of ubiquitin and one or more lysines in the substrate. Successive ubiquitylations form polyubiquitin chains that in most cases target proteins for destruction. In some instances, however, addition of ubiquitin affects the function, enzymatic activity, or subcellular localization of a protein substrate without affecting its stability (reviewed in (Komander and Rape 2012). The ubiquitin-proteasome system consists of three main enzymatic activities. Ubiquitin is first activated by an E1 activating enzyme in a process that consumes adenosine triphosphate (ATP). The ubiquitin is then transferred from the E1 to an E2 conjugating enzyme. Finally, the E2 interacts with an E3 ubiqutin ligase which also binds to the substrate, commonly (although not universally) via a short destruction motif called a "degron" sequence (discussed in the next section). This interaction ultimately promotes ubiquitin transfer to the substrate and targeting to the 26S proteasome for protein destruction **(Figure 1.2A).** (reviewed in (Nakayama and Nakayama 2006; Petroski and Deshaies 2005; Komander and Rape 2012)

E3 ubiquitin ligases involved in substrate recognition can be classified into two main groups based on their method of ubiquitin conjugation and targeting motifs: HECT (Homologous to E6-AP C-terminus) or RING (Really Interesting New Gene) (Deshaies and Joazeiro 2009). The best understood E3s with roles in cell cycle control are the cullin-RING-ligases (CRLs) as well as their relative, the anaphase-promoting complex/cyclosome (APC/C), and these will be the main focus of this dissertation work. Cullin 1 (SCF)- and Cullin 4 (CRL4)-based E3 ligase complexes adopt a similar architecture, shown in **Figure 1.2B**. The scaffold proteins Cul1 and Cul4 (cullin 4A or cullin 4B) complex with small RING finger proteins (Rbx/Roc) to form the catalytic core of CRL1 (SCF) and CRL4 complexes, respectively. Rbx 1/2 proteins are needed to recruit E2 conjugating enzymes. Cullins also bind adaptor proteins (Skp1 for CRL1 and DDB1 for CRL4) that function to bridge cullins

Figure 1.2.

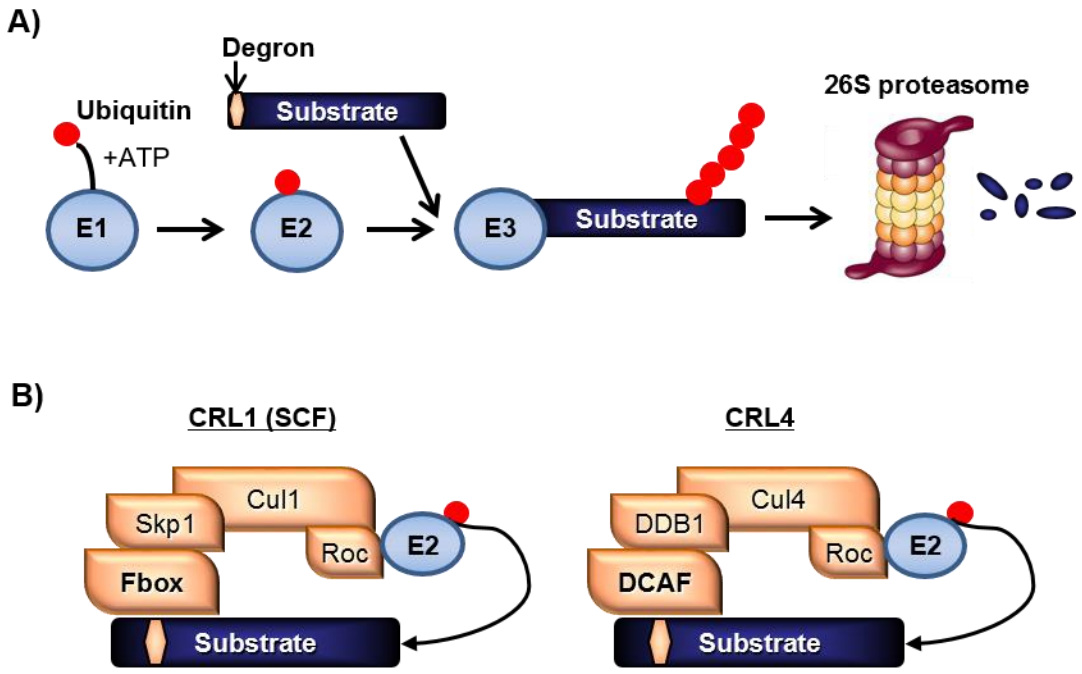

Figure 1.2. The ubiquitin proteasome pathway. (A) An overview of the three enzymatic activities involved in ubiquitin-mediated proteolysis. (B) Components of the CRL1 (SCF) and CRL4 E3 ubiquitin ligase complexes.

with a number of substrate recognition factors (SRFs) (reviewed in (Petroski and Deshaies 2005; Deshaies and Joazeiro 2009; Abbas and Dutta 2011). Substrate specificity is afforded by the large number of these SRFs; for instance, CRL1 relies on 69 F-box proteins, while CRL4 uses ~60 DCAFs, allowing for the formation of a wide variety of E3 ligase complexes to control the degradation of different cell cycle regulators (Bennett et al. 2010; Craney and Rape 2013; Jin et al. 2004).

Common mechanisms regulating E3 ligase activity and substrate recognition

As another important aspect to cell cycle control, ubiquitination reactions catalyzed by E3 ligase complexes must occur at the proper time and place. This regulation often involves modification of substrates or E3s as a prerequisite for the ubiquitination reaction, and some of these mechanisms are discussed below:

Post-translational modifications (PTMs) of substrates

Often, substrates of E3 ligase complexes are not constitutively degraded, but only in response to a particular signal. One way in which this is accomplished is through post-translational modification of the substrate degron motif. As an example, Cdk2 phosphorylates the replication factor Cdc10 dependent transcript 1 (Cdt1) at residue T29 as a prerequisite for recognition by the E3 ligase SCF^{Skp2} during S phase (Takeda et al. 2005). Hydroxylation (Ivan et al. 2001) and sumoylation (Perry et al. 2008) of degron sequences can also promote substrate ubiquitination. Interestingly, phosphorylation of degron sequences can also inhibit substrate recognition by E3 ligases. For instance, phosphorylation by cyclin E-cdk2 protects cell division cycle 6 (Cdc6) from proteolysis by preventing its association with the anaphase-promoting complex (Mailand and Diffley 2005). PTMs affecting substrate recognition do not necessarily have to occur within degron sequences. For example, our lab showed that phosphorylation of Cdt1 at its c-terminus by stress-activated mitogen-activated kinases (MAPKs) protects Cdt1 from binding $CRL4^{Cdt2}$ at

its N-terminal degron (Chandrasekaran et al. 2011).

Cycles of NEDD8 attachment and removal to CRLs

In addition to modification of substrates, the catalytic core of E3 ligases themselves can be regulated to further control ubiquitination during cell cycle progression. One of the key regulators of CRL activity is attachment of the ubiquitin-like protein NEDD8 to the cullin scaffold (Osaka et al. 2000; Sakata et al. 2007). Neddlyation induces a conformational change in the cullin that increases the activity of the CRL, while also impeding the activity of Cand1, an enzyme that promotes the turnover of CRL-receptor complexes to facilitate SRF exchange (Pierce et al. 2013; Liu et al. 2002; Wu et al. 2013). On the other hand, neddylation can be removed from cullins by the COP9-signalosome (CSN) (Lyapina et al. 2001; Cope et al. 2002). Deneddylation is blocked when the CRL is actively engaged in ubiquitination reactions, as the CSN cannot effectively recognize CRLs in these circumstances (Duda et al. 2008). In this way, E3 activity is controlled during the cell cycle via cycles of neddylation and deneddlyation. Acute inactivation of the NEDD8-E1 enzyme with the small molecule MLN4924 leads to rapid loss of all modified cullins and is frequently used in experimental manipulations to disrupt CRL targeting (Soucy et al. 2009; Lin et al. 2010).

Changes in substrate specificity promote sequential protein turnover by APC^{Cdc20}

One particular E3 ligase, APC^{Cdc20}, is unique in that it sequentially targets its cohort of substrates to promote the metaphase/anaphase transition during mitosis. This activity is largely dependent on the status of the spindle assembly checkpoint (SAC), which inhibits APC/C activity during early mitosis. The SAC helps ensure proper chromosome segregation by preventing anaphase onset until chromosomes are properly aligned on the mitotic spindle (reviewed in (Musacchio and Salmon 2007). When the SAC is active, a Mitotic Checkpoint Complex (MCC) (comprised of BubR1, Mad2, Bub3, and Cdc20) binds to and inhibits the

APC/C (Herzog 2009). Within this form of the APC/C, Cdc20 binds in a different orientation than it does within the APC/C^{Cdc20} complex that drives sister chromatid separation during anaphase. These differences in Cdc20 binding to APC/C depending on whether the SAC is active vs. inactive results in the degradation of some substrates (such as Cyclin A) before others promoting anaphase onset (like securin and Cyclin B1) (Izawa and Pines 2011; Tian et al. 2012). Additional determinants of APC/C substrate degradation ordering have been uncovered recently in budding yeast, including the dependence of Clb5 on its Cdc20-binding "ABBA" motif and interaction within the Cdk1-Cks1 complex for early degradation. Cdk1-dependent phosphorylation of securin and Dbf4 also contributes to their relatively delayed degradation (Lu et al. 2014). The combination of these factors causes the same E3 ligase to recognize its substrates at different times in mitosis, resulting in a particular order of protein turnover to promote mitotic progression. At the time of this study, this was the only E3 ligase known to sequentially target its substrates in this way, although we speculate that there are likely others (see Unanswered questions).

Mechanism of replication-coupled destruction via $CRL4^{Cdt2}$

The main focus of Chapter 2 of this dissertation is ubiquitin-mediated proteolysis by the E3 ubiquitin ligase $CRL4^{Cdt2}$. Substrate targeting by this E3 is unique in that it is linked specifically to the process of replication during S phase **(Figure 1.3A)**. Some of the first evidence for this was discovered while investigating the regulation of the origin licensing factor Cdt1. Studies in mammalian cells (Nishitani et al. 2004) and *Xenopus* egg extracts (Arias and Walter 2005) showed that Cdt1 destruction occurred in S phase independently of geminin, an inhibitor of Cdt1 function (Wohlschlegel et al. 2000; Cook et al. 2004; Lutzmann et al. 2006). It was further shown that Cdt1 is degraded by ubiquitin-mediated proteolysis during a single round of DNA replication in *Xenopus* egg extracts, suggesting a replication-dependent mechanism (Arias and Walter 2005). Replication-coupled proteolysis occurs not

only during S phase replication, but also during DNA repair synthesis in response to several damaging agents (Ralph et al. 2006; Higa et al. 2003; Jin et al. 2006; Sansam et al. 2006). Importantly, proteolysis by $CRL4^{Cdt2}$ in response to DNA damage is dependent on the DNA synthesis step during the repair process and not the DNA damage response, as the checkpoint kinases ataxia telangiectasia mutated (ATM) and ataxia telangiectasia mutated and Rad3 related (ATR) are not required (Higa et al. 2003; Arias and Walter 2006; Centore et al. 2010).

PCNA serves as the platform for replication-coupled destruction by $CRL4^{Cdt2}$

Subsequent experiments then probed the mechanism for replication-coupled destruction via $CRL4^{Cdt2}$. Cdt1 destruction was shown to be dependent on its interaction with Proliferating Cell Nuclear Antigen (PCNA), the processivity factor for DNA polymerases δ and ε, on chromatin (Arias and Walter 2006; Senga et al. 2006). Cdt1 and other substrates of $CRL4^{Cdt2}$ interact with PCNA through a PCNA interaction protein motif (PIP) box, which binds a hydrophobic pocket within the interdomain connector loop and C-terminus of PCNA (Gulbis et al. 1996). The PIP box within the substrate is critical for replication-coupled proteolysis both during S phase and during DNA repair synthesis (Arias and Walter 2006; Nishitani et al. 2006; Hu and Xiong 2006; Senga et al. 2006). Furthermore, recognition of substrates by $CRL4^{Cdt2}$ depends on the prior binding of substrates on chromatin-bound PCNA, since if steps upstream of PCNA loading are blocked, $CRL4^{Cdt2}$-mediated proteolysis cannot occur (Arias and Walter 2005, 2006; Havens and Walter 2009; Chandrasekaran et al. 2011). Also, $CRL4^{Cdt2}$ itself is recruited to chromatin during S phase and during DNA repair (Ishii et al. 2010; Jin et al. 2006), and $CRL4^{Cdt2}$-mediated destruction only occurs when Cdt1 binds DNA-bound PCNA but not soluble (free) PCNA (Havens and Walter 2009). Taken together, these results suggest a model whereby Cdt1 uses its PIP box to dock onto chromatin-bound PCNA, followed by

Figure 1.3.

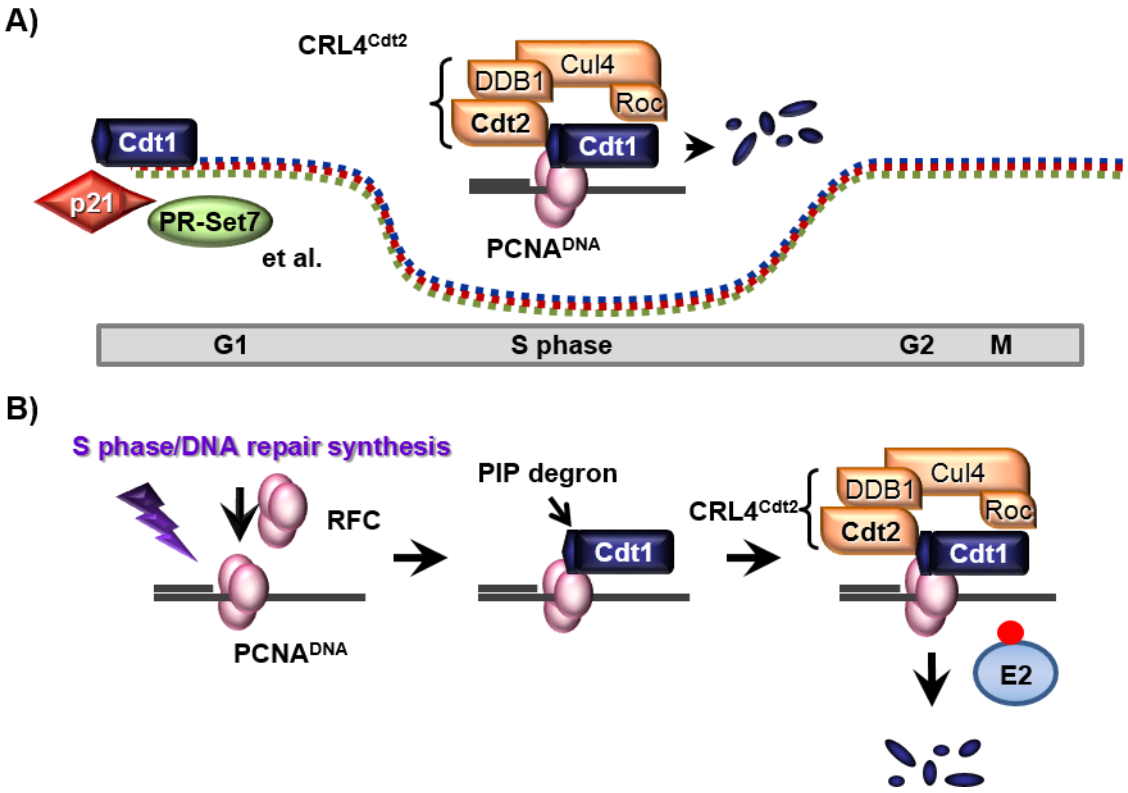

Figure 1.3. Mechanism for replication-coupled destruction of CRL4^{Cdt2} targets. (A) Ubiquitin-mediated proteolysis via the E3 ubiquitin ligase CRL4^{Cdt2} is S phase specific. (B) The mechanism for CRL4^{Cdt2} targeting involves DNA loading of PCNA, substrate recruitment via a PIP degron sequence (Cdt1 is used as an example), followed by CRL4^{Cdt2} recognition of PCNA-bound substrates and subsequent proteolysis.

recognition by CRL4^{Cdt2}, and finally ubiquitin transfer from the E2, leading to proteolysis **(Figure 1.3B)**.

Characteristics of the PIP degron sequence necessary for CRL4^{Cdt2} targeting

Many proteins contain PIP boxes that are not destroyed by CLR4^{Cdt2}, begging the question of what distinguishes *bona fide* CRL4^{Cdt2} substrates from these other PIP box-containing proteins. It was later discovered that CRL4^{Cdt2} substrates contain specialized PIP degron sequences, which are comprised of both a PIP box as well as other key residues important for binding to either PCNA or Cdt2, indicated in the alignments shown in **Figure 1.4**, (see also Figure 2 of (Havens and Walter 2011). These residues include a "TD" motif in the vast majority of CRL4^{Cdt2} substrates, which confers tight binding of substrates to PCNA along with PIP box residues (Warbrick et al. 1997; Havens and Walter 2009). The second important element distinguishing the PIP degron is a basic residue at the +4 position downstream from the PIP box (also called "B+4"). Importantly, mutation of this residue was shown to block CRL4^{Cdt2} binding to Cdt1, without affecting the interaction between Cdt1 and PCNA (Havens and Walter 2009; Michishita et al. 2011). Another feature of the PIP degron sequence is that it is transferable to heterologous substrates. Elegantly, it was shown that introduction of these key "TD" and "B+4" motifs into the PIP box of flap structure-specific endonuclease 1 (Fen1) resulted in its conversion to a CRL4^{Cdt2} substrate, even though Fen1 is not normally targeted by CRL4^{Cdt2} (Havens and Walter 2009). This portable nature of the PIP degron was taken advantage of in a variety of experiments in Chapter 2.

In addition, other residues were shown to be important for substrate interactions with PCNA and Cdt2. For instance, the "B+3" residue is also a key degron residue, as alanine substitution of this residue inhibited *Hs*Cdt1 destruction (Michishita et al. 2011). Also, substrates with internal or C-terminal PIP degron sequences contain a cluster of basic residues upstream of the PIP box **(see Figure 1.4)**; mutation of these residues is important

Figure 1.4.

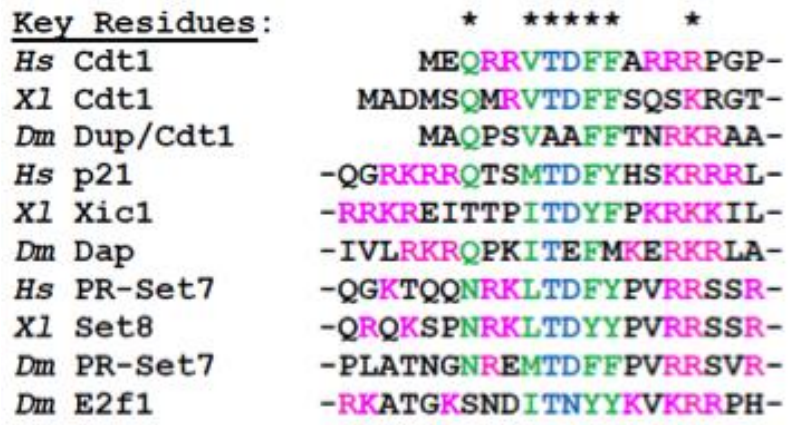

Figure 1.4. Alignment of PIP degrons of key CRL4^{Cdt2} substrates. Shown are alignments of degron sequences from flies (*Dm*), humans (*Hs*), and frogs (*Xl*). Green residues mediate PCNA interaction and blue and magenta residues mediate Cdt2 interaction. See also Figure 2 from (Havens and Walter 2011).

for $CRL4^{Cdt2}$ binding, but only when the B+4 residue is also mutated (Havens et al. 2012). Finally, an acidic residue in PCNA was identified (Asp-122), which is critical for $CRL4^{Cdt2}$ recruitment to chromatin, but not substrate interaction with PCNA (Havens et al. 2012). Likely, this is not an exhaustive list of important degron residues, and our studies in Chapter 2 suggest that there are probably other key residues for efficient PCNA and $CRL4^{Cdt2}$ binding.

Substrate ubiquitylation and beyond: E2 selection and the role of the p97 ATPase

As an additional means to regulate $CRL4^{Cdt2}$ substrate specificity, $CRL4^{Cdt2}$ uses two different ubiquitin-conjugating enzymes (UBCs or E2s) to target different substrates. In a recent study, it was shown that the UBE2G family of UBCs is important in the degradation of Cdt1, whereas UBCH8 is used in the degradation of the CDK inhibitor p21 and the histone H4 lysine 20 methyltransferase PR-Set7 (Shibata et al. 2011). In Chapter 2, we also investigate the importance of E2 selection in the temporal regulation of $CRL4^{Cdt2}$ targeting in collaboration with Anindya Dutta's lab (University of Virginia).

Once ubiquitylated by $CRL4^{Cdt2}$, substrates need to be removed from chromatin for delivery to the proteasome. Recently, the ATPase p97 was implicated in this process (Franz et al. 2011; Raman et al. 2011). A genome-wide screen showed that p97 is among the factors needed for Cdt1 ubiquitination following UV treatment (Raman et al. 2011). Cells treated with siRNA against p97 accumulate polyubiquitinated Cdt1 and on chromatin, suggesting that p97 acts downstream of the ubiquitination reaction and is required for removal of ubiquitinated substrates from chromatin for subsequent proteasomal degradation (Raman et al. 2011). Whether the timing or efficiency of this process is different between $CRL4^{Cdt2}$ substrates has not been directly investigated, however.

Regulation of the CRL4^{Cdt2} E3 ligase complex

To further regulate CRL4^{Cdt2} targeting, the activity and stability of the E3 ligase complex itself is also dynamically controlled during the cell cycle. As mentioned previously, a hyper-phosphorylated form of Cdt2 localizes to chromatin during S phase and following UV irradiation to facilitate the ubiquitylation of substrates on chromatin-bound PCNA (Ishii et al. 2010). Our lab also showed that a CDK1-dependent mechanism interferes with Cdt2 recruitment to chromatin beginning in late S phase, allowing for the stabilization of CRL4^{Cdt2} substrates at the S/G2 transition (see Appendix and (Rizzardi et al. 2014)). Finally, two independent studies showed that Cdt2 is subject to ubiquitylation and degradation by CRL1-FBXO11 (Rossi et al. 2013; Abbas et al. 2013b). Regulation of Cdt2 by CRL1-FBXO11 has been implicated in coordinating cell cycle exit and the cellular response to TGF-β (Rossi et al. 2013; Abbas et al. 2013a).

Biological importance of CRL4^{Cdt2}-mediated degradation

Although the current list of confirmed CRL4^{Cdt2} substrates is relatively short, replication-coupled destruction via this E3 is quite important for proper S phase progression, and deregulation of CRL4^{Cdt2} has been implicated in a wide variety of human cancers (Ueki et al. 2008; Liu et al. 2009; Lee and Zhou 2010). In this section, I will discuss the importance of CRL4^{Cdt2} substrate degradation during three major cellular processes: (1) DNA replication, (2) DNA repair, and (3) G1/S phase progression. The cellular roles of CRL^{Cdt2} targets and the consequences of their deregulation are summarized in **Table 1.1.**

An overview of DNA replication origin licensing and firing

To replicate large eukaryotic genomes in a relatively short amount of time in S phase, DNA replication initiates from thousands of distinct sites called origins. Origins are prepared for replication by the assembly of a multi-protein complexes called pre-replication complexes (pre-RC). Pre-RC assembly begins in telophase and continues as cells progress

through G1 (Dimitrova et al. 2002). Only origins with fully assembled pre-RCs are competent, or "licensed" for replication. These licensed origins are in a poised but inactive state in G1, but do not initiate replication (or "fire") until S phase begins **(Figure 1.5A).** It is critical that this licensing step is restricted to G1 phase, as re-licensing can result in the generation of multiple replication forks on the same DNA strand, leading to DNA re-replication. Re-replication in turn promotes double strand breaks, genome instability, and ultimately tumorigenesis (Davidson et al. 2006; Xouri et al. 2004; Arentson et al. 2002) **(Figure 1.5B)**. On the other hand, insufficient origin licensing in G1 can result in replication forks having to travel excessive distances in the process of replication, leading to fork collapse and DNA damage (Nevis et al. 2009; Shreeram et al. 2002; Teer et al. 2006) **(Figure 1.5C)**.

Origin licensing occurs in a step-wise process involving several proteins, shown in **Figure 1.6**. First, the six-subunit origin recognition complex (ORC), comprised of subunits Orc2-6, recognizes and binds to an origin of replication. Orc then recruits the replication factor cell division cycle 6 (Cdc6). The combined ATPase activity of both ORC and Cdc6 is necessary to then promote loading of the replicative helicase complex onto DNA (Randell et al. 2006; Bowers et al. 2004). The core replicative helicase, the Mini-Chromosome Maintenance (MCM) 2-7 complex, is recruited to origins by binding to the replication factor Cdt1 (Nishitani et al. 2000; Cook et al. 2004). Cdt1 itself has no enzymatic activity, but delivers MCMs to chromatin-bound Cdc6 and ORC, which both hydrolyze ATP to load MCMs onto DNA (Randell et al. 2006). ATP hydrolysis also releases Cdt1 to recruit additional MCM 2-7 hexamers (Randell et al. 2006). MCMs are loaded as head-to-head double hexamers during pre-RC formation (Remus et al. 2009; Evrin et al. 2009), with multiple rounds of MCM loading per origin (Edwards et al. 2002). Once loaded onto DNA, chromatin-bound MCM complexes mark origins as "licensed", and replication can proceed

Figure 1.5.

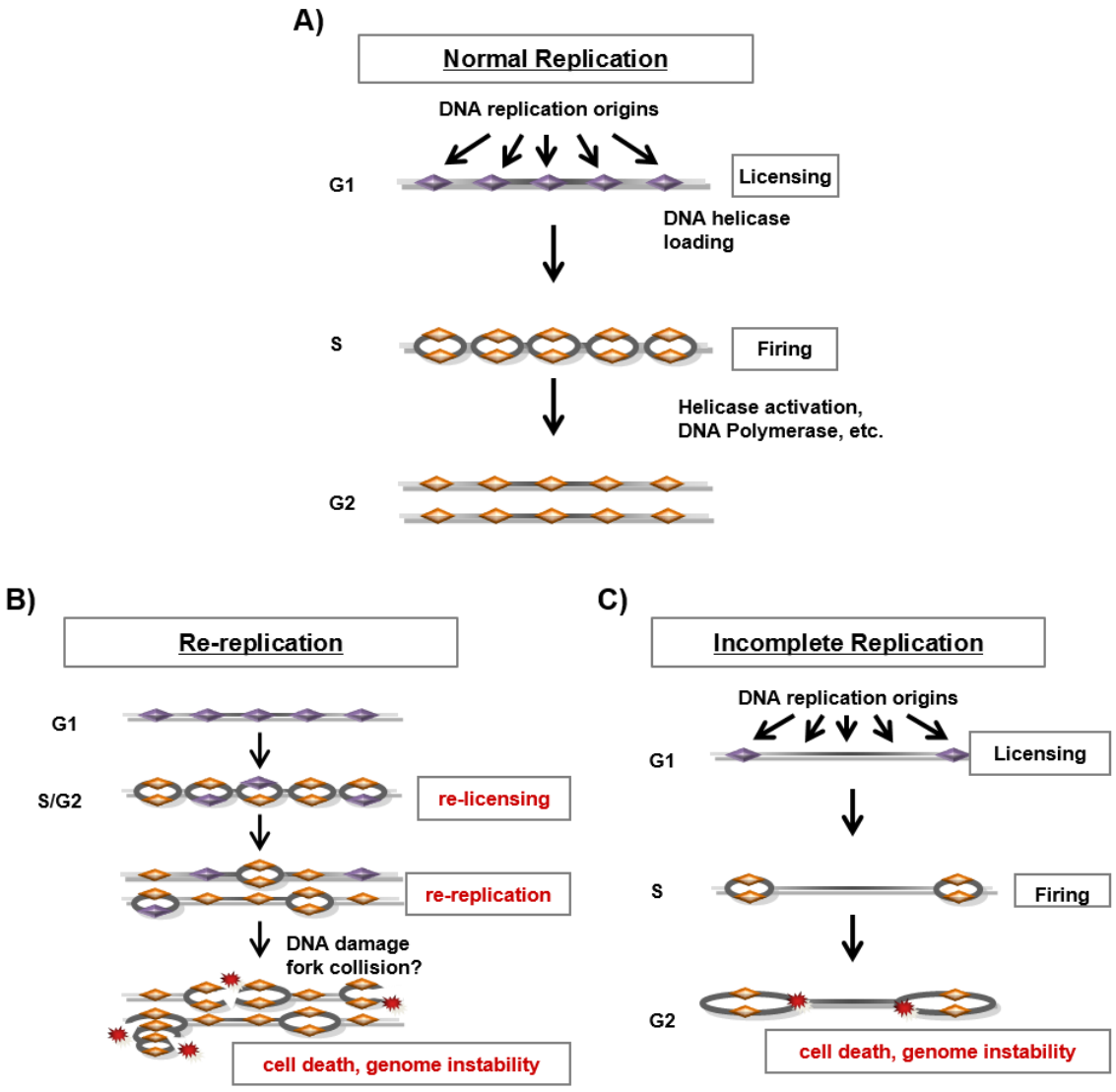

Figure 1.5. Normal replication and consequences of deregulated origin licensing. (A) During normal replication, origins are licensed during G1 (grey diamonds), but do not initiate replication or "fire" until S phase begins (yellow diamonds). Replication is completed by G2 phase. (B) Re-licensing events during S/G2 can lead to re-replication, which in turn promotes DNA damage, genome instability, and cell death. (C) Incomplete licensing during G1 can result in incomplete replication, which can also lead to fork collapse, cell death, and genome instability.

Figure 1.6.

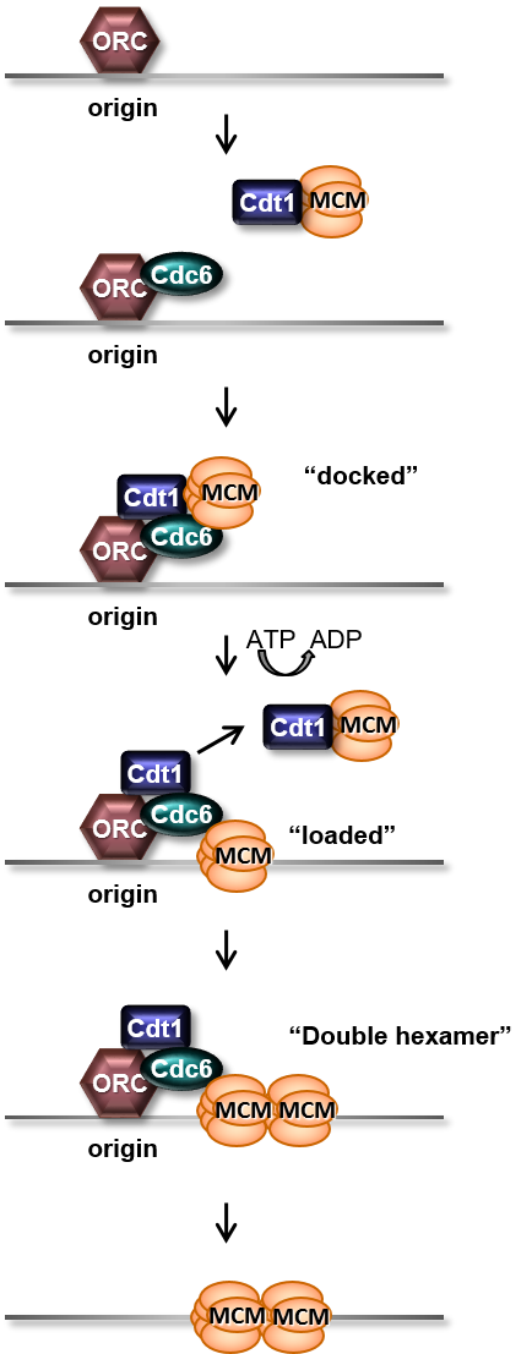

Figure 1.6. Mechanism for MCM helicase loading in G1 phase. Pre-RC assembly begins with ORC binding to origin DNA, followed by Cdc6 binding to ORC, and MCM recruitment by Cdt1. ATP hydrolysis by ORC and Cdc6 then load the MCM helicase onto DNA, which simultaneously releases Cdt1 to recruit additional MCM hexamers. Loading of a second hexamer yields a MCM double hexamer that is competent for replication. Following MCM loading, other factors involved in the licensing and are removed by various mechanisms to avoid re-replication.

from these origins once the helicase is activated upon S phase entry. At this point the replication factors ORC, Cdc6, and Cdt1 are dispensable (Donovan et al. 1997; Rowles et al. 1999), and their participation in further licensing is inhibited by several overlapping mechanisms to prevent re-replication (including $CRL4^{Cdt2}$-mediated proteolysis).

Upon the G1/S transition, a rise in S-phase CDK (both Cdk2 and Cdk1) activity, as well as Cdc7/Dbf4 (DDK) activity, results in the recruitment of additional replication initiation factors needed for complete replisome formation (involving assembly of the Cdc45-GINS-MCM2-7 (CMG) complex) and helicase activation (reviewed in (Labib 2010; Machida et al. 2005; Tognetti et al. 2014). At the same time, however, S phase CDK activity also blocks further licensing activity at origins that have already fired (Hua et al. 1997; Wheeler et al. 2008). In this way, S phase CDKs both positively and negatively affect DNA replication in S phase. Interestingly, the number of replication origins that are licensed in G1 greatly exceeds the number that actually fire in S phase (Edwards et al. 2002; Mahbubani et al. 1992; Rowles et al. 1996). It is proposed that these excess licensed origins (also referred to as “dormant” origins) serve as a backup mechanism to ensure that a sufficient number or origins fire in S phase, particularly during replication stress (Ibarra et al. 2008; Ge et al. 2007; Woodward et al. 2006). Furthermore, licensed origins do not fire synchronously, instead firing at various times in S phase (reviewed in (Aparicio 2013).

Once helicase unwinding of origin DNA occurs, DNA polymerase α/primase is recruited, which synthesizes a ~10 nt ribonucleotide primer, followed by a ~30 nt extension with deoxynucleotides. The RNA-DNA primer is then displaced by replication factor C (RFC), which in turn recruits PCNA. PCNA encircles DNA and serves as the processivity factor for DNA polymerase δ, allowing for subsequent DNA synthesis (Maga and Hubscher 2003).

Several overlapping mechanisms tightly control the MCM loading reaction to ensure that origins are licensed and replication initiates once and only once per cell cycle, that are reviewed extensively elsewhere (Arias and Walter 2007; Machida et al. 2005; Blow and Dutta 2005). The levels and activities of the licensing factors Cdc6, Cdt1, and ORC subunits peak at different times in the cell cycle, allowing only two short windows when licensing can occur. The first window occurs at the end of mitosis, before rising APC^{Cdh1} activity in G1 targets Cdc6 for degradation (Petersen 2000; Méndez and Stillman 2000). The second licensing window occurs when Cdc6 is stabilized by cyclin E-Cdk2 phosphorylation of serine 54 (Mailand and Diffley 2005), but before Cdt1 is degraded in early S phase by ubiquitin-mediated proteolysis (see next section). Also in early S phase, a member or the ORC complex, Orc1, is degraded or inactivated (Li and DePamphilis 2002; Li et al. 2004). In mammalian cells, Cdc6 is exported from the nucleus during S phase, which involves a two-step mechanism: First, Gcn5 acetylates Cdc6 at lysines 92, 105, and 109 (Paolinelli et al. 2009), and this acetylation is prerequisite for phosphorylation of Cdc6 at residue serine 106 by cyclin A-Cdk2, leading to its export to the cytoplasm (Petersen et al. 1999; Jiang et al. 1999). Additionally, levels of the inhibitor geminin rise in S phase, which prevents Cdt1 licensing activity (Wohlschlegel et al. 2000; Lee et al. 2004; Cook et al. 2004; Lutzmann et al. 2006). Finally, proteins involved in origin licensing and DNA replication control are transcriptionally regulated during the cell cycle and targeted for degradation by E3 ubiquitin ligases. The remainder of this section will cover the role of the E3 ligase $CRL4^{Cdt2}$ specifically in controlling the process of DNA replication.

Prevention of re-replication by $CRL4^{Cdt2}$-mediated degradation of Cdt1 and PR-Set7

One of the main roles of $CLR4^{Cdt2}$ targeting is to guard against re-replication through degradation of Cdt1 (Nishitani et al. 2004; Arias and Walter 2005; Senga et al. 2006; Nishitani et al. 2006) and the histone methyltransferase PR-Set7 (Jørgensen et al. 2011;

Centore et al. 2010; Oda et al. 2010; Abbas et al. 2010). Cdt1 destruction primarily prevents its further participation in origin licensing activity during S phase and during DNA damage repair. It has been shown in many different model organisms that impairment of Cdt2 targeting of Cdt1 results in high levels of re-replication and genome instability (Vaziri et al. 2003; Arentson et al. 2002; Tatsumi et al. 2006; Lovejoy et al. 2006). Cdt1 levels are also controlled by the E3 ligase SCF^{Skp2} during S phase, which requires prior cyclin A-CDK2-mediated phosphorylation of Cdt1 on residue T29 (Takeda et al. 2005; Nishitani et al. 2006). While both $CRL4^{Cdt2}$ and SCF^{Skp2} are responsible for Cdt1 degradation in S phase, the relative contribution of each of these E3 ubiquitin ligases to re-replication prevention is still unclear (see Unanswered questions).

Depletion of Cdt1 from mammalian cells using small interfering RNA (siRNA) inhibits MLN4924-induced re-replication, but only partially (Lin et al. 2010). This result suggests that $CRL4^{Cdt2}$ inactivation stabilizes a different target protein that contributes to this re-replication phenotype. This protein was soon identified as a $CRL4^{Cdt2}$ target called PR-Set7/Set8 (Jørgensen et al. 2011; Oda et al. 2010; Abbas et al. 2010; Centore et al. 2010). Origin licensing onset coincides with an increase in histone H4 Lys 20 monomethylation (H4K20me1) deposited by the PR-Set7 methyltransferase at replication origins. Artificial tethering of PR-Set7 to a non-origin genomic locus is sufficient to induce pre-RC formation on chromatin (Tardat et al. 2010). The H4K20me1 mark deposited by PR-Set7 during G2 and mitosis is also important to promote proper chromosome condensation. Inactivation of Set8 causes many aberrant phenotypes, including failed mitotic progression, gross chromosomal decondensation, and spontaneous DNA damage (Karachentsev et al. 2005; Houston et al. 2008; Rizzardi et al. 2014). Conversely, expression of $Set8^{\Delta PIP}$, which cannot be degraded by $CRL4^{Cdt2}$, results in premature chromosome compaction and abnormal H4 methylation, which also lead to G2 arrest and increased DNA damage (Centore et al. 2010;

Tardat et al. 2010; Abbas et al. 2010; Jørgensen et al. 2011) Thus, by coordinating PR-Set7 levels during the cell cycle, $CRL4^{Cdt2}$ targeting helps prevent the occurrence of re-replication and facilitates chromosome compaction prior to mitosis. Additionally, PR-Set7 is targeted by additional E3 ligases, APC^{Cdh1} specifically during G1 (Wu et al. 2010) and SCF^{Skp2} (Yin et al. 2008) during S phase, which further contribute to its dynamic cell cycle regulation.

Importance of substrate degradation to replication progression

$CRL4^{Cdt2}$ targeting also impacts replication progression in addition to controlling licensing. One of the first confirmed substrates of $CRL4^{Cdt2}$ was the *S. pombe* protein Spd1 (Holmberg et al. 2005; Liu et al. 2005). Spd1 is an inhibitor of the ribonucleotide reductase (RNR) enzyme, which synthesizes deoxyribonucleotide triphosphates (dNTPs). It is proposed that $CRL4^{Cdt2}$-mediated proteolysis of Spd1 promotes DNA synthesis during both repair and normal S phase replication by ensuring the availability of dNTPs. Disruption of $CRL4^{Cdt2}$ activity in *S. pombe* results in slow growth, defects in double strand break repair, and increased mutation rates, which are rescued (either partially or completely) in an Spd1 deletion strain (Liu et al. 2005). Lack of sequence conservation between RNR inhibitor proteins has impeded identification of mammalian counterparts for Spd1, so it is not yet clear whether this regulation by $CRL4^{Cdt2}$ occurs in human cells (Vejrup-Hansen et al. 2014).

In mammalian cells, $CRL4^{Cdt2}$ is also important for inhibition of p12, the fourth subunit of DNA polymerase δ (Terai et al. 2013; Zhang et al. 2013), which is important for effective DNA replication and cell proliferation. Degradation of p12 following UV-induced DNA damage was shown to be critical for impairing fork progression during the DNA damage response; cells expressing a stable form of p12 aberrantly undergo DNA synthesis in these circumstances, leading to decreased cell survival in response to DNA damage (Terai et al. 2013). $CRL4^{Cdt2}$-directed degradation of p12 is also evident during a normal S phase, allowing the conversion of DNA polymerase $\delta 4$ to $\delta 3$. This $\delta 3$ form of the polymerase can

more effectively engage in DNA repair processes during replication stress (Zhang et al. 2013).

Contribution of CRL4^{Cdt2}-mediated proteolysis to DNA repair

Recently, CRL4^{Cdt2} targeting was shown to influence base excision repair (BER) through degradation of the repair factor thymine DNA glycosylase (TDG) (Slenn et al. 2014; Shibata et al. 2014). TDG is involved in the BER process by removal of mispaired thymine, uracil, and certain modified cytosine residues when paired to guanine, creating an abasic site. Also, TDG participates in DNA demethylation and thereby affects epigenetic regulation of gene expression (Wu and Zhang 2014). TDG is degraded in a PIP-degron dependent manner in both *X. laevis* and mammalian culture systems, in response to both DNA damage and S phase entry (Slenn et al. 2014; Shibata et al. 2014). Expression of a stable form of TDG (ΔPIP) causes increased sensitivity to 5-FU (a uracil analog), as it leads to excessive production of abasic sites and increased checkpoint response (Shibata et al. 2014). Thus, CRL4^{Cdt2} removal of TDG may help modulate TDG levels to prevent toxicity from excess TDG.

Another DNA repair process impacted by CRL4^{Cdt2}-mediated ubiqutination is translesion synthesis (TLS), an error-prone DNA damage tolerance pathway that allows replicative bypass of DNA lesions using specialized polymerases. When replication forks encounter sites of DNA damage, PCNA becomes monoubiquitinated, which in turn promotes recruitment of TLS polymerases (Bienko et al. 2010; Watanabe et al. 2004). This monoubiquitination of PCNA is primarily controlled by the E3 ubiquitin ligase Rad18, although a recent study showed that CRL4^{Cdt2} also promotes PCNA monoubiquitination independently of Rad18 and in the absence of external damage (Terai et al. 2010). It is thought that in this way, CRL4^{Cdt2} facilitates TLS associated with stresses encountered during normal replication progression. Another way in which CRL4^{Cdt2} promotes TLS is

through degradation of p21. Through its tight interaction with PCNA, p21 was shown to block TLS polymerase recruitment to sites of UV-induced DNA damage; thus, p21 elimination by $CRL4^{Cdt2}$ promotes efficient TLS polymerase exchange for replicative bypass (Mansilla et al. 2013; Soria et al. 2008). On the other hand, $CRL4^{Cdt2}$-mediated degradation can also restrict error-prone TLS by targeting one of the main TLS polymerases in *C. elegans*, Polη. It is proposed that in this system, $CRL4^{Cdt2}$-mediated degradation facilitates removal of Polη from the replication fork after its function in TLS (Kim and Michael 2008). Whether $CRL4^{Cdt2}$ targeting regulates human Polη is still unclear, however. One reason this regulation of TLS may be particularly important during early embryogenesis in *C. elegans* is that this system is particularly resistant to DNA damage-imposed cell cycle checkpoint activation; therefore early *C. elegans* embryos may be more reliant on DNA damage tolerance mechanisms for rapid replication of damaged DNA (Kim and Michael 2008).

Control of the G1/S transition by degradation of p21 and dE2F1

In *D. melanogaster*, the $CRL4^{Cdt2}$ E3 ubiquitin ligase also controls the G1/S transition by degrading the E2F1 transcription factor. This "activator" E2F promotes the transcription of a variety of genes during G1 phase to promote S phase entry, and is cell cycle regulated. $CRL4^{Cdt2}$ contributes to this cell cycle regulation by promoting dE2F1 destruction specifically during S phase, in a manner that is defendant on the PIP motif in dE2F1 and also the Dp dimerization partner, which is necessary for dE2F DNA binding (Shibutani et al. 2008). Furthermore, expression of a ΔPIP version of dE2F results in a variety of aberrant phenotypes, including a reduced G1 population, developmental defects, and apoptosis (Shibutani et al. 2008). This $CRL4^{Cdt2}$-dependent destruction of activator E2Fs does not appear to be conserved in other species, presumably because they have adapted other mechanisms to restrain E2F activity upon S phase entry.

In Chapter 2 of this dissertation, we thoroughly investigate $CRL4^{Cdt2}$ targeting of one of the major CKIs involved at the G1/S transition, p21. p21 is targeted by $CRL4^{Cdt2}$ both during S phase and during a DNA damage response (Abbas et al. 2008; Nishitani et al. 2008; Kim et al. 2008) and purified $CRL4^{Cdt2}$ can ubiquitinate p21 *in vitro* and *in vivo* (Abbas et al. 2008). Additionally, p21 is degraded by SCF^{Skp2} during S phase (Bornstein et al. 2003) and APC/C in mitosis (Amador et al. 2007). The relative contributions of SCF^{Skp2} and $CRL4^{Cdt2}$ to the S phase degradation of p21 are currently unclear (see Unanswered questions).

In contrast to other known substrates of $CRL4^{Cdt2}$ discussed above, the reasons for replication-coupled destruction of p21 are not as well understood, however. In *C. elegans*, p21 destruction, along with Cdt1 degradation, is implicated in restraining re-replication during S phase (Kim et al. 2007). In this study, the authors attribute the persistence of p21 with low CDK2 activity and failure to promote the nuclear export of the licensing factor Cdc6, ultimately contributing to increased re-replication (Kim et al. 2007). Thus, p21 degradation may play a role in coordinating the onset of CDK2 activity to allow for Cdc6 phosphorylation and cytoplasmic export, among other events at the G1/S transition. Through its interaction with PCNA, p21 has also been shown to block replication fork progression (Waga S, Hannon GJ 1994), so degradation of p21 at the G1/S transition may relieve this inhibition to control replication onset and maintain fork speed. In support of this notion, while cells expressing low levels of p21 immediately progress through the cell cycle upon release from S phase arrest, cells with high p21 levels move much more slowly through replication in S phase (Gottifredi et al. 2004). More work clearly needs to be done to specifically show how ubiquitin-mediated proteolysis of p21 coordinates CDK levels and replication onset at the G1/S transition, which is a major topic of investigation in Chapter 2.

Table 1.1. Summary of CRL4^{Cdt2} substrate functions and consequences of their deregulation

Substrate	Normal cellular function	Phenotypes associated with deregulation
Cdt1	Replication origin licensing	Re-replication, genome instability
Set8	Deposition of H4K20me1 to promote origin licensing in G1 and chromosome condensation during G2/M	Re-replication, premature chromatin compaction in S phase, DNA damage, G2 arrest
S. pombe Spd1	Inhibits ribonucleotide reductase (RNR) to restrict dNTP production	Slow growth rate, defects in DNA repair, increased mutation rate
p12	Fourth subunit of DNA polδ; necessary for fork progression	Failure to inhibit fork progression following DNA damage, increased sensitivity to DNA damage
TDG	Base excision repair factor, DNA demethylation, epigenetic inheritance	Increased sensitivity to 5-FU; decreased cell proliferation
C. elegans Polη	TLS polymerase; replicative bypass	Increased error-prone TLS, leading to mutagenesis
p21	CDK inhibitor	Increased re-replication in combination with Cdt1 deregulation; deregulated CDK activity at G1/S?
D. melanogaster E2F1	Activator E2F transcription factor; Expression of a variety of target genes needed for S phase	Reduced G1, increased S phase population, apoptosis, developmental defects

Unanswered questions

Although much is known about the dynamic control of ubiquitin-mediated proteolysis during the cell cycle, and about the mechanism of $CRL4^{Cdt2}$ targeting in particular, studies of this regulation particularly at *transitions* between cell cycle phases have been comparatively limited. Investigation of the temporal control of E3 ligase activity and substrate recognition at these critical transition points may enhance our understanding of how normal cell proliferation is coordinated, and how cancers may arise from deregulated cell cycle transitions. Some unanswered questions in the field, which we hope to address in our own studies, include the following:

Do other E3 ubiquitin ligases besides APC/C degrade their substrates sequentially? Why is the order of substrate degradation important at cell cycle transitions?

At the time of this study, the APC/C was the only E3 ligase known to sequentially target its substrates. The order in which APC/C targeting occurs is critical to ensure proper mitotic exit and cytokinesis (Elzen and Pines 2001; Lu et al. 2014; Izawa and Pines 2011; Lindon and Pines 2004). For instance, the substrates Plk1 and Aurora A are degraded at different times as the APC/C switches from binding its activator Cdc20 and Cdh1. Expression of a non-degradable from of Plk1 causes a significant delay in mitotic exit (Lindon and Pines 2004). It is highly likely that similar E3 ligase substrate ordering occurs to properly coordinate other cell cycle transitions. In Chapter 2, we examine the temporal regulation of protein degradation mediated by one E3 ubiquitin ligase, $CRL4^{Cdt2}$, and its importance to the coordination of S phase progression.

Do E3 ligase substrates re-accumulate in a particular order?

Another interesting question is whether ordered protein re-accumulation, upon termination of E3 ligase activity, is similarly important to controlling cell cycle transitions. In our own studies, we have observed that CDK-1-dependent inhibition of the $CRL4^{Cdt2}$ E3

ubiquitin ligase results in the accumulation of its substrates at the end of S phase, and we propose that this build-up is necessary to prepare for the later functions of these proteins in mitosis and G1. Interestingly, we have seen that these substrates also accumulate to different extents at late S phase time-points (Rizzardi et al. 2014). More work is needed to further define ordered protein re-accumulation patterns and how they contribute to preparing for the next cell cycle phase.

Why is CRL4^{Cdt2}-mediated p21 destruction important to coordinating the G1/S transition? How important are other CKIs to this process?

As alluded to in the Introduction, it is clear that p21 is a *bona fide* CRL4^{Cdt2} substrate, but the importance of its degradation to S phase progression is not well defined. We speculate that p21 destruction at the G1/S transition may control the onset of S phase CDK activity needed for replication progression and several S phase events. However, this regulation has not been shown experimentally. In Chapter 2, we look more closely at the timing of p21 destruction and the consequences of manipulating the p21 degradation rate on replication efficiency in S phase. In addition to p21, mammalian cells express two other CKIs, p27^{Kip1} and p57^{Kip2}, which are cell cycle regulated. The relative contributions of these CKIs to controlling the G1/S transition are also not well understood. Whether these CKIs play redundant or separate roles from p21 in coordinating CDK activity will be an interesting topic of future investigation.

Chapter 2: Sequential Replication-Coupled Destruction at G1/S Ensures Genome Stability[1]

Introduction

A key regulatory mechanism ensuring unidirectional progression through the eukaryotic cell division cycle is the timely destruction of proteins via the ubiquitin-proteasome pathway. The precise control of ubiquitin-mediated proteolysis is critical to many cellular processes including transcription, DNA replication, DNA repair, and chromosome segregation. Deregulated protein ubiquitylation can promote aberrant cell proliferation and genome instability (reviewed in (Teixeira and Reed 2013; Nakayama and Nakayama 2006). Ubiquitin-mediated degradation requires the selection of a protein substrate by an E3 ubiquitin ligase. Several E3 enzymes recognize their targets via an amino acid binding motif in the substrate called a "degron." For the cullin family of E3 ligases, degron binding facilitates ubiquitin transfer from an associated E2 enzyme to the substrate; successive ubiquitylations direct ultimate degradation by the 26S proteasome (Petroski and Deshaies 2005; Nakayama and Nakayama 2006). Selectivity and timing of E3 ligase action by regulating degron recognition or E3 ligase activity allows oscillations in protein abundance to control key events.

It is generally presumed that an individual E3 ubiquitin ligase targets its cohort of substrates simultaneously leading to their near-synchronous degradation. Countering this

[1] Modified from Coleman KE, Grant GD, Haggerty RA, Brantley K, Shibata E, Workman BD, Dutta A, Varma D, Purvis JE, and Cook JG. 2015. *Genes & Development*, **29**: 1734-1746.

notion however, several substrates of the anaphase-promoting complex/cyclosome (APC/C), the E3 ubiquitin ligase complex regulating mitotic progression, are degraded sequentially. Mammalian APC/C^{Cdc20} triggers the degradation of substrates such as Nek2A and Cyclin A in prometaphase, well before the destruction of other APC/C substrates like securin and Cyclin B which occurs during metaphase (Elzen and Pines 2001; Hagting et al. 2002). The mechanism distinguishing early vs. late substrates involves spindle assembly checkpoint-driven changes in how the Cdc20 substrate adapter interacts with APC (Izawa and Pines 2011). Likewise, budding yeast APC/C directs the degradation of the mitotic cyclin Clb5 before securin; in this instance, the distinguishing mechanism involves Cdk1-mediated substrate phosphorylation near a Cdc20 binding motif (Lu et al. 2014). The ordered degradation of these mitotic proteins is essential for coordinated and accurate mitotic progression and cytokinesis (Elzen and Pines 2001; Lu et al. 2014; Izawa and Pines 2011; Lindon and Pines 2004). It is not yet known if similar patterns of degradation occur at other cell cycle transitions. In particular, the temporal regulation of protein degradation during S phase entry is still poorly understood. We hypothesized that the events of S phase onset must be highly temporally controlled to properly coordinate replication onset, S phase progression, and precise genome duplication.

To test this idea, we have investigated substrates of the CRL4^{Cdt2} E3 ubiquitin ligase, which triggers replication-coupled destruction of several lynchpin cell cycle proteins during S phase. In human cells, these substrates include Cdt1 (Arias and Walter 2005; Nishitani et al. 2006; Senga et al. 2006) and PR-Set7 (Abbas et al. 2010; Centore et al. 2010; Oda et al. 2010; Jørgensen et al. 2011), two factors critical to DNA replication origin licensing, the S phase cyclin-dependent kinase (CDK) inhibitor p21 (Abbas et al. 2008; Nishitani et al. 2008), the DNA polymerase delta subunit p12 (Zhang et al. 2013; Terai et al. 2013; Zhao et al. 2014), the base excision repair enzyme thymine DNA glycosylase (TDG) (Shibata et al. 2014; Slenn et al. 2014) and the nucleotide excision repair endonuclease xeroderma

pigmentosum group G (XPG) (Han et al. 2014). Each of these proteins is degraded by the same general mechanism which involves DNA loading of the sliding clamp processivity factor, proliferating cell nuclear antigen (PCNA), during DNA synthesis followed by binding of the substrate to $PCNA^{DNA}$ via a PCNA-interacting motif known as a PIP box **(Figure 2.1A)** (Arias and Walter 2006; Senga et al. 2006). PIP boxes that confer replication-coupled destruction reside in specialized motifs termed PIP degrons that include additional residues necessary for recognition by $CRL4^{Cdt2}$ (Havens and Walter 2009). The Cdt2 substrate adaptor subunit of $CRL4^{Cdt2}$ recognizes a presumed composite surface consisting of the substrate PIP degron and specific residues from $PCNA^{DNA}$ (Arias and Walter 2006; Havens and Walter 2009; Havens et al. 2012). Importantly, Cdt2 cannot stimulate substrate ubiquitylation unless the substrate is first bound to DNA-loaded PCNA, a requirement that couples substrate destruction directly to DNA synthesis (Havens and Walter 2009). Perturbations to replication-coupled destruction have profound effects on S phase progression and genome stability (Tardat et al. 2010; Arias and Walter 2005; Centore et al. 2010; Abbas et al. 2010; Shibata et al. 2014; Zhang et al. 2013; Terai et al. 2013; Oda et al. 2010; Arias and Walter 2006).

The cell cycle functions of $CRL4^{Cdt2}$ substrates vary widely, raising the possibility that they may need to be degraded at different times relative to one another to ensure orderly transition from G1 to S phase. Although the molecular mechanism of $CRL4^{Cdt2}$-mediated degradation is well-characterized, it is still unclear whether all substrates are degraded with similar timing. It is also unclear if the relative timing of substrate destruction is important for the proper coordination of S phase progression. In this study, we provide the first direct evidence of ordered substrate degradation of $CRL4^{Cdt2}$ substrates, and we show that the timing of substrate degradation is related to differences in the substrates' PIP degron affinities for Cdt2. The sequential rather than simultaneous degradation pattern is essential to avoid replication stress during S phase.

Results

$CRL4^{Cdt2}$ substrates are degraded sequentially during early S phase.

We first determined whether two $CRL4^{Cdt2}$ substrates are degraded simultaneously or in a specified order at the G1/S transition. Toward that end, we quantified the change in Cdt1 and p21 concentrations in individual late G1 *vs*. early S phase cells. We synchronized HCT116 cells in mitosis by sequential thymidine and nocodazole blocks (Chandrasekaran et al. 2011), released from nocodazole, and pulse-labeled with BrdU prior to harvesting at time points corresponding to either G1 (2.5 h after release) or early S phase (4 h after release). We then immunostained these cells for endogenous Cdt1, p21, and BrdU incorporation. Both Cdt1 and p21 were readily detectable in G1, but notably Cdt1 was mostly degraded by early S phase whereas p21 was not **(Figure 2.1B)**; p21 was more fully degraded later in S **(Figure 2.2).** We quantified the mean nuclear fluorescence intensities **(Figure 2.1C)** and scored nuclei for Cdt1 or p21 **(Figure 2.1D)**. In cells with detectable Cdt1 or p21, the concentration of Cdt1 decreased more than 10-fold between G1 (2.5 h) and early S phase (4 h), but p21 levels only decreased 2-fold during that same time period **(Figure 2.1C)**. Furthermore, far fewer nuclei retained Cdt1 at the early S phase time point (24%) than retained p21 (70%). Moreover, we detected a relatively low occurrence of BrdU-positive cells that co-stained for Cdt1 (9%), whereas BrdU/p21 double-positive cells were much more prevalent (30% of the total, and nearly half of the BrdU positive cells, suggesting that cells initiate DNA replication in the presence of p21 **(Figure 2.1E)**. We note that at this single time point after synchronization not all cells have yet entered S phase cells which contributes to the Cdt1-positive cells in **Figure 2.1D**.

A potential caveat to these immunofluorescence experiments was that the detection of endogenous Cdt1 and p21 required the use of different antibodies. To directly compare

Figure 2.1.

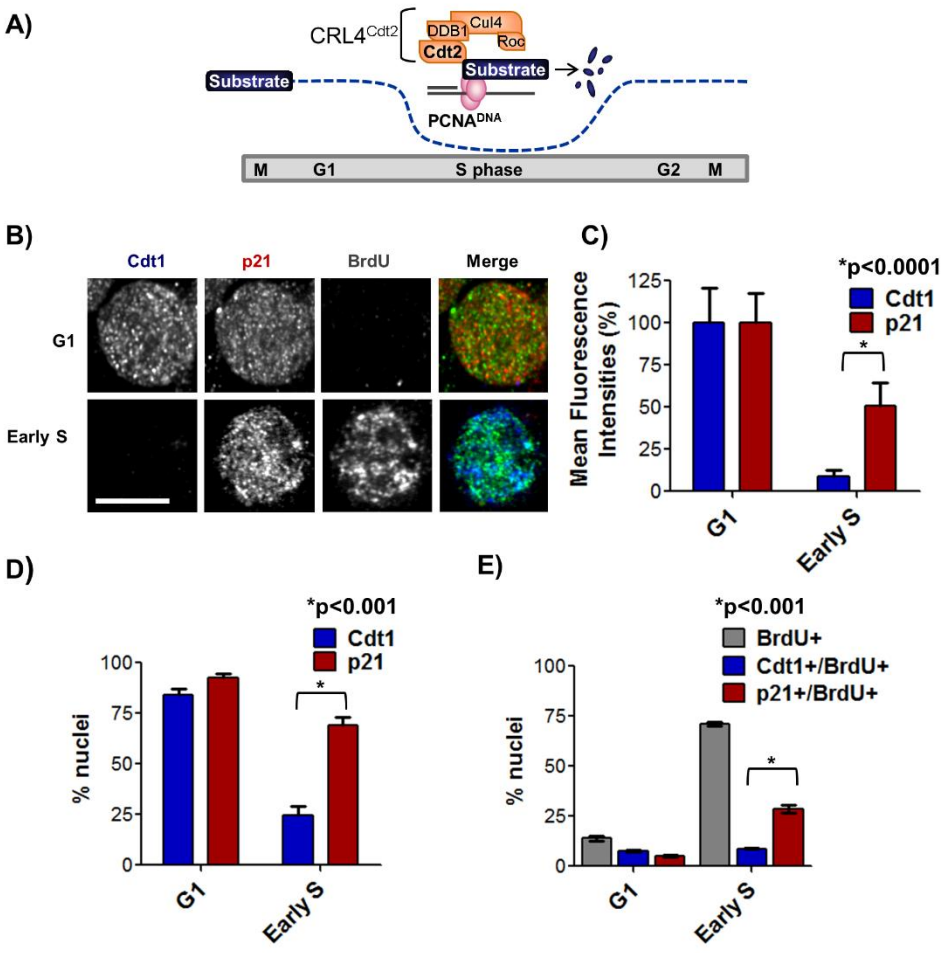

Figure 2.1. CRL4^{Cdt2} substrates are degraded in a stereotypical order during early S phase. (A) The mechanism of cell cycle regulation of CRL4^{Cdt2} substrates requires PCNA DNA loading. (B) HCT116 cells were synchronized by sequential thymidine and nocodazole treatment and fixed at 2.5 h (G1) or 4 h (early S) after nocodazole release. Cells were labeled with BrdU 30 minutes prior to fixation and staining with the indicated antibodies. Scale bar = 5 μm. (C) Average fluorescence intensities relative to G1 from 3 independent experiments; n = 15. (D) Percentage of nuclei positively stained by anti-Cdt1 or anti-p21; n = 650. (E) Percentage of nuclei positively staining with the indicated antibodies from three independent experiments; n=200. Error bars indicate standard deviations.

Figure 2.2.

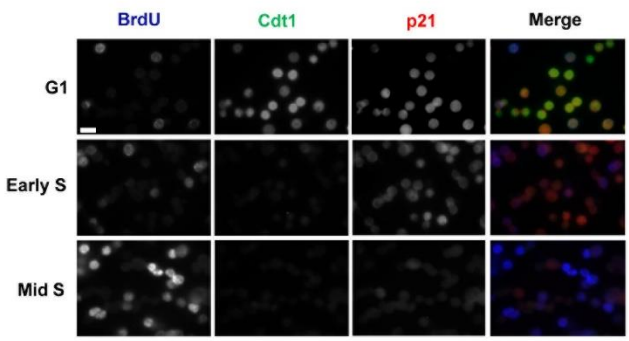

Figure 2.2. Sequential destruction of CRL4^{Cdt2} targets during the G1/S transition. HCT116 cells were synchronized by sequential thymidine and nocodazole treatment and fixed at 2.5 h (G1), 4 h (early S), or 5.5 h (mid S) post nocodazole release. Cells were labeled with BrdU 30 minutes prior to fixation and staining with the indicated antibodies. Scale bar = 10 μm.

the rates of Cdt1 and p21 degradation using the same detection method, we generated fluorescent fusions. We fused cyan fluorescent protein (CFP, “mCerulean3”) to the C-terminus of Cdt1 and yellow fluorescent protein (YFP, “Venus”) to the N-terminus of p21 bearing a nuclear localization signal; these arrangements leave the regions of each protein that direct replication-coupled destruction unperturbed. We expressed them from a single bicistronic mRNA in which the two fusions are separated by a viral self-cleaving sequence from porcine teschovirus “P2A” (Kim et al. 2011) **(Figure 2.3A).** We integrated the bicistronic cassette into U2OS cells at a single FRT locus under control of a doxycycline-inducible promoter; the parent cells were engineered to constitutively express a histone H2B-mCherry fusion. Addition of doxycycline to the culture medium resulted in a dose-dependent induction of both fusions, and importantly, no uncleaved protein was detectable even at the highest concentrations **(Figure 2.3A).** Induction with 20 ng/ml doxycycline produced YFP-p21 at close to endogenous levels, and Cdt1-CFP was moderately overproduced, so we selected this concentration for subsequent experiments **(Figure 2.3A, lane 3).** Importantly, both fusions showed the same stability as their endogenous counterparts **(Figures 2.4A and 2.4B)**, and much higher levels of expression were required to produce detectable cell cycle perturbations **(Figure 2.4C-E)**. Based on our immunostaining results **(Figure 2.1)**, we predicted that Cdt1-CFP would be consistently degraded before YFP-p21 and that in asynchronous populations we would observe YFP single positive cells but few CFP single-positive cells. To test this prediction, we imaged fixed asynchronous, unperturbed cells by fluorescence microscopy **(Figure 2.3B)**. We identified nuclei and scored them as either YFP (p21) positive, CFP (Cdt1) positive, double positive, or double negative. Among cells with detectable fluorescence expression, double-positives were the most abundant class representing cells presumed to be in either G1 or G2 phase (31%). (Of note, we did not achieve 100% expression under these induction conditions meaning that we cannot conclude that all double-negative nuclei are in S phase.)

Strikingly however, YFP-p21 single positives represented a significant subpopulation (22%) whereas Cdt1-CFP single positive were exceedingly rare (0.3%) **(Figure 2.3C)**. Altogether, these results suggest that the $CRL4^{Cdt2}$ substrates Cdt1 and p21 undergo sequential rather than simultaneous degradation upon S phase entry during an unperturbed cell cycle. This finding prompted investigation into the molecular mechanism of this differential targeting.

$CRL4^{Cdt2}$ substrates are degraded sequentially during DNA repair synthesis.

Since most DNA repair processes involve a DNA synthesis step, PCNA is loaded during DNA repair similar to its DNA loading during S phase. Consequently, $CRL4^{Cdt2}$ substrates are also degraded during DNA repair (Nishitani et al. 2008; Abbas et al. 2008; Senga et al. 2006; Abbas et al. 2010). We took advantage of this knowledge to induce synchronous PCNA loading and therefore simultaneous and robust replication-coupled destruction in otherwise asynchronous populations. We employed a semi-quantitative immunoblotting strategy to compare the relative degradation kinetics during DNA repair for $CRL4^{Cdt2}$ substrates **(Supplementary Figure 2.5 and Materials and Methods).** To determine whether $CRL4^{Cdt2}$-mediated destruction also occurs sequentially during DNA repair, we irradiated HCT116 cells with 20 J/m^2 UV and monitored levels of three $CRL4^{Cdt2}$ targets – Cdt1, PR-Set7, and p21 – in a time course. Similar to our analysis of the G1/S transition, Cdt1 was degraded dramatically faster than p21. By 15 minutes post-irradiation, Cdt1 was already more than 50% degraded, but p21 persisted much longer and was not substantially degraded until 60-120 minutes post-irradiation (**Figure 2.6A**, compare lanes 2 and 5 to lane 1). The half-life of Cdt1 was only 9 min, but p21 was degraded with an average half-life of 53 min; the half-time for PR-Set7 degradation was intermediate at 23 min **(Figure 2.6A)**. Importantly, we observed the same sequential relationship among the

Figure 2.3.

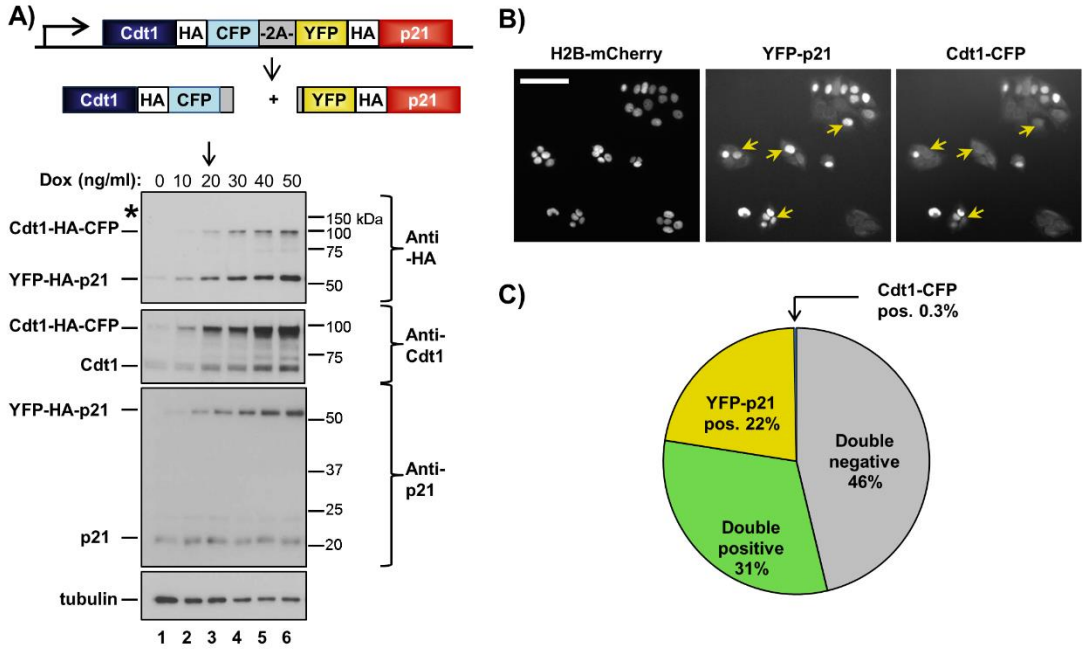

Figure 2.3. Cdt1-CFP is degraded more rapidly than YFP-p21 in unperturbed cells. (A) Schematic of the bicistronic expression construct (top); Cdt1-HA-mCerulean3 (CFP) and Venus (YFP)-HA-p21 are produced from a single mRNA due to the presence of a viral self-cleaving peptide "2A." (Bottom) The resulting Cdt1 and p21 fusions were expressed from a single FRT locus in U2OS cells after doxycycline induction with the indicated concentrations for 20 h; the arrow marks the concentration used for imaging, and the asterisk marks the predicted size of the fusion in the absence of 2A-mediated cleavage. (B) A representative field showing double-negative, double positive and YFP (Venus) single positive cells; four single positive cells are marked with arrowheads. Scale = 100 µM. (C) Quantification of asynchronous Cdt1-mCerulean3 and Venus-p21-expressing U2OS cells. Averages from three fields of cells (n>150 per field) were scored as double-negative, double-positive, or single positive.

Figure 2.4.

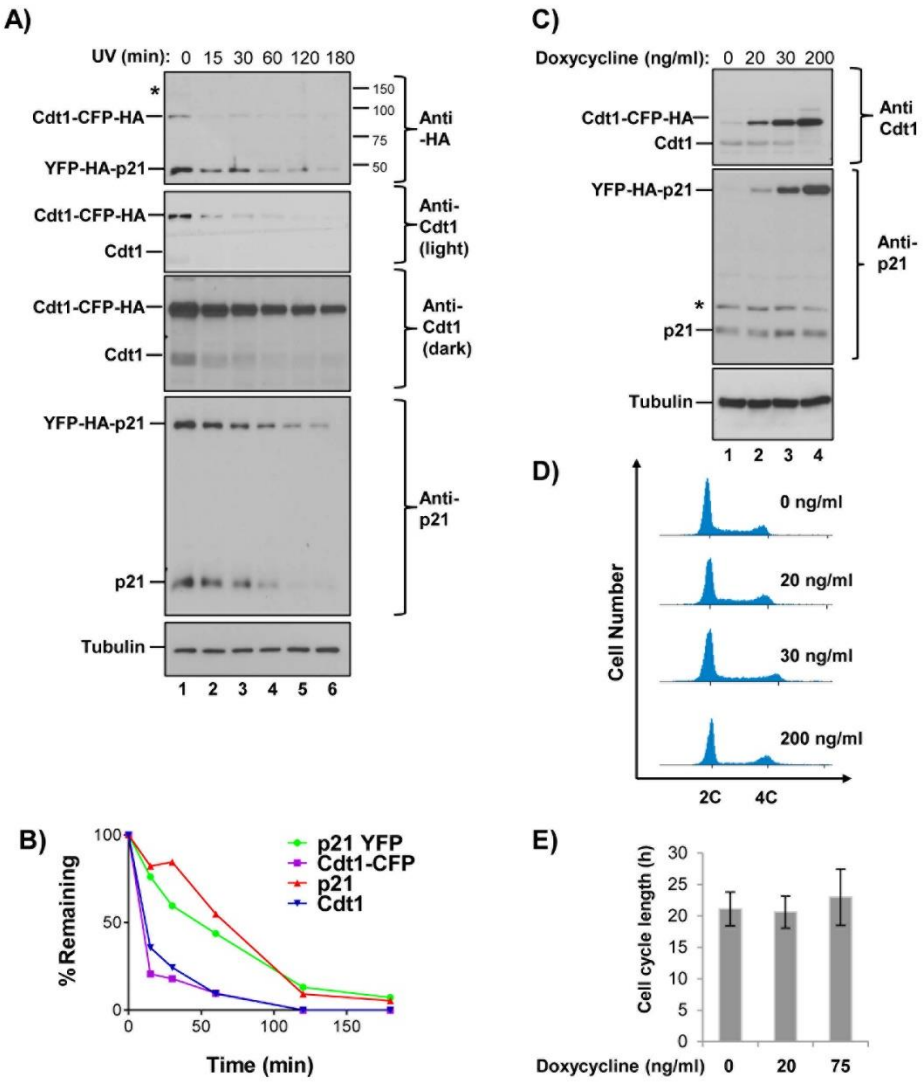

Figure 2.4. YFP-p21 and Cdt1-CFP fusion protein expression and validation. (A) Asynchronously proliferating U2OS cells expressing Cdt1-CFP-P2A-YFP-p21 were treated with 20 J/m2 UV and collected at the indicated times. The asterisk (*) marks the predicted position of the uncleaved fusion which is undetectable. (B) Quantifications of immunoblots from A. (C) U2OS cells were treated with the indicated concentrations of doxycycline to induce expression of YFP-p21 and Cdt1-CFP fusion proteins; fusions were detected by immunoblotting. (D) Cells treated with the indicated doxycycline concentrations as in (C) were analyzed by flow cytometry for DNA content. (E) Live cell movies of cells induced with the indicated doxycycline concentrations were analyzed for cell cycle length. Twenty cells (0 ng/ml and 20 ng/ml) and 19 (75 ng/ml) cells were counted from one mitotic event to the next mitotic event. Error bars indicate standard deviations.

$CRL4^{Cdt2}$ substrates using other damaging agents such as oxidative damage **(Figure 2.6B)** and the radiomimetic bleocin (data not shown). Moreover, the degradation order was similar in other cell lines including U2OS and immortalized primary fibroblasts (NHF-hTERT) **(Figure 2.6C)**. We also observed the same relative degradation order in cycloheximide-treated cells **(Figure 2.5B)** and that p21 stably expressed from a heterologous promoter was degraded with the same kinetics as endogenous p21 **(Figure 2.5B and 2.7A)**. These observations eliminated the possibility that the particularly slow p21 degradation reflected a contribution from p53-dependent p21 induction. We note that *p21* is a well-known DNA damage-inducible gene making the degradation of p21 protein after DNA damage somewhat counter-intuitive. p21 induction and cell cycle arrest typically occurs at lower doses and at much later time points after DNA damage (Bendjennat et al. 2003; Pagano et al. 1994); in agreement with these previous studies, we also observed that p21 induction and cell cycle arrest only occurred 24 h after we treated HCT116 cells with 2-5 J/m^2 UV **(Figures 2.5C and 2.5D)**. On the other hand, $CRL4^{Cdt2}$-mediated p21 destruction within 2-3 hours was the predominant response to higher doses of UV (20 J/m^2) used throughout this study. HeLa cells which are functionally p53-deficient also degraded Cdt1 more rapidly than they degraded PR-Set7 (**Figure 2.5E**). A recent study implicated the Tripartite Motif 39 (TRIM39) protein in regulating p21 degradation by blocking Cdt2 binding and inhibiting p21 degradation (Zhang et al. 2012). We tested a mutant form of p21 that fails to bind TRIM39 described in that study (p21-K153A), but observed no appreciable acceleration in its rate of degradation compared to the WT version (**Figure 2.5F**). Thus, we determined that slow p21 degradation is common to many human cell lines and must be via a mechanism unrelated to *de novo* protein synthesis or interaction with TRIM39.

The Cdt1 PIP degron confers an accelerated degradation rate.

Human Cdt1 codons 1-28 encode its single PIP degron, and when fused to a heterologous substrate, this sequence is sufficient to confer $CRL4^{Cdt2}$-mediated degradation

Figure 2.5.

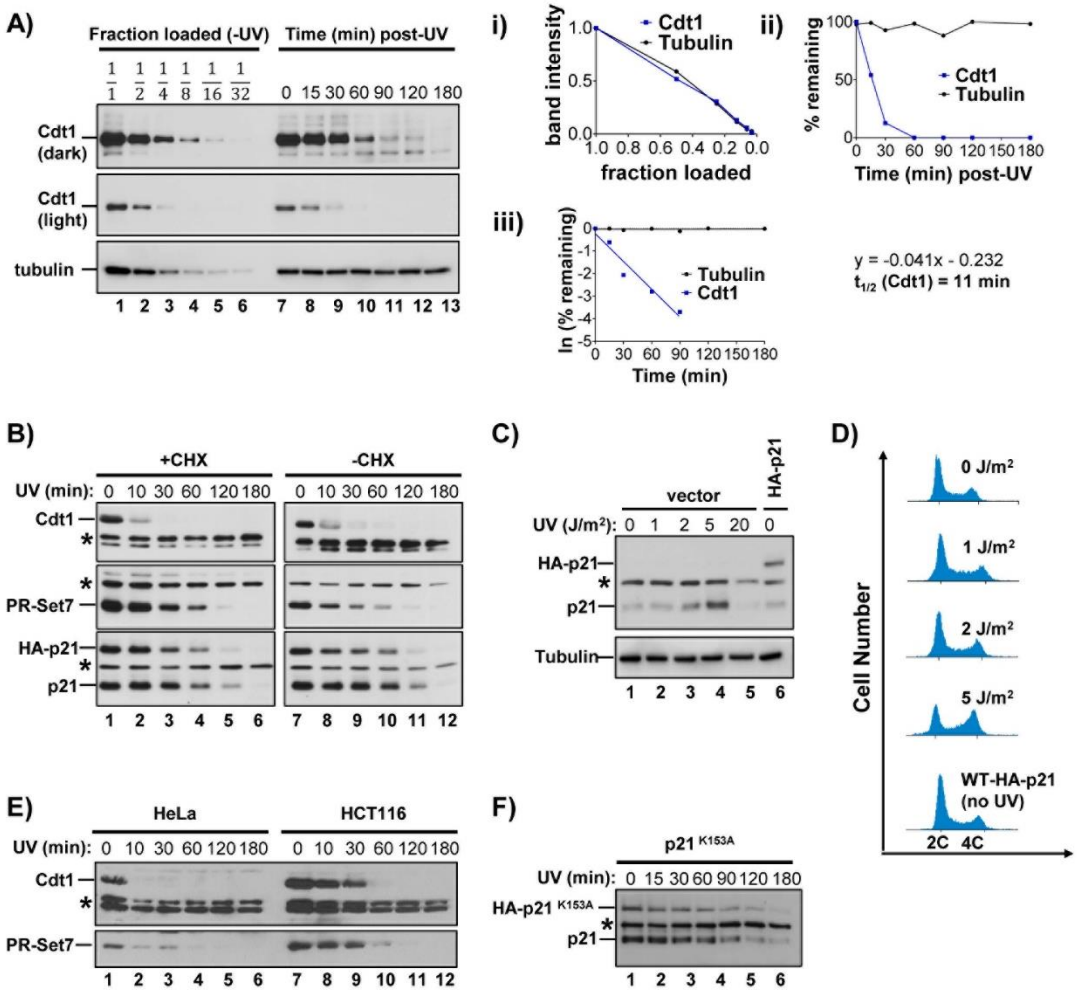

Figure 2.5. p21 protein degradation is independent of DNA damage-inducible expression. (A). Example of semi-quantitative immunoblot analysis of substrate degradation kinetics. (Lanes 1-6, (i): Two-fold serial dilutions of HCT116 cell lysate were immunoblotted for endogenous Cdt1 and tubulin (light and dark exposures are shown). Lanes 7-12, (ii): HCT116 cells were irradiated with 20 J/m^2 UV, harvested at the indicated time points, and probed for endogenous Cdt1 and tubulin. Band intensities from multiple exposures were used to generate graphs of lysate loaded (i) and Cdt1 degradation (ii). (iii) Semi-log plot of % remaining values used for half-life determinations. (B) HCT116 cells were subjected to 20 J/m^2 UV and treated with cycloheximide (10 µg/ml) immediately after irradiation (lanes 1-6) or left untreated (lanes 7-12). Cells were harvested at the indicated time points for immunoblot analysis. (C) Asynchronous HCT116 cells were treated with the indicated doses of UV and collected after 24 h for immunoblot analysis. (D) Cells treated as in (C) were analyzed by flow cytometry for DNA content. HCT116 cells stably expressing wild-type HA-tagged p21 used in Figure 4A are included for comparison. (E) HeLa cells were subjected to a UV time-course and compared to HCT116 cells. (F) HCT116 cells expressing ectopic HA-p21 deficient for TRIM39 binding (K153A) were treated with 20 J/m^2 and harvested at the indicated time-points for immunoblot analysis of ectopic and endogenous p21 levels.

Figure 2.6.

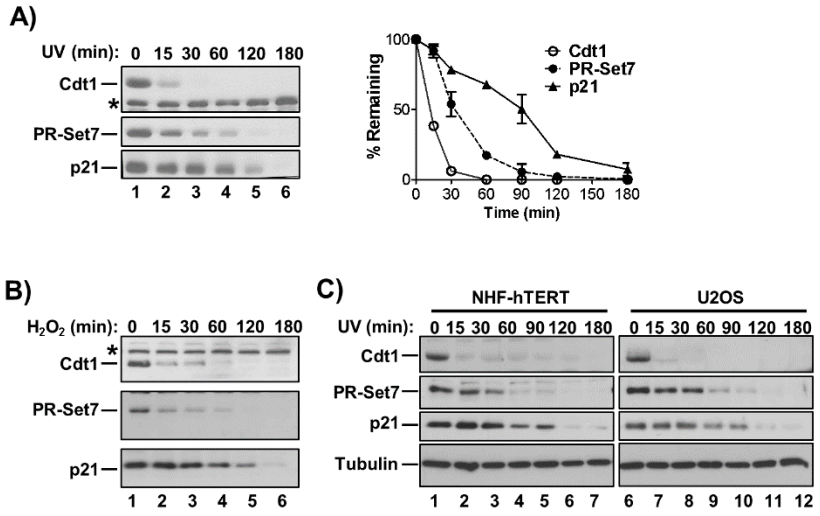

Figure 2.6. CRL4^{Cdt2} substrates are degraded sequentially during DNA repair synthesis. HCT116 cells were treated with (A) 20 J/m^2 UV or (B) 100 μM tert-butyl peroxide and harvested at the indicated times after treatment for immunoblot analysis. Non-specific bands serving as loading controls are indicated by asterisks (*). Quantifications of immunoblots from a minimum of three biological replicates of the UV time course are plotted. (C) NHF-hTERT cells (lanes 1-7) or U2OS cells (lanes 8-14) were treated with 20 J/m^2 UV and harvested at the indicated time points as in (A). Error bars indicate standard error of the mean (SEM).

(Senga et al. 2006; Rizzardi et al. 2014). Given our finding that Cdt1 is consistently the most rapidly degraded among the $CRL4^{Cdt2}$ substrates tested, we sought to determine if the Cdt1 PIP degron is sufficient to confer the fast kinetics of degradation. We therefore fused Cdt1 1-28 to the N-terminus of an epitope-tagged p21 and compared this fusion to a correspondingly epitope-tagged WT p21. We generated stable HCT116 cell lines producing these fusions at near-endogenous levels and utilized the same UV irradiation strategy to induce synchronous replication-coupled destruction as in **Figure 2.6**. Firstly, the addition of an N-terminal HA epitope tag to p21 had no measureable effect on degradation kinetics; both endogenous and tagged p21 were degraded at the same rate and substantially slower than endogenous Cdt1 **(Figure 2.7A)**. Second, constitutive expression of HA-p21 from a heterologous promoter had no effect on p21 degradation kinetics **(Figure 2.5B and Figure 2.7A)** and did not alter cell cycle phase distribution **(Figure 2.5C lane 6 and 2.5D**). Strikingly however, the PIP^{Cdt1}-p21 chimera was degraded much more rapidly than either WT p21 or endogenous p21, and this chimeric protein more closely resembled the degradation kinetics of endogenous Cdt1 with a half-life of just 20 min **(Figure 2.7B)**. A PIP^{Cdt1}-p21 chimera in which key amino acids of the Cdt1 PIP degron were mutated to alanine ($PIPm^{Cdt1}$-p21) was degraded with kinetics similar to both WT HA-p21 and endogenous p21 as expected **(Figure 2.7C)**. Thus, addition of the Cdt1 PIP degron to the N-terminus of p21 is sufficient to confer accelerated p21 degradation.

We considered several explanations for the rapid degradation of the PIP^{Cdt1}-p21 fusion: the addition of a second PIP degron, the N-terminal location of the PIP degron, or the PIP degron sequence itself. To test the idea that rapid degradation is achieved simply by the presence of two degrons, we disrupted the native p21 PIP degron sequence in the PIP^{Cdt1}-p21 chimera leaving only the one Cdt1 PIP degron ,"PIP^{Cdt1}-p21PIPm". We confirmed p21 PIP degron impairment in a control experiment **(Figure 2.8A and 2.8B)**. The PIP^{Cdt1}-p21PIPm fusion was still degraded faster than endogenous p21 **(Figure 2.7D)**, indicating

that the presence of two degron sequences did not account for the accelerated degradation of the PIP^{Cdt1}-p21 fusion in **Figure 2.7B**. The native PIP degron sequences of Cdt1 and p21 are located at either the N- or C-terminus of each protein respectively; thus, the relative location of the PIP degrons could impact accessibility to PCNA and/or $CRL4^{Cdt2}$. Importantly, when we fused a second copy of p21's PIP degron to its own N-terminus, this PIP^{p21}-p21 fusion was degraded slowly like endogenous p21 **(Figure 2.7E)**. Finally, we fused the p21 PIP degron to an HA-tagged form of Cdt1 lacking its own native PIP degron. We confirmed that the tag did not disrupt WT Cdt1 degradation kinetics **(Figure 2.7F)** and that deleting Cdt1's PIP degron stabilized Cdt1 independently **(Figure 2.8C)**. Cdt1 bearing a single PIP degron derived from p21 was degraded more slowly than WT Cdt1, particularly at later time points **(Figure 2.7F)**. These experiments yield several important mechanistic insights: the PIP degron sequence itself carries intrinsic and transferable information dictating the degradation kinetics, the location of the PIP degron sequence has little impact on degradation kinetics, and an additional PIP degron sequence is insufficient to enhance the degradation rate.

The accelerated degradation of the PIP^{Cdt1}-p21 fusion during DNA repair suggested that a similar fusion would be degraded with faster kinetics in early S phase since the same ubiquitylation pathway applies to both S phase and DNA repair. To test that idea, we fused YFP to the C-terminus of PIP^{Cdt1}-containing p21 and integrated this doxycycline-inducible fusion into U2OS cells expressing histone H2B-mCherry. As a control we integrated a YFP-p21 fusion to create a separate cell line. The arrangement of these fusions was designed to avoid perturbing the relevant PIP degrons. Of note, high concentrations of doxycycline induced substantial p21 overproduction and G1 accumulation indicating that both fusions are likely active CDK inhibitors **(Figures 2.9A and 2.9B),** but cells can tolerate moderate p21 overproduction (e.g. from induction with 10-30 ng/ml) with no detectable change in in cell cycle phase distribution **(Figure 2.9B).** Moreover, the UV-triggered degradation of

Figure 2.7.

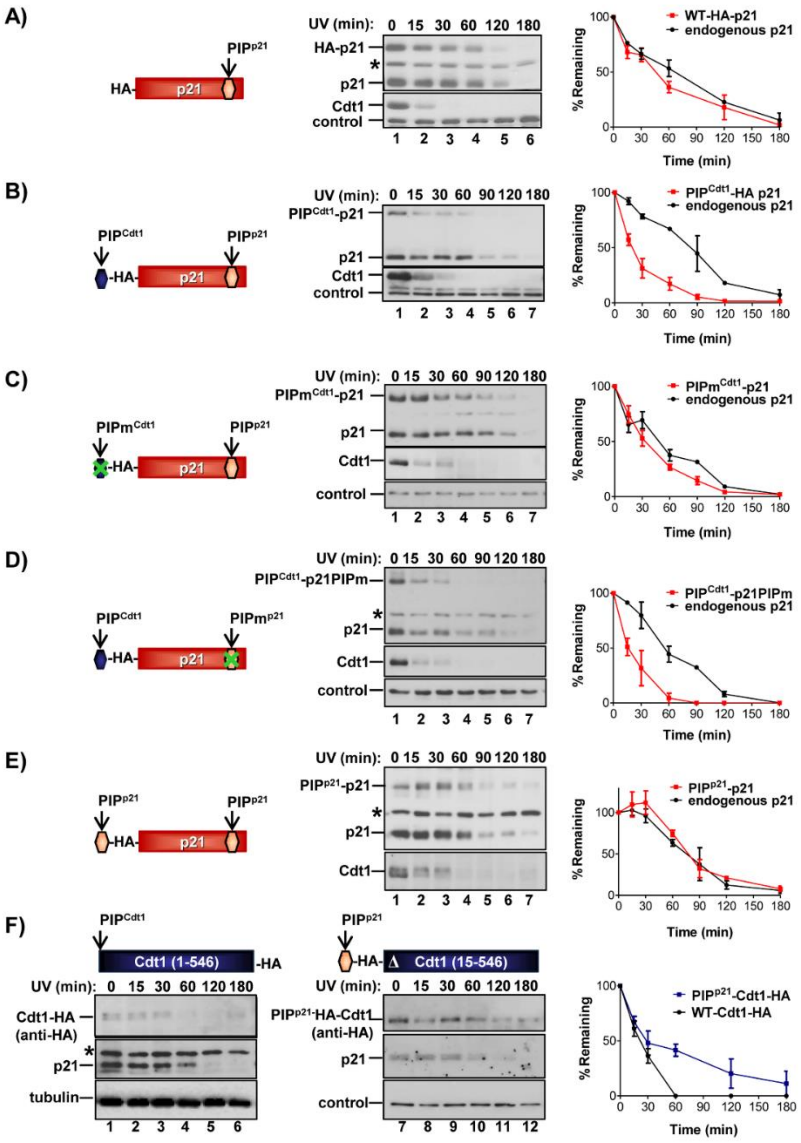

Figure 2.7. The Cdt1 PIP degron confers accelerated degradation to p21 during DNA repair. (A) HCT116 cell lines were generated that stably produce (A) HA-tagged WT-p21, (B) HA-tagged PIP^{Cdt1}-p21, (C) HA-tagged $PIPm^{Cdt1}$-p21 bearing inactivating mutations in the Cdt1 PIP degron, (D) HA-tagged PIP^{Cdt1}-p21 fusion with the native p21 PIP degron inactivated, or (E) PIP^{p21}-p21 with the native p21 PIP degron added to the N-terminus. (F) HA-tagged WT Cdt1 or Cdt1 lacking its native PIP degron ("Δ") but fused to the p21 PIP degron was expressed from an inducible promoter in U2OS cells with 20 ng/ml doxycycline.. These cell populations were treated with 20 J/m^2 UV and harvested at the indicated times for immunoblot analysis. Quantifications of immunoblots for ectopic and endogenous p21 and Cdt1 proteins are from two independent experiments; error bars indicate SEM.

Figure 2.8.

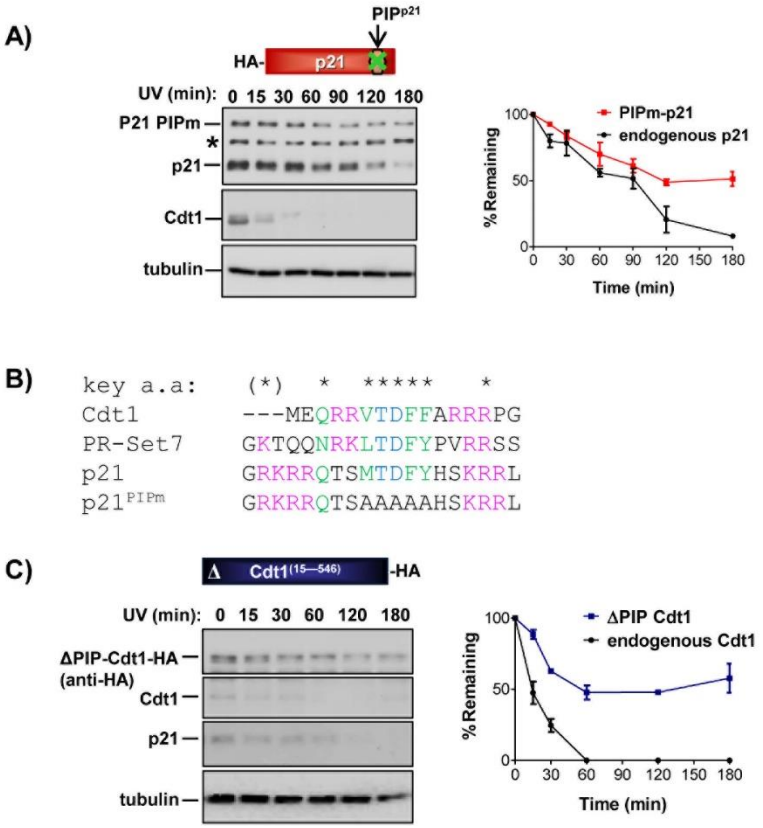

Figure 2.8. Mutation of PIP degron sequences impairs CRL4^{Cdt2}-mediated proteolysis. (A) Cells expressing ectopic HA-tagged p21 bearing alanine substitutions in p21 amino acids 146-150 were treated with 20 J/m^2 UV and harvested at the indicated time-points for immunoblot analysis. (B) Alignment of the PIP degron sequences from human Cdt1, PR-Set7, and p21. Basic residues are in magenta, hydrophobic residues in green, and the conserved T and D common to PIP degrons are in blue. (C) Cdt1 15-546 lacking the native PIP degron and tagged at the C-terminus was expressed from a doxycycline-inducible promoter in U2OS cells (20 ng/ml doxycycline), then analyzed as in A.

PIP^{Cdt1}- p21-YFP was accelerated compared to normal YFP- p21 or endogenous p21 similar to the HA-tagged fusions in Figure 2.7B **(Figure 2.9C).**

We induced expression of both p21 fusions to similar levels (10 ng/ml for WT and 30 ng/ml for PIP^{Cdt1}-p21) and imaged unperturbed proliferating cells for at least 16 hours, capturing fluorescence images of histone H2B-mCherry and YFP-p21 every ten minutes **(representative Supplementary videos 1 and 2)**. We subjected the videos to computational segmentation using the histone H2B-mCherry to mark and track nuclei and then automatically quantified the average fluorescence intensity of YFP in both lines **(see Methods)**. Each set of fluorescence intensities was normalized from zero (minimum) to 1 (maximum) for 50 cells that we selected for expression of the fusion and that underwent both mitosis and a complete degradation/re-accumulation cycle (i.e. S phase) within the recorded time. The dynamics of YFP-p21 degradation are shown for these cells as a heat map in **Figure 2.10A** with the first data point plotted for each cell corresponding to the video frame containing the cell division that produced that cell. Fitting these *in silico* aligned traces for each cell to an inverse sigmoidal curve yielded T_d, the time from mitosis to the half-point of degradation **(Figure 2.10B)**. We then calculated the relative maximal rates of degradation from the slopes at each T_d and noted that the degradation rate of the PIP^{Cdt1}-containing fusion was more than 5 times that of the fusion bearing only the native p21 PIP degron.

Differential recruitment of PCNA/Cdt2 by PIP degrons

We next generated new degron fusions in which either the Cdt1 or p21 PIP degron plus a nuclear localization signal (NLS) was fused to glutathione-S-transferase (GST). These fusions created an artificial substrate for replication-coupled CRL4^{Cdt2}-mediated proteolysis and had the added benefit of isolating the Cdt1 and p21 PIP degrons from their respective full-length proteins **(Figure 2.11A)**. We monitored the degradation kinetics of the GST

fusions after UV irradiation as before and found that PIP^{p21}-GST was degraded more slowly than PIP^{Cdt1}-GST, similar to the relationship between the endogenous proteins from which they were derived **(Figure 2.11A)**.

Two critical interactions for productive replication-coupled destruction are binding of the PIP degron to DNA-loaded PCNA ($PCNA^{DNA}$) and subsequent recruitment of CRL4 through substrate interaction with the substrate receptor, Cdt2. Differences in affinities for $PCNA^{DNA}$ and/or Cdt2 could explain why proteins containing the Cdt1 PIP degron are consistently degraded before proteins with the p21 PIP degron. To test this idea, we produced the same PIP^{Cdt1}-GST and PIP^{p21}-GST constructs in bacteria, isolated the recombinant proteins on glutathione beads and used them to retrieve $PCNA^{DNA}$ and Cdt2 from sonicated chromatin fractions of human cell lysates. We had previously used this strategy to analyze interactions of full-length Cdt1 with $PCNA^{DNA}$ and Cdt2 (Chandrasekaran et al. 2011). As controls we included a full-length GST-tagged p21 and a PIP mutant form of p21 which cannot bind PCNA, PIP_mp21-GST (Rizzardi et al. 2014). As expected, the PIP mutant p21, unlike the WT p21, did not bind $PCNA^{DNA}$ **(Figure 2.12)**.

First, although equal amounts of solubilized chromatin were incubated with the two PIP degron fusions, the p21 PIP degron retrieved approximately three times more PCNA than the Cdt1 PIP degron did under the same conditions **(Figure 2.11B, compare lanes 3 and 4)**. This tight binding of p21 to PCNA is consistent with prior studies (Arias and Walter 2006; Gulbis et al. 1996). Surprisingly, even with this strong relative binding to PCNA, the p21 PIP degron did not recruit proportionately more Cdt2 **(Figure 2.11B, compare lanes 3 and 4).** In fact, PIP^{Cdt1}-GST retrieved more Cdt2 than PIP^{p21}-GST did, despite holding 3-fold less $PCNA^{DNA}$ **(Figure 2.11B, lanes 3 and 4)**. The significantly better Cdt2 binding with PIP^{Cdt1} GST was most readily apparent when we directly compared equal levels of co-purified PCNA; PIP^{Cdt1}-GST bound more than 5-fold more Cdt2 than PIP^{p21}-GST did for the same amount of co-purified PCNA **(lanes 3 and 4, Figure 2.11C and D)**. Thus, the Cdt1 PIP

Figure 2.9.

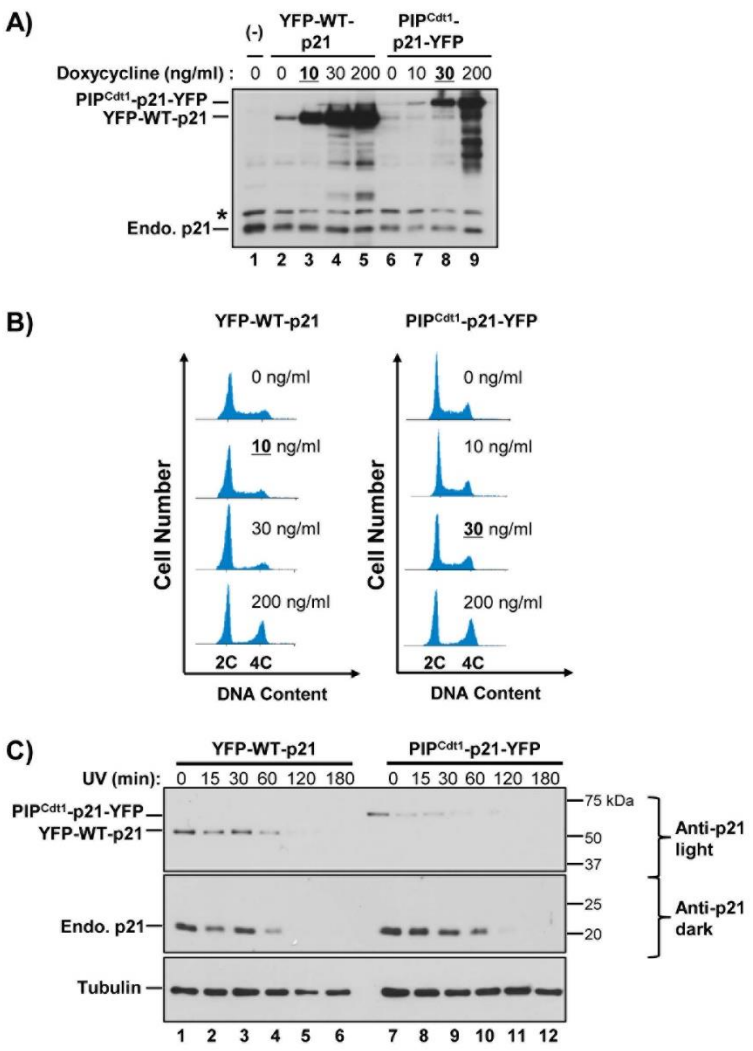

Figure 2.9. Validated YFP-p21 and PIP^{Cdt1}-p21-YFP fusion regulation and function. (A) Asynchronous U2OS cells expressing either YFP (Venus)-p21 or PIPCdt1-p21-YFP fusions were induced with the indicated concentrations of doxycycline and then subjected to anti-p21 immunoblot analysis. (* indicates a non-specific band that serves as a loading control.) (B) Flow cytometry analysis of DNA content of cells expressing YFP fusion proteins shown in (A). Doxycycline concentrations of each cell line used in the imaging analysis in Figure 5 are underlined. (C) Asynchronous U2OS cells expressing either YFP-p21 or PIP^{Cdt1}-p21-YFP proteins (induced with 20 ng/ml doxycycline) were treated with 20 J/m^2 UV and collected at the indicated times for immunoblot analysis.

Figure 2.10.

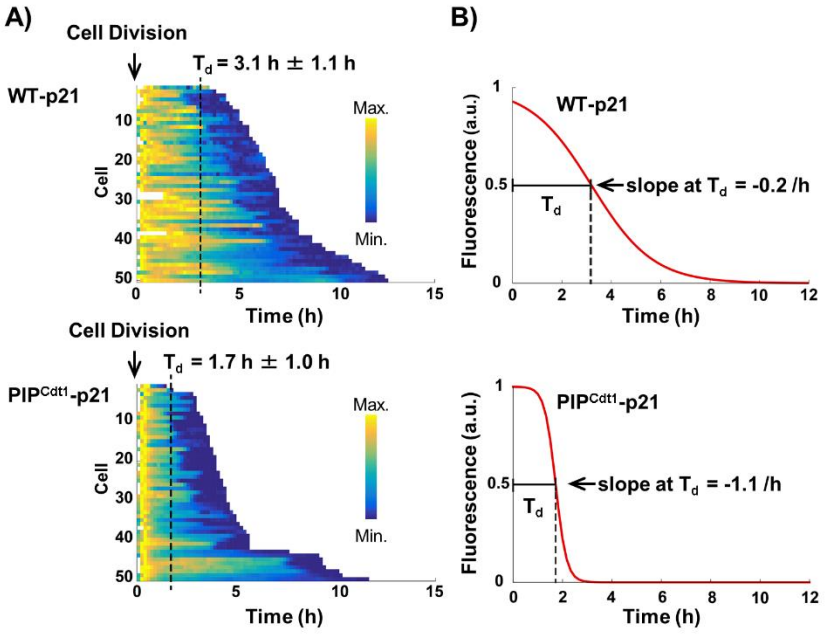

Figure 2.10. The Cdt1 PIP degron confers accelerated degradation to p21 at G1/S. (A) Heat maps for the kinetics of YFP-p21 and PIP^{Cdt1}-p21-YFP degradation in 50 asynchronously proliferating cells generated by high content live cell imaging. Expression was induced with 30 ng/ml doxycycline for YFP-WT-p21 and 10 ng/ml doxycycline for PIP^{Cdt1}-p21-YFP (see Supplementary Figure 5) and individual cell fluorescence intensity traces were computationally aligned to mitosis (t=0). Fluorescence intensities were normalized to individual minima and maxima (see Methods). (B) Data were fit to sigmoidal curves, and the average time for degradation from mitosis to the half minimum fluorescence intensity, "T_d," is marked with black dashed lines on both the heat maps and the plots. The slopes at T_d are indicated.

Figure 2.11.

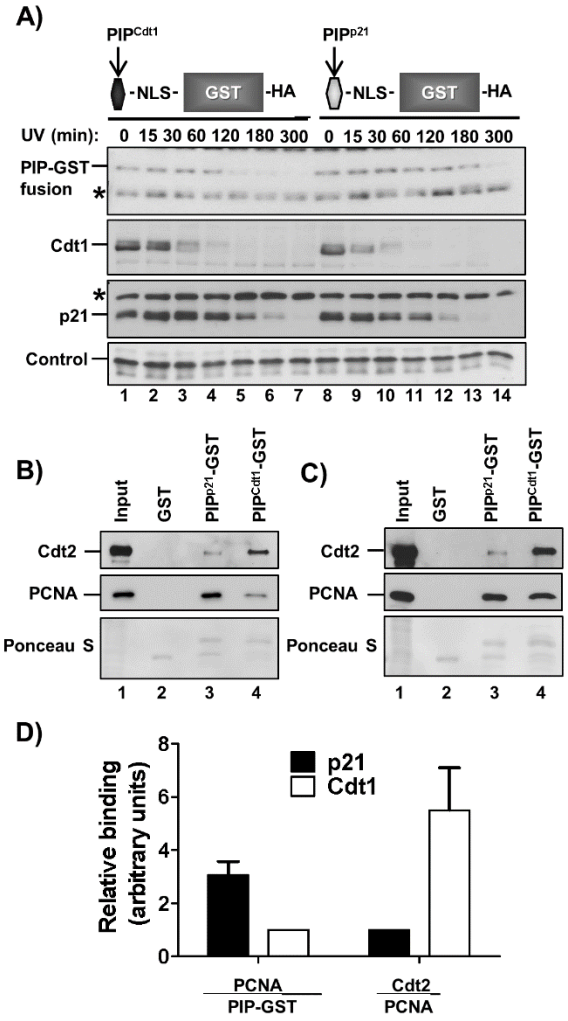

Figure 2.11. The Cdt1 PIP degron binds more Cdt2 than the p21 PIP degron. (A) HCT116 cells stably expressing either Cdt1 PIP (aa 1-28) or p21 PIP (aa 137-164) fused to the N-terminus of GST were UV-treated and harvested for immunoblot analysis at the indicated times. (B) PIP-GST fusion proteins were purified from *E.coli* lysates with glutathione-sepharose beads and incubated with sonicated chromatin fractions from UV-irradiated 293T cells. Bound proteins were eluted in 2X SDS buffer and subjected to immunoblot analysis with the indicated antibodies. Lanes 2-4 contained equivalent amounts of GST fusions. (C) PIP degron-bound proteins were prepared as in (B), but loaded equivalently for co-purified PCNA. (D) Quantification of the relative amounts of bound PCNA and Cdt2, based on two independent experiments; error bars indicate standard deviations.

Figure 2.12.

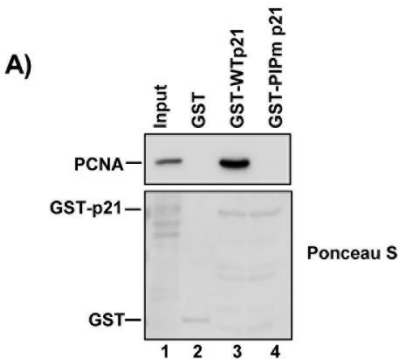

Figure 2.12. p21^{PIPm} (PIP degron mutant) fails to bind PCNA^{DNA}. (A) The indicated GST fusion proteins were purified from *E.coli* lysates with glutathione-sepharose beads and incubated with sonicated chromatin fractions from UV-irradiated 293T cells. Bound proteins were eluted in 2X SDS buffer and subjected to immunoblot analysis after normalizing for bound GST. (B) Alignment of PIP degron sequences from human Cdt1, PR-Set7, p21 and p21^{PIPm}. Positions previously shown to be important for CRL4^{Cdt2}-mediated degradation are shown in red.

degron more efficiently recruits Cdt2, and this effect likely contributes to its accelerated degradation via the $CRL4^{Cdt2}$ E3 ubiquitin ligase.

We also considered a potential role for ubiquitin E2 utilization in the differential degradation of Cdt1 and p21. Ubiquitylation by cullin E3 ligases is catalyzed by associated E2 ubiquitin-conjugating enzymes (UBCs), and our recent study showed that ubiquitylation of p21 and Cdt1 is carried out by different E2s: UBE2G1+UBE2G2 for Cdt1 and UBCH8 for p21 (Shibata et al. 2011). Different E2s may be responsible for the different degradation rates and further, exchanging the PIP degrons might have led to E2 switching. To test this hypothesis, we used RNAi-mediated depletion of the relevant E2s to determine if thePIP^{Cdt1}-p21 fusion **(diagramed in Figure 2.7B)** relies on the E2 that normally targets Cdt1 (i.e. UBE2G1+UBE2G2). As shown in **Figure 2.13A and 2.13B** however, the PIP^{Cdt1}-p21 fusion, just like endogenous p21, was stabilized in UBCH8-depleted cells, whereas its typical accelerated degradation pattern was observed in both control and UBE2G1+UBE2G2-depleted cells. Thus, we concluded that degradation of PIP^{Cdt1}-p21 still involves the same E2 as normal p21, arguing against an E2 switch. Substrate features separate from those directly responsible for E3 recruitment must control E2 specificity, but that discrimination plays little role in the rate of $CRL4^{Cdt2}$-mediated degradation.

Delayed p21 degradation facilitates normal S phase progression.

We next sought to probe the physiological importance of sequential $CRL4^{Cdt2}$ substrate degradation. Specifically we tested the consequences of imposing the early Cdt1 degradation pattern on p21. For this purpose, we stably produced siRNA-resistant versions of the PIP^{Cdt1}-p21 and WT-p21 described in **Figure 2.7** in HCT116 cells. We depleted endogenous p21 and analyzed cell cycle profiles by flow cytometric measurement of BrdU incorporation and DNA content **(Figure 2.14A).** Neither siRNA depletion of p21, nor stable expression of WT-p21 had a substantial effect on overall cell cycle distribution in these cells

Figure 2.13.

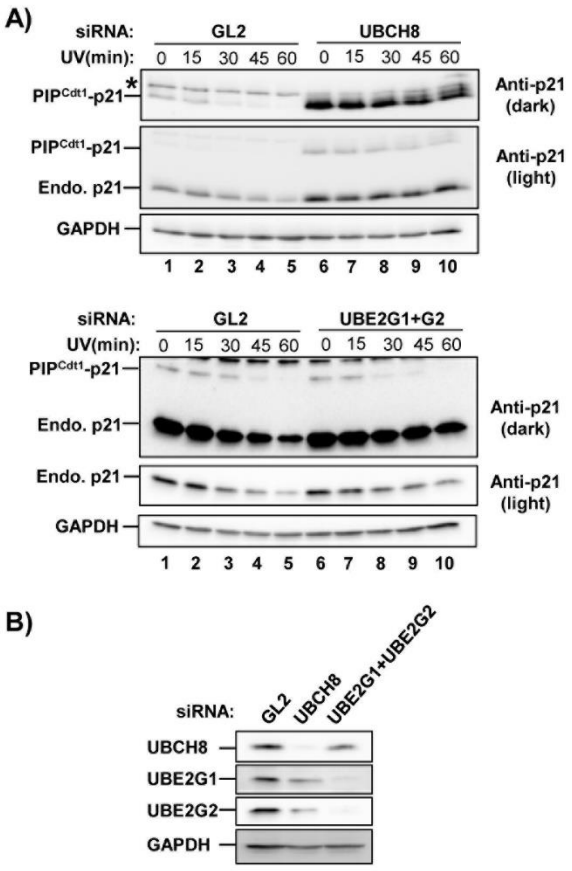

Figure 2.13. The Cdt1 PIP degron fused to p21 is still a substrate for the p21-specific E2 (UBCH8). (A) HCT116 stably expressing PIP^{Cdt1}-p21 were depleted of UBCH8 or UBE2G1 +UBE2G2 as in Shibata et al. 2011. Cells were treated with cycloheximide for 10 min before 20 J/m^2 UV irradiation, collected at the indicated times after UV treatment and then analyzed for ectopic and endogenous p21 by immunoblotting; GAPDH serves as a loading control. (B) Immunoblot analysis of siRNA transfected cells to assess E2 depletion.

(Figure 2.14B), but we noted that p21 depletion caused an increase in a sub-population of cells of intermediate DNA content (i.e. S phase) that were not actively synthesizing DNA. We scored this population as "BrdU^{neg} /S phase", and following p21 depletion, there were 3x more BrdU^{neg}/S phase cells compared to control cells. This phenotype was complemented by ectopic WT-p21 (without causing cell cycle arrest), but strikingly PIP^{Cdt1}-p21 cells still generated the BrdU^{neg} /S phase subpopulation **(Figure 2.14A and 2.14B)**. PIP^{Cdt1}-p21 was produced at levels similar to endogenous p21 in control RNA-treated cells which suggests that the phenotype of the PIP^{Cdt1}-p21 line is the kinetics of p21 degradation rather than insufficient p21 **(Figure 2.14C).**

The increase in cells that reached mid-S phase but then stopped DNA synthesis (BrdU^{neg} /S phase) suggested that premature p21 degradation leads to difficulty in maintaining active replication. If true, then these cells may experience higher than normal rates of endogenous DNA damage which could render them more sensitive to additional damage or replication stress. To test that idea more directly, we produced the same p21 fusions as YFP-tagged forms **(i.e. Figure 2.10)** in U2OS cells and then challenged them to recover from a strong replication block. We depleted endogenous p21 **(Figure 2.15A)**, and then held cells in hydroxyurea for 16 h to induce replication stalling. We immunostained for a marker of DNA damage often associated with replication stress, γ-H2AX, and found the expected high percentage of positively-staining cells in all HU-arrested populations (Figure 7D and E). Releasing cells into fresh medium allowed S phase resumption within 12 h in cells expressing normal p21 as measured by both flow cytometry **(Figure 2.15B)** and elimination of γ-H2AX foci **(Figure 2.14D and 2.14E)**. In contrast to both siRNA controls and p21-depleted cells complemented with WT-p21 however, p21-depletion caused 2-fold more retention of γ-H2AX signal 12 h after HU release **(Figure 2.14D 12 h, and 2.14E)**. Strikingly, cells expressing PIP^{Cdt1}-p21 to similar levels as WT-p21 **(Figure 2.15A)** retained as much

Figure 2.14.

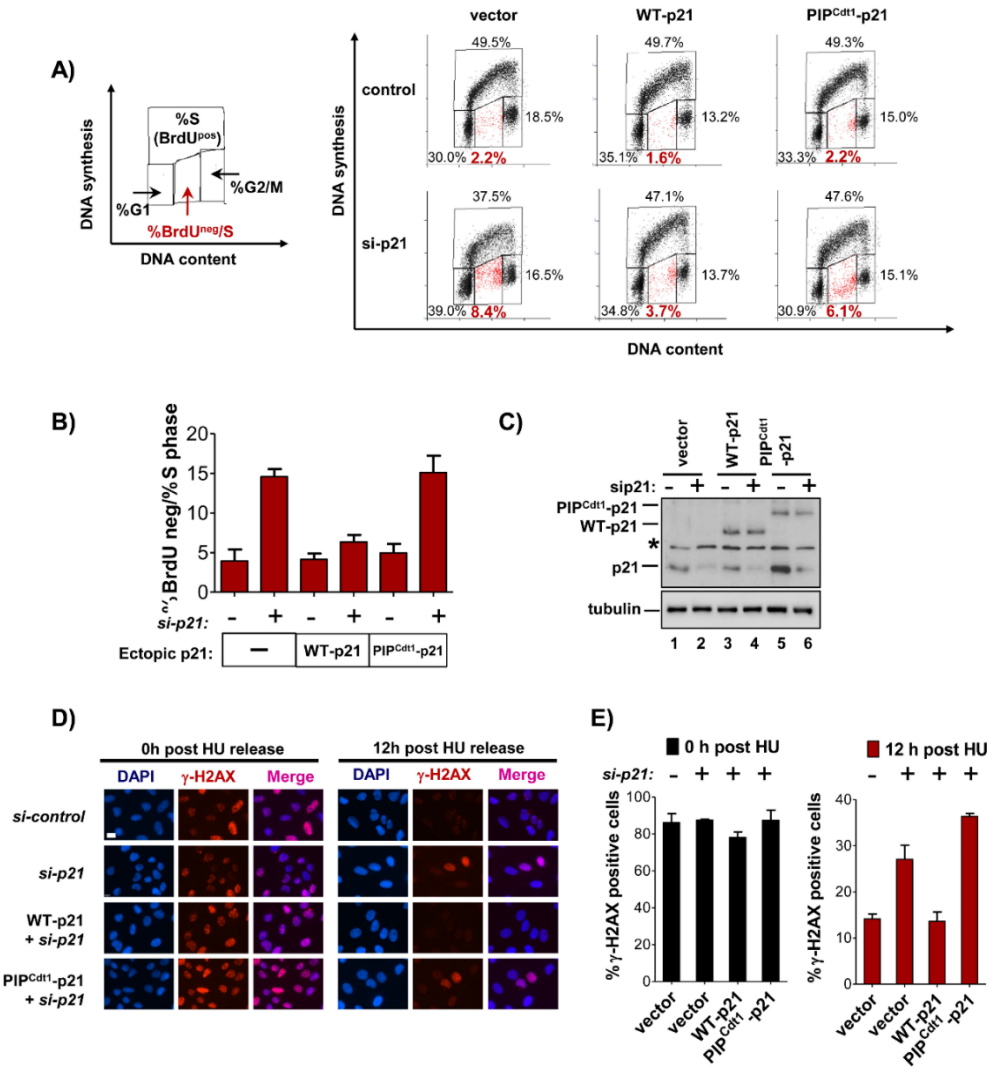

Figure 2.14. Accelerating p21 degradation promotes replication stress. (A) Asynchronously growing HCT116 cell lines stably-expressing the indicated HA-tagged p21 fusions were treated with 100 nM of control or p21 siRNA for 48 h. Cells were labeled for 1 h with BrdU and analyzed by flow cytometry with anti-BrdU antibody to detect DNA synthesis (y-axis) and with propidium iodide for DNA content (x-axis). Flow cytometry gating for distinguishing BrdU negative S phase cells is indicated in the schematic. Percentage of the total population in each gated cell cycle phase is indicated on the plots. (B) Percentage of BrdU negative/S phase cells in samples from (B); error bars indicated standard error of the mean. (C) Immunoblots of endogenous and ectopic p21 in (B). (D) U2OS cells producing the indicated p21-YFP fusions (induced with 10 ng/ml doxycycline) were treated with 2 mM HU for 16 h and subsequently released into fresh medium for 12 h, as indicated. Representative images (D) show γ-H2AX staining of cells for each condition, and the percentage of γ-H2AX positive cells is quantified in (E). Scale bar = 30 μm. For quantifications > 200 nuclei from randomly-selected fields were counted for each condition, and error bars represent standard deviations from two independent experiments. p=<0.05

Figure 2.15.

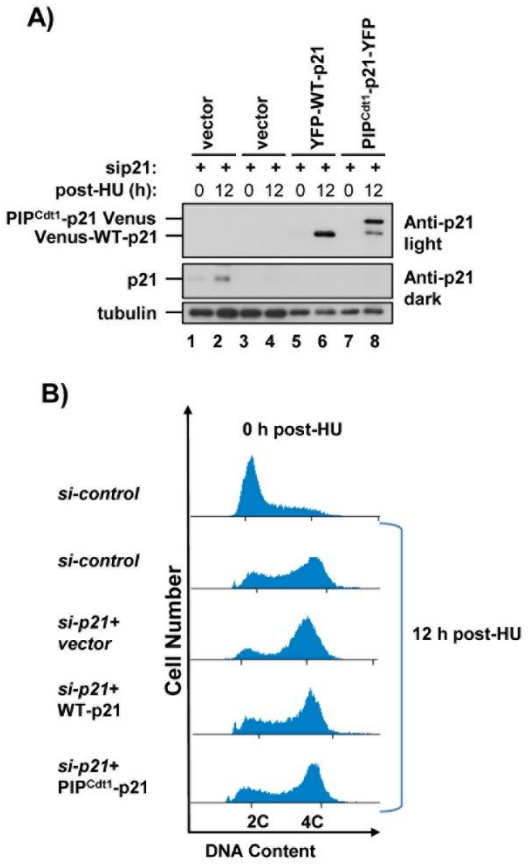

Figure 2.15. HU-mediated replication-coupled destruction and recovery. A) Immunoblot and (B) flow cytometry analysis of samples from HU arrest and release experiment in Figure 7D. Cells were treated with 100 nM siRNA and 10 ng/ml doxycycline as indicated.

γ-H2AX signal as p21-depleted cells did **(Figure 2.14C and D)**. Altogether, these results indicate that the normal delayed p21 degradation in early S phase contributes to robust replication progression during S phase. Furthermore, the absence of p21 during early S phase sensitizes cells to subsequent replication stress and DNA damage.

Discussion

In this study we provide conclusive evidence that despite being subject to the same targeting mechanism, several substrates of the $CRL4^{Cdt2}$ E3 ubiquitin ligase are degraded in a conserved and stereotypical order. In particular, p21 degradation is significantly delayed relative to Cdt1 (and PR-Set7) both during early S phase and during DNA repair. As a result, early S phase cells and cells beginning DNA repair lack Cdt1 but still have abundant p21. Several other studies (Nishitani et al. 2008; Shibata et al. 2011; Bendjennat et al. 2003; Zhang et al. 2013; Abbas et al. 2008, 2010) explored $CRL4^{Cdt2}$ substrate degradation kinetics, and late p21 degradation is detectable in those studies but had not been investigated. We note also that these three proteins appear to re-accumulate at the end of S phase in reverse order relative to the order in which they are degraded (Nishitani et al. 2008; Rizzardi et al. 2014; Abbas et al. 2010).

Based on our observations, early Cdt1 degradation relative to p21 in S phase is likely due to differences in the efficiency with which different PIP degrons recruit Cdt2 **(Figure 2.16A)**. It is not yet clear however why the Cdt1 PIP degron confers weaker PCNA binding but more efficient Cdt2 recruitment. Detailed structural information about the interaction of p21's PIP degron with PCNA is available (Gulbis et al. 1996), and a collection of alanine substitutions at sites critical for PCNA binding or Cdt2 recruitment block replication-coupled destruction (Arias and Walter 2006; Havens and Walter 2009). Interestingly however, none of those previously-studied positions are significantly different between the p21 and Cdt1 PIP degrons **(Figure 2.8B)**. We presume that the substantially more efficient *in vitro* Cdt2

recruitment by the Cdt1 PIP degron is the major reason for faster Cdt1 degradation *in vivo*, but other mechanisms may also contribute. Among these factors are differences in ubiquitylation processivity as is observed among substrates of the APC/C (Rape et al. 2006). Strikingly, p21's PIP degron binds $PCNA^{DNA}$ *in vitro* more efficiently than Cdt1's PIP degron does **(Figure 2.11).** It is possible that the p21-$PCNA^{DNA}$ interaction is in fact too tight for maximally-efficient degradation compared to other $CRL4^{Cdt2}$ substrates, but this idea has not yet been explored. Tight PCNA binding by p21 has been suggested to compete with other PCNA binding proteins (Warbrick et al. 1997; Ducoux et al. 2001; Arias and Walter 2006), and so we have considered the possibility that competition among PIP degrons contributes to their order of degradation. We have not observed however any evidence for competition effects at either the endogenous levels of $CRL4^{Cdt2}$ substrates or when they are moderately overproduced. For example the ~2-fold increase in PIP degron from the ectopic fusions in **Figure 2.7A** and **2.7B** had no effect on the rates of endogenous Cdt1 and p21 degradation. Thus we do not favor a model in which the higher affinity of Cdt2 for Cdt1 leads to slower p21 degradation strictly through competition for either PCNA or Cdt2.

By fusing Cdt1's PIP degron to p21, we created a scenario in which p21 is expressed in G1 but degraded prematurely at the beginning of S phase rather than at the normal time well after S phase is underway. Interestingly, the consequences of accelerating the timing of p21 degradation are very similar to depleting cells of p21 altogether with respect to replication stress. The striking similarity of cells expressing the PIP^{Cdt1}-p21 fusion to p21-depleted cells indicates that a critical period for p21 expression is early S phase since PIP^{Cdt1}-p21 cells have sufficient p21 in G1. Cells lacking p21 in early S showed both an increase in the proportion of cells that failed S phase and a reduced ability to recover from a strong replication block. Particularly with respect to the increase in $BrdU^{neg}$ /S phase cells, we were initially surprised to observe what appeared to be a mid-to-late S phase phenotype since mid-S phase cells have already degraded p21. In addition, the recovery from an HU

block seems unrelated to the degradation rates of the p21 fusions during the arrest since both are degraded at 0 h. We consider however that these phenotypes are a downstream consequence of insufficient p21 in early S phase leading to overall higher levels of endogenous damage prior to or during the HU block and a longer recovery time. Even in the absence of HU treatment, we observed a small (though not statistically significant) increase in γ-H2AX positive proliferating cells expressing only the prematurely degraded p21 (data not shown). The combination of preexisting replication stress with an HU challenge could account for the poor recovery from replication arrest.

Our findings suggest a model for the need to degrade Cdt1 at the very beginning of S phase but delay p21 degradation until later in S phase **(Figure 2.16B).** In normal cells Cdk2 activity begins to rise in late G1 due to the increase in cyclin E, but p21 is still present **(Figure 2.1).** Once S phase begins and PCNA is loaded at early-firing origins, the continued presence of p21 restrains S phase progression by slowing the rise of Cdk2 activity. In this model, early S phase cells have lower total Cdk2 activity than mid-S cells but the intermediate Cdk2 activity supports some origin firing and PCNA loading. During this early S phase period, Cdt1 is rapidly degraded to prevent origin re-licensing and re-replication. This rapid degradation may be particularly important because two of the blocks to re-replication, the geminin inhibitor protein and cyclin A, are lower in early S phase than when they reach maximal levels later in S (Wohlschlegel et al. 2000; Girard et al. 1991; Rosenblatt et al. 1992). If p21 is degraded prematurely, Cdk2 activity may rise too early leading to more origins firing at the beginning of S phase than normally should, and subsequent replication stress. In support of that notion, manipulations in both yeast and *X. laevis* experimental systems that shift origin firing towards early S phase induce replication stress markers (Woodward et al. 2006; Gibson et al. 2004; Mantiero et al. 2011). Replication fork speed may also be affected by p21 tightly bound to PCNA (Waga et al.,1994). The aggregate of

Figure 2.16.

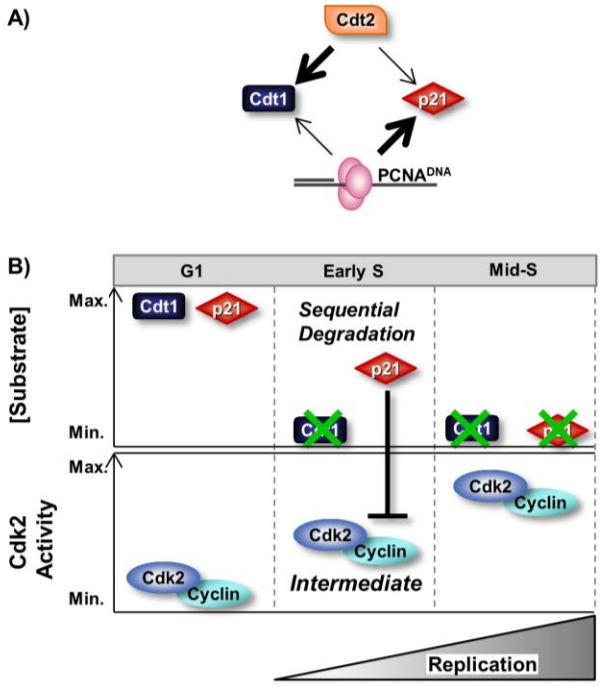

Figure 2.16. Model (A) Despite lower binding affinity for PCNA, the Cdt1 PIP degron recruits more Cdt2 than the p21 PIP degron does. (B) The normal relatively delayed degradation of p21 by $CLR4^{Cdt2}$ permits only intermediate Cdk2 activity in early S phase rather than maximal activity at S phase onset. The more gradual degradation of p21 prevents replication stress (see Discussion).

effects such as these may explain the higher likelihood of S phase failure in cells that prematurely degrade p21. We conclude therefore that some key molecular events at the G1/S transition must happen in a defined order to ensure a normal S phase progression. These findings raise the possibility that many aspects of cell cycle transitions are also programmed to occur in a stereotypical sequence to ensure genome stability.

Materials and Methods

Cell culture and manipulations

HCT116 and HEK 293T cells were obtained from ATCC and cultured in Dulbecco's modified Eagle's medium (DMEM) (Sigma) supplemented with 10% fetal calf serum (Sigma). U2OS TRex cells were a gift from John Aster (Malecki et al. 2006) NHF-hTert cells are normal human fibroblasts immortalized with telomerase. HCT116 cells were synchronized in prometaphase by treatment with 2 mM thymidine for 18 h followed by release into 100 nM nocodazole. To obtain populations of cells in either G1 or early S phase, cells were released from the prometaphase arrest by mitotic shake-off, re-plated in complete medium, and collected at either 2.5 h (G1) or 4 h (early S phase). To arrest replication forks and measure recovery, U2OS cells expressing empty vector, wild-type p21, or PIP^{Cdt1}-p21 were treated with 2 mM hydroxyurea (HU) for 16 h and released into fresh media. UV irradiation experiments were performed using a single dose of 20 J/m^2 in a Stratalinker (Stratagene, La Jolla, CA). Additional DNA damage repair triggers used were 100 µM tert-butyl peroxide (Sigma) and 10 µg/ml bleocin (EMD Millipore). Lentiviral packaging was performed by standard protocols in 293T cells followed by selection with 1 µg/ml puromycin. Synthetic duplexed RNA oligonucleotides were synthesized by Life Technologies; Luciferase (5'- CUUACGCUGAGUACUUCGA-3'); p21-2 (5'-AACAUACUGGCCUGGACUGUU-3'), UBCH8 (5'- GCAAGAACCAGAAAGAGAA-3') UBE2G1 (5'– GGGAAGAUAAGUAUGGUUA-3') UBE2G2 (5'-

UGACGAAAGUGGAGCUAAC-3'). Significance testing utilized the two-tailed Student t test on at least 3 biological replicates.

Antibodies

Antibodies were purchased from the following sources: p21, PCNA, and anti-HA from Santa Cruz; PR-Set7 and Cdt1 from Cell Signaling Technologies, alpha-tubulin, GAPDH, and GST from Sigma, anti-BrdU from BD Biosciences, anti-phospho-Histone H2A.X (Ser139) from EMD Millipore, anti-HA from Roche Life Sciences, anti-UBCH8 and anti-UBE2G1 from Protein tech, and anti-UBE2G2 from Thermo Scientific. Antibodies to human Cdt1 (Cook et al. 2004) and Cdt2 (Abbas et al. 2008) have been described previously. AlexaFluor 488, Rhodamine Red-X, and Cy5 donkey secondary antibodies for immunofluorescence microscopy were obtained from Jackson ImmunoResearch Laboratories.

Plasmids and recombinant protein preparation

For expression in mammalian cells, wild-type (WT) p21, PIP^{Cdt1}-p21, PIP^{Cdt1}-GST, PIP^{p21}-GST, WT Cdt1 bearing an HA epitope tag, Cdt1 15-546-HA ("ΔPIP") , and PIP^{p21}-Cdt1-HA alleles were subcloned into pENTR vectors and subsequently transferred into a retroviral vector, pQCXIP CMV TO/DEST (Campeau et al. 2009) (Addgene ID: # 17386) or to pDESTJC16 or pDESTJC17 by Gateway cloning. K153A mutation in p21 was generated through site-directed mutagenesis. Lentiviral $PIPm^{Cdt1}$-p21, PIP^{Cdt1}-p21PIPm, PIP^{p21}-p21, and PIPm-p21 plasmids were generated by sucloning cDNAs into a pCDH IRES mcherry vector (System Biosciences). pBabe-puro-H2B-mCherry was subcloned from PGK-H2B-mCherry (gift from Mark Mercola, Addgene plasmid # 21217) into pBabe-puro using standard methods. pDESTJC16 and 17 are a derivatives of pcDNA5/FRT/TO-Venus-Flag-Gateway (gift from Jonathon Pines, Addgene plasmid # 40999) in which the hygromycin resistance gene has been replaced with either the puromycin orthe nourseothricin

resistance genes respectively using standard methods. pEXP-JC17- Cdt1-mCerulean3-P2A-Venus-NLS-p21, pEXP-JC17-2HN-Venus, and pEXP-JC17-Venus-NLS-p21 were generated by Gateway cloning from pENTR vectors. Both Venus and mCerulean3 fluorophores were selected for their relative brightness and rapid fluorescence maturation. Plasmids for expressing WT and PIPm-p21 glutathione-S-transferase (GST) fusions were generated by recombinational Gateway cloning (LR clonase, Invitrogen) between pENTR plasmids and pDEST15. Additional plasmids for PIP^{Cdt1}-GST and PIP^{p21}-GST fusions were constructed by subcloning cDNAs into pET11b vector (Novagen). The PIP mutants were generated by site-directed mutagenesis to introduce alanine codons a positions corresponding to Cdt1 amino acids 5 through 8 or p21 amino acids 146-150. PIP degron fusions carried human Cdt1 amino acids 1-28 or human p21 amino acids 137-164. GST fusions were transformed into BL21 (DE3) cells (Invitrogen) and partially purified as described previously (Cook et al. 2004).

Protein lysate preparation

Whole-cell lysates were prepared either by direct lysis of equal cell numbers in 2X Laemmli sample buffer with 10% β-mercaptoethanol or in CSK buffer (Cook et al. 2002) supplemented with 0.1% Triton X-100 and protease and phosphatase inhibitors. Densitometry analysis of immunoblots of lysates was performed using NIH Image J software (normalized to tubulin expression). At least two film exposures were chosen for quantifications of each protein analyzed, such that one lane of each exposure was of equal band intensity and thereby served as a normalization control. Quantifications represent percentages of each protein remaining relative to the starting amount prior to UV irradiation (time=0 min). Half-lives were estimated from semi-log plots of the ln (% remaining) vs time.

GST pull-down assays

Recombinant GST fusion proteins described above were immobilized on glutathione-

sepharose 4B resin (GE Healthcare). UV-irradiated HEK293T cells were lysed in CSK buffer (supplemented with 0.1% Triton-X-100 plus protease and phosphatase inhibitors). Chromatin fractions were prepared as described previously (Cook et al. 2002) and subjected to low-power sonication of Triton-insoluble pellets to fragment DNA-bound material. Soluble chromatin fractions were clarified by centrifugation at 13,000 x g for 15 min at 4°C and incubated with bound GST fusion proteins for 3 h with rotation at 4°C. Beads were washed three times in supplemented CSK buffer and bound proteins were eluted by boiling for 5 minutes in 40 µl 2X SDS sample buffer.

Immunofluorescence microscopy

HCT116 cells synchronized in either G1 or early S phase were pulse-labeled with 50 µM bromodeoxyuridine (BrdU) for 30 min prior to fixation in 2% paraformaldehyde for 15 minutes. DNA was denatured with 1.5 N hydrochloric acid for 15 min. Cells were permeabilized with 0.5% Triton-X-100 for 5 minutes and then blocked in 0.1% BSA for 1 hour. Incubations with primary and fluorescent secondary antibodies were performed in 0.1% BSA for 1 hour at 37°C and washes were for 10 minutes at room temperature. DAPI (4',6-diamidino-2-phenylindole) staining (0.1 µg/ml) was performed for 10 minutes, and cells were mounted using Prolong Gold Antifade Reagent (Life Technologies/Molecular Probes).

For indirect immunofluorescence microscopy, images were acquired using Velocity Software and a 60X/1.42NA (PlanApo) DIC oil immersion objective mounted on a Olympus 1X81 inverted microscope equipped with a Hamamatsu Orca ER cooled CCD camera. For fluorescence intensity measurements, the average values for integrated nuclear Cdt1 and p21 fluorescence from control and experimental cell samples were subjected to background subtraction to obtain the specific nuclear fluorescence levels.

Flow cytometry analysis

Cells to be analyzed by flow cytometry were labeled with 10 μM BrdU for 1 hour prior to trypsinization and fixation in 70% ethanol. Nuclei were stained with anti-BrdU antibody (BD Biosciences) followed by AlexaFluor 488-labeled secondary antibody (Jackson ImmunoResearch) and counterstained with propidium iodide. Flow cytometry analysis was performed using a Cyan FACScan (DakoCytomation) and Summit v4.3 software (DakoCytomation).

Fixed cell imaging analysis

Asynchronous U2OS cells expressing Cdt1-mCerulean3-P2A-Venus-p21 induced with 20 ng/ml doxycycline were fixed with 2% paraformaldehyde using standard methods and imaged on a Nikon Ti Eclipse inverted microscope running NIS Elements software V4.30.02 with an Andor ZYLA 4.2 camera using a 20X objective. Images of randomly-selected fields were collected in all three channels (CFP, YFP, and RFP) using exposure times producing approximately equivalent nuclear fluorescence in the three channels. ImageJ (V1.49p) was used to identify nuclei on the H2B-mCherry images using the nucleus counter plug-in from the ImageJ Cookbook. Cells were scored for Venus and/or mCerulean3 expression over three randomly-selected fields (n>150 per field).

Live-cell imaging analysis

Asynchronous U2OS cells stably expressing histone H2B-mCherry and PIP^{Cdt1}-p21-Venus, or Venus-NLS-p21 were plated on 35 mm glass bottom plates (In Vitro Scientific) in imaging media (phenol-red free DMEM (Invitrogen) supplemented with 10% FBS and 1X pen/strep) approximately 24 hours before being imaged. Cells were imaged for a minimum of 18 hours using a Nikon Ti Eclipse microscope operated by NIS Elements software V4.30.02 with an Andor ZYLA 4.2 camera and a custom stage enclosure to ensure constant temperature, humidity, and CO_2 levels. Protein expression was induced with 10 ng/ml

(PIP^{Cdt1}-p21), or 30 ng/ml (Ven-NLS-p21) doxycycline 20 hours before imaging. Fresh media with doxycycline was added 5 hours before imaging. Images were flat-field corrected using NIS Elements. 50 cells of each line were selected for analysis based on Venus expression and visualization of a complete cycle (minimum mitosis to S phase degradation).

Single-cell fluorescence intensity was quantified using custom MATLAB software, which is available upon request. In each frame, the nuclei of individual cells were identified using an adaptive threshold followed by watershed segmentation of the H2B-mCherry channel. Cells were tracked through consecutive frames by tracking nearest nuclear centroids between frames. The resulting nuclear borders were used to quantify average fluorescence intensity from other channels (e.g., p21-Venus). Missing time points, which were generally no more than 1-2 frames, were interpolated linearly. To compare the decay kinetics of individual cells, fluorescence intensity was normalized between 0 and 1. The delay time, T_d, was calculated by fitting each trace to an inverse sigmoidal Boltzmann curve, $f(t) = \frac{1}{1+\exp\left(\frac{t-t_d}{t_s}\right)}$.

CHAPTER 3: IDENTIFICATION OF MECHANISMS CONTRIBUTING TO ORIGEN LICENSING INHIBITION DURING CELLULAR QUIESCENCE[2]

Introduction

In Chapter 1, I discussed the origin licensing reaction, in which origins are rendered competent for replication by the chromatin-loading of the MCM helicase. This licensing reaction is highly regulated to ensure that it only occurs during G1 phase and is restricted beyond the G1/S transition to prevent DNA re-replication. As mentioned in Chapter 1, restriction of new origin licensing during S and G2 phases is accomplished by a variety of overlapping mechanisms, including transcriptional regulation of licensing proteins, Cdc6 nuclear export, expression of protein inhibitors (e.g. geminin), and ubiquitin-mediated proteolysis via SCF^{Skp2}, $CRL4^{Cdt2}$, and the APC/C E3 ubiquitin ligases (reviewed in (Arias and Walter 2007; Blow and Dutta 2005; Sclafani and Holzen 2007; Machida et al. 2005).

Another point in the cell cycle in which licensing activity is strictly inhibited is during cellular quiescence (G_0). In fact, the absence of chromatin-bound MCMs is a distinguishing feature of quiescent cells, as it helps maintain them in their non-proliferative state (Malumbres and Barbacid 2001). How licensing activity is restricted during G_0 is still not entirely understood, however. One of the major mechanisms known to limit licensing in quiescence is ubiquitin-mediated proteolysis of the licensing factor Cdc6 by APC^{Cdh1}, which

[2] Results from Chapter 3 are currently unpublished.

is highly active in G_0 cells (Petersen 2000). Also, in some cell lines, Cdt1 levels are transcriptionally downregulated as cells exit the cell cycle (Xouri et al. 2004; Mailand and Diffley 2005). It was shown previously, however, that reconstitution of Cdc6 expression in quiescent REF52 cells cannot overcome the resistance to licensing during cell cycle exit (Cook et al. 2002), suggesting the existence of additional mechanisms.

In developing hypotheses for additional factors restricting licensing activity during G_0 phase, we considered recent evidence from our lab implicating stress-activated mitogen-activated protein kinase (MAPK) activity in the regulation of origin licensing. The stress MAPKs p38 and JNK are activated by a variety of environmental and genotoxic stressors and play key roles in controlling cell proliferation among other important processes (Wagner and Nebreda 2009; Thornton and Rincon 2009) **(Figure 3.1A)**. In the study from our lab, we observed that induction of the stress MAPK pathway using acute stressors such as sorbitol treatment promotes phosphorylation of the Cdt1 licensing factor; this MAPK-induced phosphorylation has two important effects on Cdt1 regulation: (1) It results in increased Cdt1 stability by preventing Cdt1 binding to Cdt2, abrogating $CRL4^{Cdt2}$-mediated ubiquitination, and (2) it disrupts Cdt1 function in origin licensing. In this same paper, our lab also observed an inverse relationship between stress MAPK levels and the timing of licensing onset in G1; In G_0 cells, stress MAPK activity is quite high, but these levels drop coincidentally with the onset of MCM loading during G1 (Chandrasekaran et al. 2011) **(Figure 3.1B)**. Previous studies also showed that p38 activity is important for establishing contact inhibition in response to serum withdrawal (Faust et al. 2005) as well as controlling cell cycle exit in primary myoblasts (Perdiguero et al. 2007). Whether this elevated stress MAPK activity in G_0 is linked to inhibition of licensing activity is still unclear.

Based on this collective evidence, we hypothesized that stress MAPK activity contributes to licensing inhibition in G_0, through direct phosphorylation of Cdt1 or perhaps

Figure 3.1.

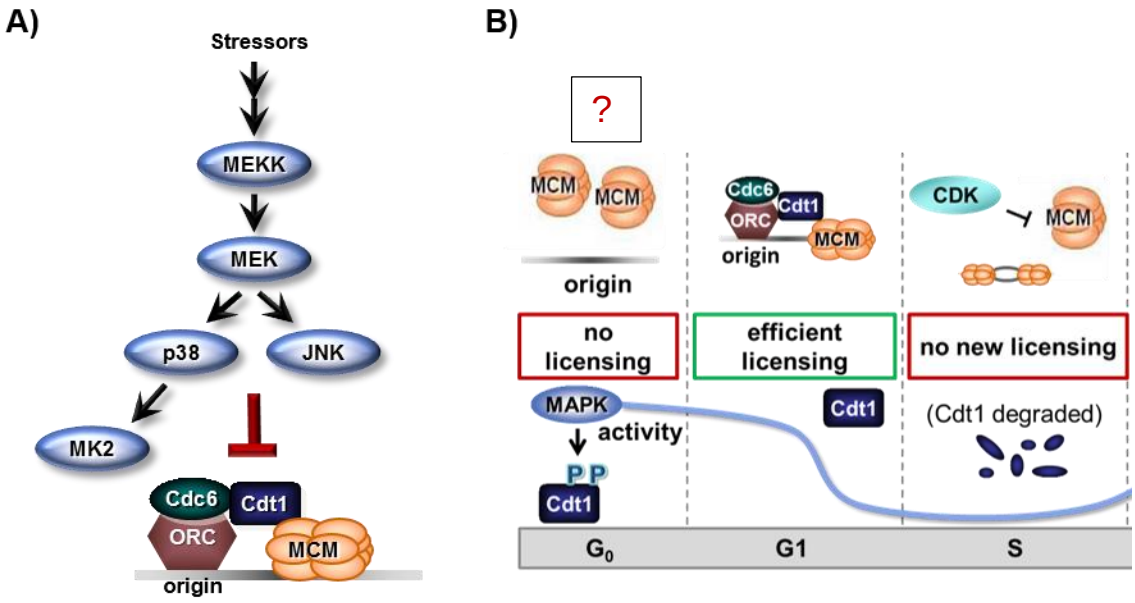

Figure 3.1. Regulation of MCM loading (licensing) and stress MAPK activity during the cell cycle. (A) Pathway for activation of the stress MAPKs p38 and JNK upon acute cellular stress. Stress MAPK activity blocks MCM loading (Chandrasekaran et al. 2011). (B) *(top)* MCM loading status during the cell cycle. Licensing is allowed only in G1, but blocked in quiescence and beyond the G1/S transition. Mechanisms contributing to licensing inhibition in G_0 are the focus of Chapter 3. *(bottom)* Stress MAPK activity (and Cdt1 phosphorylation by stress MAPKs) is inversely correlated with MCM loading during the cell cycle.

other licensing factors. In this project, we tested our hypothesis by combining stress MAPK inhibition with artificial restoration of the licensing factors Cdc6 and Cdt1 in quiescent T98G cells. While results confirmed previous observations of licensing inhibition, Cdt1 phosphorylation, and elevated stress MAPK activity in G_0 phase, addition of pharmacological inhibitors of stress MAPKs had little effect on restoring licensing activity during G_0. Therefore, we turned our attention to identifying differential regulators of MCM loading in G_0 vs. G1 cells in an unbiased mass spectrometry screen. Using this approach, we were able to identify novel MCM interactions, including some with previously characterized roles in cell proliferation control. Here, I summarize these findings and discuss optimization of the original mass spectrometry screen for better detection of MCM regulators contributing to quiescence establishment and maintenance.

Results

Quiescent cells are resistant to MCM loading despite artificial restoration of licensing factors.

To determine whether there are other mechanisms contributing to the inhibition of MCM loading during quiescence besides Cdc6 degradation by APC^{Cdh1}, we artificially restored licensing factors Cdc6 and Cdt1 to quiescent cells. Serum-starved T98G cells are distinguished by the absence of Cdc6 and Cdt1, in agreement with previous observations (Mailand and Diffley 2005); levels of Cdc6 and Cdt1 re-accumulate upon cell cycle re-entry and progression into late G1, coinciding with the timing of MCM chromatin loading **(Figure 3.2A)**. We reconstituted Cdt1 expression in these cells by stable integration of a wild-type Cdt1 construct and infection with an adenovirus encoding a stable, APC^{Cdh1}-resistant form of Cdc6 (“S3D”). Despite ectopic expression of Cdc6 and Cdt1 to G1 levels, when we performed chromatin fractionations to compare relative amounts of chromatin-bound MCMs, we found that quiescent cells were still resistant to MCM loading in comparison to G1 cells, in agreement with published results (Cook et al. 2002) **(Figure 3.2B, compare lanes 2 and**

Figure 3.2.

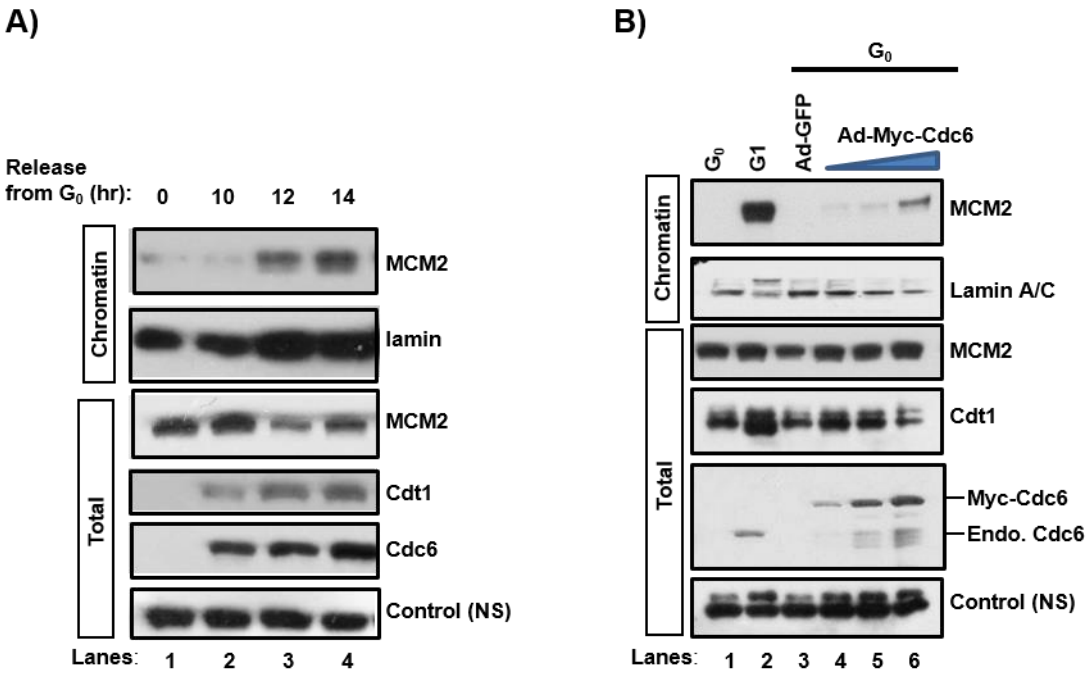

Figure 3.2. Quiescent cells are resistant to MCM loading. (A) T98G cells were serum-starved for 48 h and then released into complete medium for the indicated times. Cell lysates were fractionated to monitor the chromatin association of MCM2 by immunoblotting. In parallel, immunoblots were performed on whole cell lysates for total MCM2, Cdt1, and Cdc6. (B) T98G cells stably expressing Cdt1-WT-V5 were serum-starved (lane 1), released from quiescence and collected at 12 h in late G1 (lane 2), or serum-starved and infected with either control Ad-GFP adenovirus or Ad-mycCdc6-S3D at various multiplicity of infection (MOI) values: (MOI= 10, 25, and 50 ffu/cell for lanes 4,5, and 6 respectively). Chromatin fractions (top) and whole cell lysates (bottom) were analyzed by immunoblotting for the indicated proteins.

6). Thus, we concluded that there are other mechanisms besides the absence of licensing factors to account for MCM loading inhibition in G_0.

Stress MAPK inhibition is not sufficient to restore MCM loading to quiescent cells.

As mentioned in the Introduction, we speculated that high stress MAPK levels in G_0 cells could be a contributing factor to MCM loading inhibition, given our previous observation that sorbitol-induced MAPK activation was sufficient to block licensing activity (Chandrasekaran et al. 2011). Indeed, we did observe evidence for upregulated stress MAPK in G_0 cells, in line with published findings. For instance, we performed a time-course experiment to monitor MCM loading and phospho-p38 levels in T98G cells following release from quiescence into G1 phase, and saw that these markers were inversely correlated; phopho-p38 levels, indicative of p38 activation, were elevated in G_0 cells and decreased in late G1 cells, coinciding with the onset of MCM loading **(Figure 3.3A).** Furthermore, phosphorylation of a downstream target of p38, MAPKAP-K2, was high in G_0 arrested cells and low in G1. **(Figure 3.3B)**. Interestingly, we also observed that Cdt1 was predominately in its phosphorylated, licensing-deficient, form in G_0 cells as evidenced by its reduced electrophoretic mobility, and that Cdt1 de-phosphorylation occurred in late G1 **(Figure 3.3B)**. Based on this evidence, we hypothesized that stress MAPK inhibition, either through the use of pharmacological inhibitors or siRNAs targeting p38 and JNK, would overcome the restriction to licensing in G_0 by reducing the inhibitory phosphorylation of Cdt1 and perhaps other licensing factors. When we reconstituted Cdc6 and Cdt1 expression in quiescent cells and treated them with pharmacological inhibitors for p38 and JNK, we did not observe a rescue in licensing activity to G1 levels, however **(Figure 3.3C, lanes 2 and 6).** In the same experiment, inhibition of p38 and JNK isoforms with siRNAs produced similar results (data not shown). These results encouraged us to investigate other potential mechanisms for licensing inhibition during G_0.

Figure 3.3.

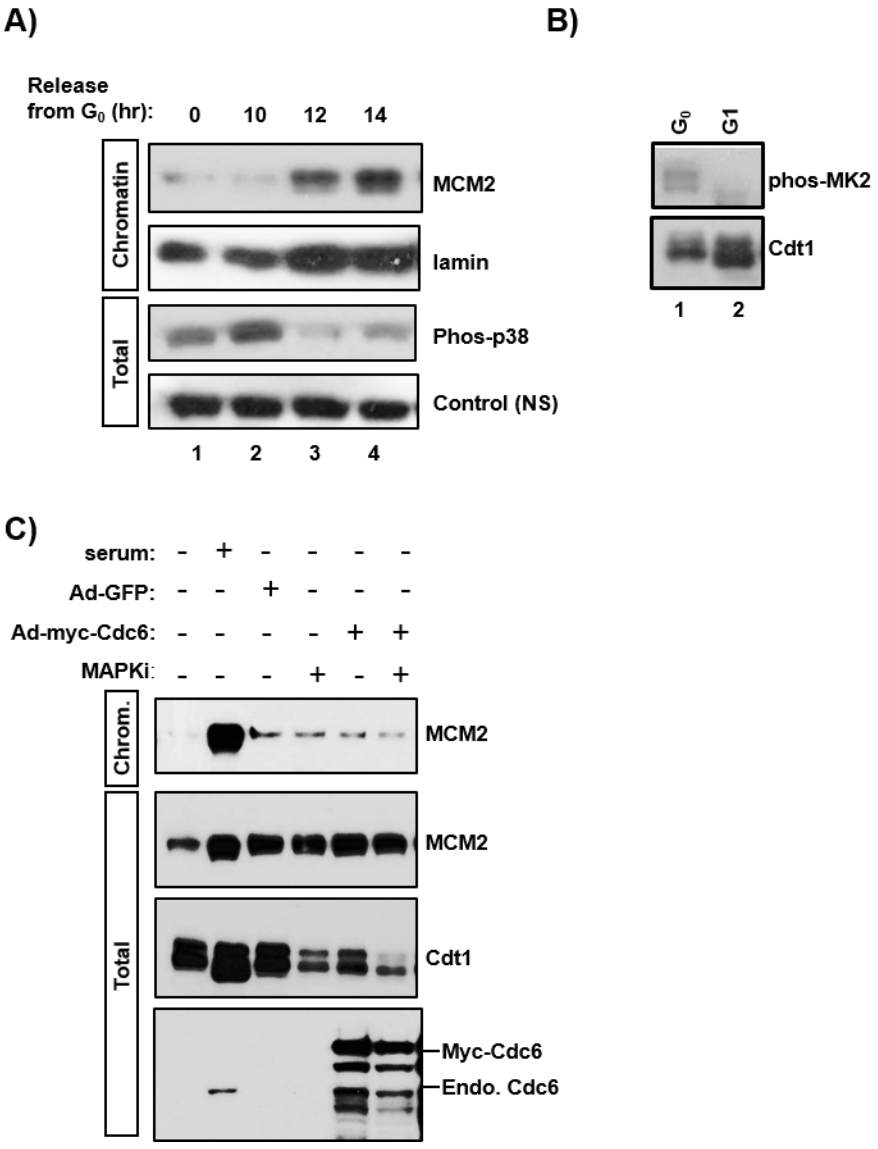

Figure 3.3. Inhibition of elevated stress MAPK activity in G_0 cells is insufficient to restore licensing activity. (A) T98G cells were rendered quiescent and re-stimulated for the indicated times with medium containing 10% FBS. Chromatin fractions (top) and whole cell lysates (bottom) were prepared and analyzed by immunoblot for the indicated proteins. (B) T98G cells were either rendered quiescent (G_0) or re-stimulated and harvested in late G1 (12 h post-serum). Lysates were analyzed for p-MAPKAP-K2 and Cdt1 levels by immunoblot. (C) T98G cells with stably integrated Cdt1-WT-V5 were serum-starved or re-stimulated to enter late G1 (indicated by - and + serum, respectively) and infected with adenoviral constructs and treated with MAPK inhibitors as indicated. Cells were infected with an MOI=25 of either control Ad-GFP or Ad-myc-Cdc6 adenoviruses for 24 h prior to harvesting. MAPK inhibitor treatments were performed for 4 h prior to harvesting with inhibitors targeting both p38 and JNK (see Methods).

MS/MS analysis of protein interactions with G_0 vs. G1 MCM complexes

In developing alternative hypotheses, we considered the possibility that MCM-interacting proteins could be contributing to the dynamic regulation of origin licensing in G_0 vs. G1 in two different ways: (1) Protein factors may preferentially bind MCMs in G_0 to block helicase-loading, or (2) MCM-interacting proteins may promote helicase-loading only in proliferating cells **(Figure 3.4A)**. These possibilities are not mutually exclusive. Therefore, to identify differential MCM interactions fitting into these two categories, we performed an unbiased mass spectrometry screen in collaboration with Ben Major's lab. We synchronized T98G cells in either G_0 or G1 as described in Methods, prepared lysates, and performed large-scale immunoprecipiations (IPs) of MCM complexes from each set of lysates using an antibody against endogenous MCM2. Large-scale anti-MCM2 IPs were performed in triplicate along with negative control samples for each condition (lysates incubated with beads but no antibody) and subjected to on-bead trypsin digestion and filter-aided sample preparation (FASP) clean-up before liquid chromatography and MS/MS analysis (according to Major Lab protocols).

Prior to mass spectrometry, we verified the efficiency of each IP by using a small amount (10%) in immunoblot analyses for MCM subunits **(Figure 3.4B)**. We also checked that cells were properly synchronized by monitoring Cdc6 and Cdt1 levels by immunoblot **(Figure 3.4C)** and by performing flow cytometry analysis of DNA synthesis (BrdU incorporation) vs. DNA content (PI staining) **(Figure 3.4D)**. Cdc6 and Cdt1 levels were low in G_0 cells, and the majority of cells (90.0%) had a 2C DNA content and did not incorporate BrdU, indicating that these cells were synchronized appropriately. We did note that while most cells in our G1 sample (12 h post-serum) did not incorporate BrdU during the labeling period (68.6%), a percentage showed evidence of BrdU incorporation to indicate early S phase entry (25.1%). However, Cdt1 levels were still very high in G1-synchronized samples (**Figure 3.4C**) indicating that most of the cells had not yet entered S phase. In the

Figure 3.4.

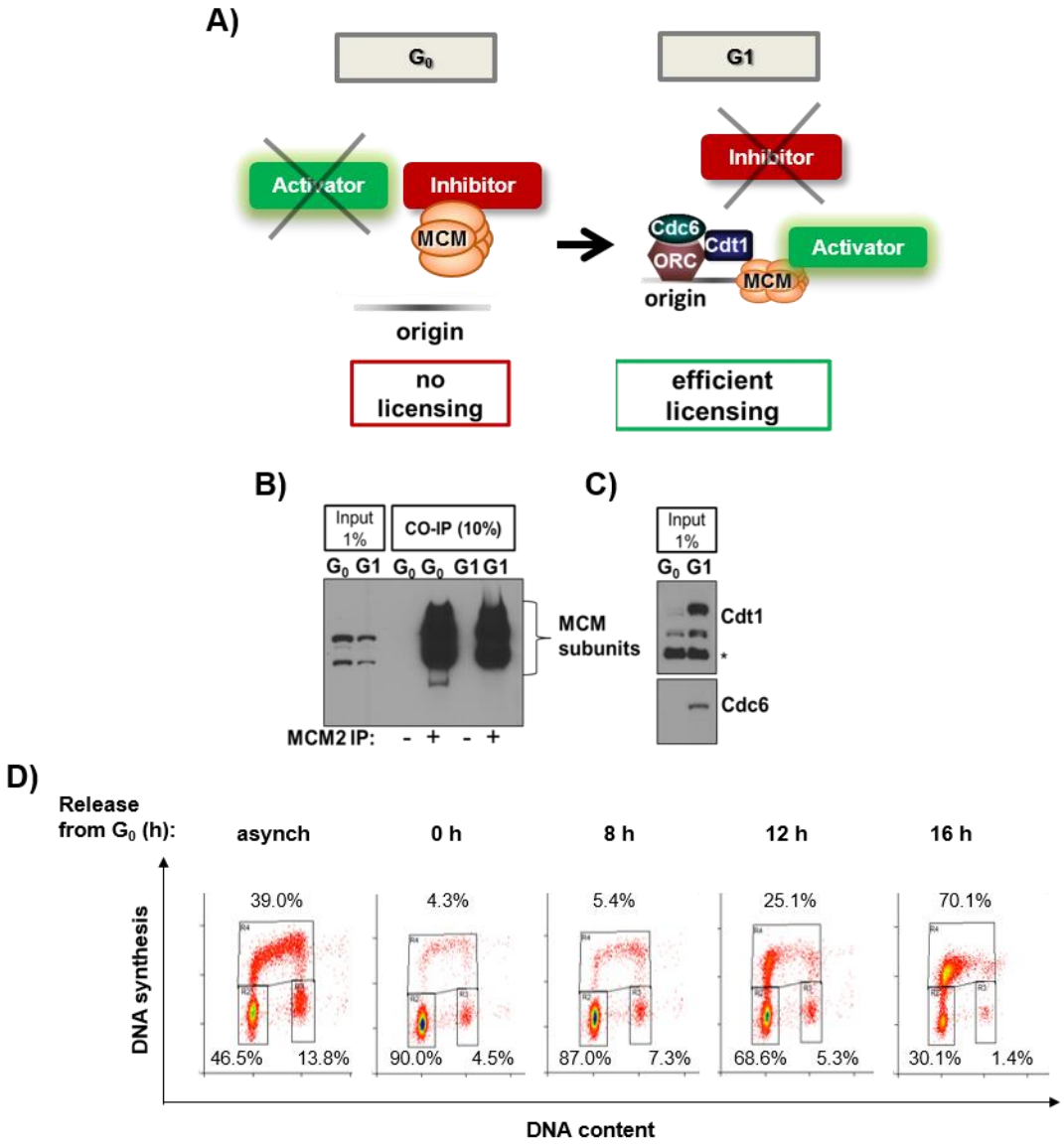

Figure 3.4. Verification of G_0 and G1 synchronizations and MCM purification strategy prior to MS/MS analysis. (A) Hypothesis for MCM complex regulation in G_0 vs. G1 cells. Either an inhibitor molecule preferentially binds MCM complexes in G_0 cells that is absent/inactive during G1, or an activator molecule enhances licensing activity exclusively in G1 cells but not G_0 cells. (B) T98G cells were synchronized in either G_0 or late G1 (12 h post serum re-stimulation). Lysates were used in CO-IPs with or without an antibody against endogenous MCM2, as indicated. Purification of MCM complexes was verified using 10% of each CO-IP sample in immunoblot analysis with a pan-MCM antibody. Remaining sample was used as one replicate for our LC-MS/MS analysis (C) Whole cell lysates from cells synchronized as in (B) were analyzed by immunoblot for Cdt1 and Cdc6 levels. (D) T98G cells were synchronized in G_0 and released into complete medium containing serum for the indicated times. Cells were labeled for 1 h with BrdU prior to fixation and analyzed by flow cytometry with anti-BrdU antibody to detect DNA synthesis (y-axis) and with propidium iodide for DNA content (x-axis).

future, a slightly earlier time-point (10-11 h) should be collected to ensure that late G1 samples are void of any early S phase cells that could skew results.

As expected, resulting MS/MS datasets confirmed the presence of all six subunits forming the MCM2-7 heterohexamer with high sequence coverage (>50%) in both the G_0 and G1 anti-MCM2 IP samples, but not in the respective control samples **(Table 3.1)**. While many novel MCM-interactions were identified in both the G_0 and G1 conditions, there were few associated proteins identified which bound exclusively in G_0 or G1 lysates. A subset of proteins fitting into each of these categories is shown in **Table 3.2**. We further prioritized our list of MCM interactions based on variety of different factors such as the SAINT algorithm (a bioinformatics tool that assigns confidence values to protein-protein interaction data) (Choi et al. 2011), relative abundance in IP samples (normalized spectral abundance factors (NSAF) values) (Paoletti et al. 2006), Gene Ontology (GO) term analysis, known involvement in cell cycle regulation, etc. Based on this analysis, we generated a list of high-priority candidates for further follow-up experiments **(Table 3.3)**. The full dataset is uploaded as a **supplemental file** to this dissertation.

Validation of prioritized MCM interactions

Our first goal was to validate our list of MCM interactions by co-immunoprecipitation and immunoblot analysis. To facilitate these experiments, we obtained cloned open reading frames (ORFs) of candidate genes from the Human ORFeome collection v5.1, and generated Flag-tagged expression constructs using Gateway cloning with a custom lentiviral vector (pHAGE-CMV-FLAG-DEST, gift from Ben Major). We also obtained cloned cDNAs for mammalian expression from other sources. We transiently transfected HEK293T cells with expression vectors for 24 h and immunoprecipitated MCM complexes using an MCM2 antibody. We then detected co-immunoprecipitated target proteins using an antibody against the N-terminal FLAG tag in each construct. Using this approach and with the help of

a rotation student at the time, Jacob Matson, we were able to validate at least 8 interactions from our list **(see Table 3.3)**. We also used these vectors to generate stable cell lines in T98G cells for validation. **Figure 3.5** shows examples of validated MCM interactions using this approach.

Table 3.1. Detection of MCM subunits in MS/MS IP samples

	CO006_MCM2/3_G0_Kate			CO010_MCM2_G0_Kate			CO014_MCM2_G0_Kate_2nd		
Gene Name	Tot SC	Unique SC	%Seq coverage	Tot SC	Unique SC	%Seq coverage	Tot SC	Unique SC	%Seq coverage
MCM2	*208*	*34*	*38.4*	*338*	*105*	*62.7*	*679*	*115*	68.4
MCM7	176	53	49.7	229	97	63	420	110	68.8
MCM4	167	59	61.5	375	110	67.2	766	131	70.1
MCM6	98	40	39.5	255	88	61.8	347	102	66.7
MCM3	76	33	41.3	133	63	56.7	223	90	70.8
MCM5	65	24	33.7	130	61	53.5	230	63	56.7

	CO005_MCM2/3_G1_Kate			CO009_MCM2_G1_Kate			CO013_MCM2_G1_Kate_2nd		
Gene Name	Tot SC	Unique SC	%Seq coverage	Tot SC	Unique SC	%Seq coverage	Tot SC	Unique SC	%Seq coverage
MCM2	*101*	*30*	35.7	*191*	*70*	*45.9*	*398*	*89*	*61.4*
MCM7	116	49	53.3	170	69	50.1	266	82	61.8
MCM4	105	49	52	154	78	51.2	509	100	62
MCM6	158	41	48.7	157	64	42.3	222	66	57.4
MCM3	117	38	45.2	103	63	51.6	145	67	58
MCM5	63	22	32.3	92	52	46	135	53	47

Table 3.2. Examples of novel constitutive, G_0-induced, and G1-induced MCM interactions.

Constitutive interactions

Uniprot ID	Gene Name	description	siRNA phenotypes	partners of note	Avg Saint	Max Saint
P51610	**HCFC1**	VP16, regulation of I	Increased cell number in G1, small nucl	transcription factors	0.60	0.97
Q86UU1	**PHLDB1**	pleckstrin homology	Decreased nuclei size in G2M	sh3kbp1 (only one partner)	0.7077	0.986
P19474	**TRIM21**	E3 Sjogren syndrome antigen A1	dec influenza rep'n Synthetic lethal with Ras	Cul1-Skp2, fadd, interferon r	0.9998	1
Q9UBP0	**SPAST**	spastin	Increased G1 DNA content, synth let w	partners in protein sorting, st	0.6102	0.935
O43150	**ASAP2**	Arf-GAP		fak2	0.8093	0.987
P14136	**GFAP**	glial fibrillary acidic protein	Increased circadian period length	transcription factors, f box pr	0.1473	0.884
Q07666	**KHDRBS1**	KH domain-containir	cell division, ciliogenesis, HR	pi3K, prmt1, src, chromatin r	0.7173	0.999
Q13425	**SNTB2**	Beta-2-syntrophin	ciliogenesis	mark2, dystrophin	0.6373	0.951
P51610	**HCFC1**	VP16	ncreased cell number in G1, small nucle	transcription factors	0.6003	0.967
Q96B97-2	**SH3KBP1**	SH3 domain-containing kinase-binding protein 1	cell division, ciliogenesis		0.5495	0.929
Q9Y5B9	**SUPT16H**	chromatin-specific transcription elongation factor 140 kDa subunit	cell division, ciliogenesis,	TONSL, MCM4, SSRP1, BR	0.5355	0.949
Q9Y294	**ASF1A**	Histone chaperone ASF1A	cell division, synthetic lethal with ML	MCM subunits, RIF1,	0.378	0.773
Q13263-2	**TRIM28**	Transcription intermediary factor 1-beta	cell division, cell viability, ciliogenesi	cul1, cul3, CDK2, E2Fs	0.3257	0.8
P49815-2	**TSC2**	Tuberin	cell division, ciliogenesis		0.3012	0.831
Q6SZW1-2	**SARM1**	sterile alpha and TIR motif	cell division, genome stability		0.2985	0.899
	SCLY	selenocysteine lyase	cell division, ciliogenesis		0.2832	0.865

G_0-induced interactions

Uniprot ID	Gene Name	description	siRNA phenotypes	partners of note	Avg Saint	Max Saint
P46939	**UTRN**	dystrophin-related protein 1	cell division, ciliogenesis, HR	mark2 kinase (cytoskeleton)	0.8333	1
Q8WXX5	**DNAJC9**	DnaJ (Hsp40) homolog, subfamily C, member 9	cell growth and viability (fly)	cul1 cul3	0.1203	0.722
Q3V6T2	**CCDC88A**	G{alpha}-interacting	none significant	bard1, smad, AKT	0.157	0.942
P57721	**PCBP3**	poly(rC) binding protein 3	HepC replication blocked	transcription factors, RNA BP	0.2885	0.768
P15531	**NME1**	NM23 nucleoside dip	cell proliferation, HepC replication	aurorak, rora	0.3227	0.737

G1-induced interactions

Uniprot ID	Gene Name	description	siRNA phenotypes	partners of note	Avg Saint	Max Saint
P47756	**CAPZB**	F-actin capping protein	some nuclear parnters (p53, ER, brca1)		0.5667	0.943
Q9Y4B5	**SOGA2**	coiled-coil domain-containing protein 165	no hits	ATM/ATR substrate, Mark2 an	0.4667	0.785
Q9BXF6	**RAB11FIP5**	Rab effector protein, vesicle trafficing protein	Increased gamma-H2AX phosphorylation		0.4015	0.849
Q96HA7-2	**TONSL**	Tonsoku-like protein	cell division, cell cycle regulation,	ASF1a, MCM subunits, SUPT	0.3858	0.751
Q9UQF2	**MAPK8IP1**	JNK MAP kinase scaffold 1	cell division, cell proliferation	JNK, c-jun,	0.3568	0.939

Table 3.3. List of prioritized hits from MS/MS screen for validation experiments

Gene ID	Gene Name	source of vector	expression vector (Midi	validated by CO-IP?
9479	MAPK8IP1	K. Verhey	pcDNA 3 Flag	no
6737	TRIM21	ORFeome library	Flag-nterm (Major)	yes
4659	PPP1R12A	ORFeome library	Flag-nterm (Major)	no
51540	SCLY	ORFeome library	Flag-nterm (Major)	yes
90957	DHX57	ORFeome library	Flag-nterm (Major)	no
10657	KHDRBS1 (Sam68)	Addgene	pcDNA3 HA N-term	yes
3054	HCFC1	ORFeome library	Flag-nterm (Major)	yes
30011	SH3KBP1	ORFeome library	Flag-nterm (Major)	yes
11198	SUPT16H	Jurgen Marteijn	GFP HA PLHLX	published
4796	NFKBIL2 (TONSL)	ORFeome library	Flag-nterm (Major)	yes
25842	ASF1A	ORFeome library	Flag-nterm (Major)	published
3191	HNRNP1			
10155	TRIM28	Addgene	pKH3-HA	no
23098	SARM1			
7249	TSC2	ORFeome library	not cloned yet	
23234	DNAJC9			
5905	RANGAP1	ORFeome library	Flag-nterm (Major)	yes
26056	RAB11FIP5			
6749	SSRP1	Jurgen Marteijn	GFP clonech (N and C-te	published
9782	MATR3	ORFeome library	N-term FLAG	
57488	ESYT2	ORFeome library	not cloned yet	
23255	KIAA0802 (SOGA2)	ORFeome library	not cloned yet	
4830	NME1	ORFeome library	Flag-nterm (Major)	yes
832	CAPZB	ORFeome library	Flag-nterm (Major)	
23187	PHLDB1	ORFeome library	Flag-nterm (Major)	no
8853	ASAP2	ORFeome library	not cloned yet	
2670	GFAP	ORFeome library	Flag-nterm (Major)	
7248	TSC1	ORFeome library	not cloned yet	
~~7402~~	~~UTRN~~	~~TOO BIG!~~		
55704	CCDC88A			
54039	PCBP3			
6683	SPAST			

Figure 3.5.

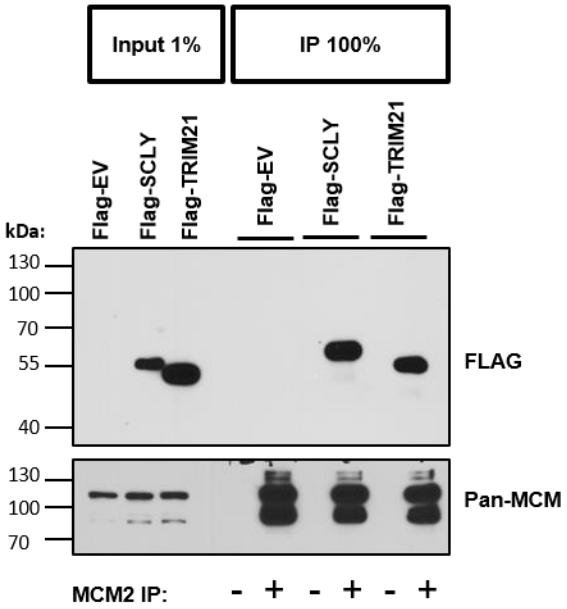

Figure 3.5. Validation of MS/MS interactions. Candidate genes were cloned into a custom Gateway lentiviral vector (pHAGE-CMV-FLAG-DEST), and resulting vectors were then transfected into HEK293T cells for expression of Flag-tagged proteins of interest. Lysates were prepared 24 h following transfection and used as input in Co-IPs with or without MCM2 antibody. Interactions with MCM complexes were verified by immunoblot analysis of Co-IP samples with an antibody against the N-terminal Flag tag in each expression construct. Shown are two examples of validated interactions with TRIM21 and SCLY.

Discussion

Here, we show that inhibition of MCM loading in quiescence requires additional mechanisms other than APC^{Cdh1}-mediated proteolysis of Cdc6. This conclusion was based on our observation that forced expression of both Cdc6 and Cdt1 in quiescent T98G cells, even above normal G1 levels, was insufficient to fully restore licensing activity. Therefore, we sought to define additional mechanisms explaining the inherent resistance of quiescent cells to origin licensing. In pursuing our original hypothesis that high stress MAPK activity may be involved in this licensing block, we showed that pharmacological inhibition of the stress MAPKs p38 and JNK was also insufficient to overcome MCM loading inhibition in G_0. Thus, either stress MAPK activity may be completely unrelated to licensing control in these conditions, or it may be involved in combination with other redundant mechanisms and signaling pathways. Additional pharmacological screening (with or without inhibition of stress MAPKs) may provide insight into other pathways that could potentially be important to establishing unlicensed chromatin in G_0.

Therefore, we developed an alternative hypothesis that differential MCM interactions in G_0 and G1 cells could impact MCM loading status. We were successful in developing a system to test this hypothesis through LC-MS/MS analysis of MCM binding proteins from G_0 vs. G1 cellular extracts. As evidence that MCM complexes were purified successfully for analysis, we were able to detect all six subunits of the MCM2-7 heterohexamer with high sequence coverage. We were also able to confirm some published MCM interactions in our screen, including ASF1a, SUPT16H, TONSL, MMS22L, and SSRP1 (O'Connell et al. 2010; Groth et al. 2007). On the other hand, we also failed to detect other known MCM binding proteins in our G1 sample, including Cdt1 (Cook et al. 2004), Cdc6 (Shin et al. 2003), the histone acetyltransferase HBO1 (Burke et al. 2001), ORC subunits (Bell and Dutta 2002) and Keap1 (much to the dismay of the Major lab!). We acknowledge that our

synchronization was imperfect, as a percentage of cells had started to enter early S phase at the time of collection (25%). In future attempts, we should collect a slightly earlier time-point (~10-11 hr post serum re-stimulation), to ensure a true late G1 population and enhance our abilities to detect MCM interactions known to occur at this point in the cell cycle.

Nevertheless, we did successfully uncover some novel MCM interactions which were validated by co-immunoprecipitation and immunoblotting. For instance, one of these interactions was with Sam68 (KHDRBS1), which was never shown previously. Sam68 is a nuclear RNA binding protein associated with various processes in mRNA metabolism (Chawla et al. 2009). A natural isoform of this protein (Sam68ΔKH) is expressed specifically in quiescent cells, and transfected Sam68ΔKH inhibits serum-induced DNA synthesis, which is overcome by Sam68 expression. Thus, Sam68 is proposed to control G1/S progression (Maurier 1997). Whether the Sam68ΔKH isoform preferentially interacts with MCM complexes from quiescent cells to inhibit MCM loading will be an interesting topic for future interrogation.

Another interesting MCM binding protein identified was Nme1 (NM23-H1), which we also observed was a G_0-induced MCM interaction. The traditionally described role for Nme1 is to synthesize nucleoside triphosphates other than ATP; however, increased evidence has shown alterative roles for this protein in other processes, including differentiation, proliferation, and development (Choudhuri et al. 2010). Microarray analysis comparing the expression profiles of BJAB (B-cell line) cells transfected with an expression construct for NM23-H1 or vector only revealed significant changes in genes involved in cell cycle control, apoptosis, and p53 activities. For instance, NM23-H1 expression caused reduced expression of cyclins and CKIs and reduced cell growth, implicating NM23-H1 in the control of cell proliferation (Choudhuri et al. 2010). Whether NM23-H1 is differentially regulated in

quiescent cells to affect the expression of these proliferative genes is not yet clear, and is something we are interested in following up on.

Finally, an additional protein identified from our screen was Host Cell Factor 1 (HCFC1), which was previously shown to be involved in cell cycle control and plays several roles in transcriptional regulation by tethering the chromatin modifying enzyme Set1/Ash2 and Sin3 histone deacetylase (HDAC) complexes together. Interestingly, a 50-kDa N-terminal fragment of HCFC1, arising from proteolysis of the full-length protein, was identified only from whole cell lysates of peripheral blood mononucleocytes (PBMCs) and primary fibroblasts which were arrested in G_0 (Scarr et al. 2000). It would be interesting to determine whether this truncated fragment also influences MCM loading status in quiescent cells in follow up experiments.

Among these previously uncharacterized MCM interactions were also some that we deemed unlikely to occur under physiological conditions. These include proteins like TRIM21 and RANGAP1, which are primarily localized to the cytoplasm in interphase, among other likely contaminants such as cytoskeletal proteins, ribosomal proteins, heatshock proteins, and elongation factors. These contaminant proteins are to be expected in any mass spectrometry experiment (Mellacheruvu et al. 2013), but we should prioritize optimizing our screening method to reduce the number of these false positives and enhance our detection of weaker affinity/transient interactions. One potential improvement a current graduate student is already employing involves proximity-dependent labeling of proteins neighboring the MCM complex by fusing MCM subunits to the promiscuous biotin ligase BirA*. Upon addition of biotin to cultured cells, the BirA* fusion will only biotinylate proteins within a 10nm radius; the biotinylated proteins can then be isolated from lysates by affinity purification over streptavidin resin (Roux et al. 2012). In this way, we may be able to maximize the number of *bona fide* interactions occurring during the biotin labeling period,

and reduce the number that occur as post-lysis artifacts. As further improvement to our original screen, nuclear fractionation of lysates prior to purification of MCM complexes may also help eliminate unlikely cytoplasmic interactions. We hope that with these improvements, we will be able to further characterize proteins that preferentially bind to MCMs in either G_0 or G1 (see Chapter 4).

Materials and Methods

Cell culture and manipulations

T98G glioblastoma cells were cultured in Dulbecco's modified Eagle's medium supplemented with 10% fetal bovine serum (Sigma). To synchronize cells in quiescence, serum was removed from confluent cells for 48 h; cells were re-stimulated to enter G1 phase by re-plating at a 1:3 ratio into fresh medium containing 10% serum. Cdc6 levels were restored to quiescent cells by infecting cells with Ad-mycCdc6-S3D adenovirus 24 h prior to harvesting. MAPK inhibitors (Sigma) were added at the following concentrations for 4 h prior to collection: p38 inhibitor SB203580 at 30 μM and c-Jun N-terminal kinase (JNK) inhibitor SP600125 at 100 μM.

Antibodies

Antibodies were purchased from the following sources: lamin A/C, Cdc6 (180.2), and PCNA (F-2) from Santa Cruz Biotechnologies; phospho-p38 and phospho-MAPKAP-K2 from Cell Signaling Technologies; anti-FLAG from Sigma, MCM2 from Bethyl Labs; BrdU and MCM2 (BM28) from BD Biosciences; and HRP or Dylight 488 secondary antibodies from Jackson Labs. Antibody against Cdt1 was described previously (Cook et al. 2004). Pan-MCM antibody was a gift from D. MacAlpine (Duke University).

Plasmids and recombinant protein preparation

Wild-type Cdt1 and Cdt1 5A alleles bearing a V5 tag (not in frame!) were sub-cloned into vector pCLXSN for retroviral packaging. For mass spec validation experiments, pDONR223 vectors containing candidate genes were obtained from the Human ORFeome collection v.5.1; expression plasmids were generated by Gateway cloning into a pDEST Phage N-terminal Flag vector (gift from Ben Major). Retroviral and lentiviral packaging and infection were performed using standard methods. Stable cell lines were selected using 500 ng/ml G418 (for pCLXSN vector) and 1 μg/ml puromycin (for N-terminal Flag vector). Ad-GFP and Ad-mycCdc6-S3D adenoviruses were prepared as described previously (Cook et al. 2002).

Protein lysate preparation

Protein lysates were prepared by re-suspending cells in CSK buffer (Cook et al. 2002) supplemented with 0.1% Triton-X-100 and protease and phosphatase inhibitors. Chromatin fractions were isolated as described previously by the addition of micrococcal nuclease and $CaCl_2$ to Triton-insoluble pellets to release chromatin-bound proteins (Cook et al. 2002).

Large-scale MCM2 immunoprecipitation for LC-MS/MS analysis

Four 15 cm dishes of T98G cells were either rendered quiescent according to the protocol above (G_0 sample) or re-stimulated from quiescence with media containing 10% FBS for 12 h (G1 sample). Cells were harvested and lysed in co-IP #3 buffer (50 mM HEPES pH=7.2, 33 mM KAc, 0.5 mM EDTA, 0.5 mM EGTA, 0.1% Triton-X-100 and 10% glycerol with protease and phosphatase inhibitors). Cells were lysed on ice for 20 minutes with gentle sonication to release chromatin-bound proteins. Lysates were divided in half and incubated for 1 h with either 5 ug anti-MCM2 antibody (Bethyl Labs) or without antibody (negative control sample) with rotation at 4°C. Lysates were then added to 20 μl protein A

agarose beads (Roche Life Sciences) and incubated for another 2 h at 4°C; beads were washed three times with co-IP #3 buffer and stored at -80°C prior to mass spectrometry analysis (10% was retained for immunoblot analysis). Samples were processed for LC-MS/MS according to Major Lab protocols.

Flow cytometry analysis

Cells to be analyzed by flow cytometry were labeled with 10 μM BrdU for 1 hour prior to trypsinization and fixation in 70% ethanol. Nuclei were stained with anti-BrdU antibody (BD Biosciences) followed by AlexaFluor 488-labeled secondary antibody (Jackson ImmunoResearch) and counterstained with propidium iodide. Flow cytometry analysis was performed using a Cyan FACScan (DakoCytomation) and Summit v4.3 software (DakoCytomation).

CHAPTER 4: CONCLUSIONS AND FUTURE DIRECTIONS

We have clearly shown from our studies in Chapter 2 that $CRL4^{Cdt2}$ substrates are degraded sequentially during the G1/S transition and during DNA repair synthesis. Furthermore, we demonstrated that these differences in targeting are related to PIP degron sequences within substrates. In our comparison of Cdt1 vs. p21, we found that their respective PIP degron sequences confer differences in binding to PCNA/Cdt2 to explain the very different destruction rates of these two substrates. Finally, we concluded that delayed p21 degradation is critical for proper replication progression in S phase, as premature p21 degradation promotes increased replication stress and DNA damage. These results demonstrate the importance of ordered protein destruction for proper coordination of S phase replication, and further suggest that substrate ordering may occur via different E3s involved at other cell cycle transitions to control key events.

This work has several implications in future studies of cell cycle transitions. While many past studies have identified molecular events occurring at these transitions, very few have characterized relationships among these events and their importance to cell cycle progression, like we have described here for Cdt1 vs. p21 degradation patterns. Based on these findings, we conclude that the four-stage model of the cell cycle introduced in Chapter 1 may be too simplistic; “sub-phases” may exist between cell cycle phases to help anticipate the next cell cycle phase, and to ensure that cell cycle progression occurs appropriately. From these studies, we have also developed tools to manipulate these inter-molecular relationships and assess the consequences on replication progression. Using our novel

live-cell imagining approach, we have further defined degradation patterns of $CRL4^{Cdt2}$ substrates on a much more detailed time-scale than would be accomplished using conventional biochemical methods. Going forward, this work will hopefully inspire future studies from our lab and others toward developing a more refined kinetic map of cell cycle events, allowing others to explore new molecular relationships and to more accurately test treatments specific to a given phase.

Despite these accomplishments, there are still several outstanding questions from this project that will require more work to resolve. These are highlighted below:

Future Directions for Chapter 2

Which specific amino acid residue(s) contribute to differential recruitment of PCNA/Cdt2 by PIP degrons?

Although we confirmed that the PIP degron sequences ultimately determined the degradation rates of $CRL4^{Cdt2}$ substrates, we did not pinpoint which specific degron residues accounted for these differences in targeting. As shown in the alignment in **Figure 1.4**, although the "TD" and "B+4" residues are conserved between all substrates examined in this study, there are some variations in a few key degron residues that may confer differences in binding to either PCNA or Cdt2 (or both). There is a phenylalanine residue within the PIP box of Cdt1 (QRRVTDF**F**) that differs from the tyrosine residue at that same position within both PR-Set7 and p21. Also, PR-Set7 and p21 contain a basic patch of amino acids upstream of the PIP box that is not found in Cdt1. Further mutational analyses will be needed to interrogate whether any of these different residues (or combinations of residues), accounts for the different rates of $CRL4^{Cdt2}$-mediated proteolysis. I did create an additional allele of p21 in which its native PIP degron sequence was converted to match the sequence of the Cdt1 PIP degron. Oddly, when I performed a UV chase experiment to measure its degradation kinetics, I saw that it was not degraded at all (similar to ΔPIP). Thus, sequence

context of PIP degron sequences may also be important for their proper recognition. Ultimately, our goal will be to deduce the minimal destruction motif necessary to confer "Cdt1-like" or "p21-like" degradation kinetics.

Are there additional mechanisms to explain the different substrate degradation rates?

We discovered that the Cdt1 PIP degron binds Cdt2 more efficiently than the corresponding p21 sequence, providing one mechanism for its accelerated degradation via the same E3 ligase complex. However, this is probably not the only explanation for why these degron sequences are targeted differently. For instance, we have considered the possibility that some substrates of $CRL4^{Cdt2}$ could be more processive than others, leading to preferential multiubiquitination and earlier degradation. More processive substrates would obtain polyubiquitin chains in a single $CRL4^{Cdt2}$ binding event, whereas distributive substrates would require multiple rounds of binding. In fact, differences in the processivity of ubiquitination were observed between substrates of the APC/C during the mitosis/G1 transition, which also accounts for their ordered degradation (Rape et al. 2006). Therefore, it is conceivable that Cdt1 may be more processive and prone to earlier ubiquitination than p21*; in vitro* and *in vivo* ubiquitination assays with purified proteins may be helpful in further understanding the timing and extent of ubiquitination of different $CRL4^{Cdt2}$ substrates.

$CRL4^{Cdt2}$ substrate degradation timing may also be influenced by PTMs or preferential binding to other proteins. As an example, we have shown that stress MAPK phosphorylation of Cdt1 at the C-terminus blocks the association of Cdt2 with the N-terminal PIP degron, resulting in Cdt1 stabilization (Chandrasekaran et al. 2011). Stress MAPK phosphorylation of p21 has also been reported to affect its stabilization (Kim et al. 2002). I have already observed that inhibition of stress MAPK phosphorylation had no appreciable effect on the rates of Cdt1 and p21 destruction by $CRL4^{Cdt2}$ following UV irradiation (unpublished observations). There could potentially be other kinase signaling pathways

intersecting with $CRL4^{Cdt2}$ targeting that we are currently unaware of. In Chapter 2, I also saw that abrogation of p21 binding to the protein TRIM39 did not affect its degradation pattern, but there could also be other undiscovered p21 binding partners that delay its replication-coupled destruction.

Finally, other processes downstream of the ubiquitination event may influence the timing of proteasomal degradation. As mentioned in the Introduction, the p97 enzyme was recently shown to be important for stripping ubiquitinated substrates from chromatin before their delivery to the 26S proteasome. Perhaps there could be differences in the timing or efficiency with which p97 acts on different $CRL4^{Cdt2}$ targets. Bolstering this hypothesis, our *in vitro* binding assay shows that p21 binds PCNA more efficiently than Cdt1 does; the PCNA-p21 interaction could in fact be too tight to allow for efficient p97-mediated removal of ubiquitinated p21 from chromatin, contributing to delayed p21 destruction. Future work needs to be done to test this idea, although we briefly started pilot experiments to test sensitivity of substrates to the p97 inhibitor NMS-873 (SelleckChem).

How is Cdk activity correlated with the rate of p21 destruction by $CRL4^{Cdt2}$?

Here, we showed that premature p21 degradation in asynchronously proliferating cells causes replication defects during S phase. To further investigate how early p21 degradation influences S phase progression, synchronization experiments should also be performed to measure BrdU incorporation at the G1/S transition in cells complemented with either WT-p21 or PIP^{Cdt1}-p21 alleles. We predict that in agreement with our model, accelerated p21 degradation will result in high CDK activity in early S phase, leading to premature origin firing and replication stress. While we speculate that delayed p21 degradation controls the timing of CDK activation, we did not actually provide evidence for this correlation. Future studies should be focused on determining how p21 destruction rates coincide with CDK activity at time-points corresponding to the G1/S transition, using either

histone H1 kinase assays or some other readout for CDK2 activity (Cdc6 export from the nucleus, for example). In addition, p21 levels in early S phase could play a role in modulating replication fork speed, as the p21 interaction with PCNA was shown to inhibit fork progression (Waga S, Hannon GJ 1994). DNA fiber combing assays or thymidine incorporation assays may reveal these differences in replication rates in cells complemented with either WT-p21 or PIP^{Cdt1}-p21 alleles.

Does premature p21 degradation promote re-replication?

According to our model, we predict that if p21 is degraded prematurely, this could present a situation in which CDK levels rise too soon at the G1/S transition when other licensing factors are still present (like Cdt1), which could promote the occurrence of re-licensing and re-replication. In our flow-cytometry analysis, we did not detect an appreciable difference in the percentages of re-replicating cells in cells with prematurely degraded p21, however. A re-replication phenotype may be more readily detected by co-depletion of additional factors that normally restrain re-replication in proliferating cells, such as the Cdt1 inhibitor geminin. Also, fiber combing assays may be more ideal than flow cytometry analysis for showing re-replication events that occur only in early S phase. It is possible that these cells do not progress far enough to show >4C DNA content by flow cytometry analysis owing to checkpoint arrests.

Does ordered substrate re-accumulation by $CRL4^{Cdt2}$ occur at the end of S phase? Why?

While we have clearly shown that substrate ordering occurs at the G1/S transition, we have yet to test whether $CRL4^{Cdt2}$ targets also re-accumulate in a defined order. Future live-cell imaging analysis of fluorescently-tagged Cdt1 and p21 fusion proteins will focus on capturing the S/G2 transition to further discern substrate re-accumulation patterns. If ordered re-accumulation does occur in live cells, we will then investigate the consequences

of manipulating this order using cell lines and reagents generated in the course of this study. Considering our results from Chapter 2, we also consider it likely that the order of substrate re-accumulation is determined by PIP degron sequences, and similar PIP swap experiments should be designed to test this possibility.

What are the relative contributions of SCF^{skp2} and $CRL4^{Cdt2}$ to S-phase proteolysis?

In the Introduction, I mentioned that several substrates of $CRL4^{Cdt2}$ are also targeted by another S-phase specific E3 ubiquitin ligase, SCF^{Skp2}, including p21, PR-Set7, and Cdt1. The relative contribution of these E3 ligases to S phase proteolysis is not yet understood, however. Current evidence suggests that these two pathways are not entirely redundant. For example, Skp2 knockout mice are viable, but still exhibit a variety of defects, including enlarged nuclei, polyploidy, reduced growth rate, and apoptosis (Nakayama et al. 2000). On the other hand, targeted Cdt2 gene deletion in mice results in early embryonic lethality (Liu et al. 2007), and acute depletion of Cdt2 results in massive re-replication that is not affected by co-depletion of Skp2 (Kim et al. 2008). We hypothesize that SCF^{Skp2} may play a more important role later in S phase than $CRL4^{Cdt2}$; the rationale here is that SCF^{Skp2} targeting requires CDK2-mediated phosphorylation of substrates, and prior degradation of p21 via $CRL4^{Cdt2}$ may allow the onset of CDK activity necessary for this to occur. In this regard, our observation of the relatively delayed timing of p21 destruction at the G1/S transition may also have implications for controlling the timing of Cdk2-mediated phosphorylation of substrates required for SCF^{Skp2} targeting. Further examination of the timing with which these E3 ubiquitin ligases act on their substrates will be interesting to explore in future experiments.

Future Directions for Chapter 3

As noted in the Discussion section for Chapter 3, using our large-scale MCM2

immunoprecipitation and LC-MS/MS approach, we were able to uncover some previously uncharacterized MCM interactions. Further follow-up analyses is warranted to determine their roles in controlling origin licensing/DNA replication. For instance, our next step after validation of interactions by co-IP and western blotting (which we have already accomplished for some proteins on our list) will be to perform further functional analyses to manipulate the expression/activity of candidate proteins. We will perform siRNA knockdowns and over-express candidate MCM interactors and determine cellular consequences for MCM loading during G_0/G1 as well as cell cycle progression (measured by flow cytometry analysis of DNA content). We will also assess expression levels and subcellular localization of candidate interactions in a variety of cell types to further define their involvement in controlling origin licensing and replication onset. Hopefully, based on these analyses, we will be able to better define the roles of these proteins in establishing and maintaining unlicensed chromatin during quiescence.

Future directions for this project will also prioritize improving our original screening approach. Our original experiment had some obvious limitations, including the fact that our list of G_0- and G1-induced MCM interactions was relatively short and inconclusive. As mentioned in the Discussion of Chapter 3, we are currently developing an alternative screening strategy which exploits the promiscuous biotin ligase BirA*. We hope that proteins purified using this proximity-dependent labeling approach represent more probable MCM interactions and that this technique allows for identification of weaker affinity/ transiently-associated proteins. If we still do not uncover many proteins that differentially bind G_0 and G1 MCM complexes, we may also explore other potential explanations for licensing inhibition in G_0. For instance, we could perform phospho-enrichment prior to mass spectrometry analysis to identify dynamically regulated phosphorylation sites between purified G_0 and G1 MCM complexes. Even if our candidate proteins are not necessarily involved in licensing control, we could also investigate their involvement in other aspects of

cell cycle regulation. Ultimately, we hope that any new MCM interactions we uncover from these screens will increase our understanding of MCM loading regulation during the cell cycle.

Success with these screens will greatly facilitate studies of quiescence control in several ways. The identification of new MCM loading inhibitors in quiescent cells may provide new biomarkers to further distinguish quiescent vs. proliferating cells in culture. Also, increased understanding of their function in maintaining quiescence may allow us to make more accurate predictions on how to manipulate cell proliferation pharmacologically. A defining feature of several types of cancer cells is their inability to establish and maintain cellular quiescence. Identification of hits from our screen which are also differentially regulated in cancer cells will be quite impactful, as such information may potentially guide therapeutic efforts to selectively target cancer vs. normal cells.

APPENDIX: CDK1-DEPENDENT INHIBITION OF THE E3 UBIQUITIN LIGASE, CRL4^{CDT2}, ENSURES ROBUST TRANSITION FROM S PHASE TO MITOSIS[3]

Project Summary

In addition to my main dissertation work detailed in Chapters 2 and 3, I also made substantial contributions to another publication investigating the inhibition of CRL4^{Cdt2} targeting during the S/G2 transition. In this paper, on which former graduate student Lindsay Rizzardi is first-author, we discovered that the CRL4^{Cdt2} substrates p21, Cdt1, and PR-Set7 re-accumulate beginning in late S phase, in spite of the persistence of PCNA^{DNA}. Furthermore, these substrates are protected from UV-triggered CRL4^{Cdt2} targeting during mitosis. We demonstrated that a CDK1-dependent mechanism blocks CRL4^{CDT2} activity during the S/G2 transition by interfering with CDT2 recruitment to chromatin. Based on this evidence, we conclude that the CDK1-dependent override of replication-coupled destruction in late S phase contributes to substrate re-accumulation at this point in the cell cycle, allowing for the efficient transition from S phase to mitosis.

My specific contributions to this paper are listed below. Portions of text from the manuscript highlighting these findings are indicated by **[ ]**.

Contributions to Rizzardi et al., 2014

(1) The UV-triggered degradation of CRL4^{Cdt2} substrates Cdt1, p21 and PR-Set7

[3] Modified from Rizzardi, L.F., D. Varma, K.E.Coleman, J.P. Matson, S. Oh, **J.G. Cook**. (2014) CDK1-dependent Inhibition of the E3 Ubiquitin Ligase, CRL4^{CDT2}, Ensures Robust Transition from S Phase to Mitosis. *J. Biol. Chem*. **290**: 556-567.

is blocked in nocodozole-arrested cells **(Figure A.2A and B)**.

(2) CDK-1 inhibition with the drug RO-3306 was shown to block the re-accumulation of substrates during the late S phase/G2 transition. I provided flow cytometry analysis to show that synchronized cells treated with RO-3306 experienced a G2 arrest as expected, but were still allowed to progress normally through late S phase **(Figure A.4A and B)**.

(3) Similarly to WT-p21, a p21 construct harboring alanine substitutions at two phosphorylation sites previously reported to stabilize p21, T57 and S130 (HA-p21-AA), was still resistant to $CRL4^{Cdt2}$-mediated proteolysis in mitosis. This result further suggests that $CRL4^{Cdt2}$ is itself inhibited during this transition, and that direct substrate phosphorylation is not required for protection from $CRL4^{Cdt2}$-mediated destruction in mitosis **(Figure A.5A)**.

(4) While PCNA is still recruited to chromatin in nocodozole-arrested cells, Cdt2 is not. This inhibition of Cdt2 chromatin association prevents recognition of $CRL4^{Cdt2}$ substrates in mitosis, leading to their stabilization **(Figure A.6A)**.

(5) Cdt2 chromatin binding is lost as CDK1 activity rises in late S phase, coinciding with the timing of substrate re-accumulation (with Jacob Matson) **(Figure A.6C)**.

Introduction

Ubiquitin-mediated degradation of cell cycle proteins is essential to ensure timely cell cycle transitions that maintain genome integrity. Conversely, cell cycle-dependent protein stabilization by preventing ubiquitination allows rapid protein accumulation at the right time to bring about robust cell cycle transitions. Replication-coupled destruction is a particularly important protein control mechanism that coordinates the degradation of a cohort of proteins with the process of DNA synthesis. Much has been learned about how replication-coupled

destruction is initiated in S phase (Arias and Walter 2005; Kim et al. 2008; Tardat et al. 2010; Terai et al. 2013; Zhang et al. 2013), but less is known about how it is inhibited as S phase ends.

Among the cohort of human proteins reported to be subject to replication-coupled destruction are CDT1, SET8, p12, the CDK inhibitor p21, and most recently, thymine DNA glycosylase (TDG) (Shibata et al. 2014; Slenn et al. 2014). Their destruction in S phase is particularly critical to ensure precise and efficient genome duplication (Arias and Walter 2005; Kim et al. 2008; Tardat et al. 2010; Terai et al. 2013; Zhang et al. 2013; Shibata et al. 2014; Slenn et al. 2014). CDT1 is required in G1 for rendering DNA replication origins competent for initiation in S phase (a process termed origin licensing) (Nishitani et al. 2000; Maiorano et al. 2000). SET8 is the sole enzyme responsible for histone H4 lysine 20 monomethylation (H4K20me1) and, like CDT1, is also required for origin licensing (Tardat et al. 2010). Degradation of CDT1 and SET8 at the onset of S phase restricts DNA replication to no more than once per cell cycle by preventing re-licensing of replicated origins. Failure to degrade either CDT1 or SET8 results in multiple rounds of origin firing leading to DNA re-replication and ultimately significant DNA damage and genome instability (Arias and Walter 2005; Tardat et al. 2010; Abbas et al. 2010; Arias and Walter 2006; Kerns et al. 2007; Li and Blow 2005; Takeda et al. 2005; Vaziri et al. 2003; Yoshida et al. 2005). Likewise, persistence of human thymine DNA glycosylase in S phase slows proliferation (Shibata et al. 2014). Degradation of p21 in early S phase stimulates CDK2 activity which in turn, triggers key S phase events including DNA replication initiation and origin licensing inhibition (Abbas et al. 2008; Nishitani et al. 2008). During S phase, p12 levels are 35% of their G2/M and G1 levels resulting in the presence of both Polδ3 (Polδ lacking p12) and Polδ4 (Polδ containing p12) during S phase (Zhang et al. 2013). Since the two forms of Polδ have

complementary biochemical properties (Zhang et al. 2013; Meng et al. 2010), $CRL4^{CDT2}$-mediated degradation of p12 during S phase may be important for DNA replication fidelity.

Each of the proteins known to be subject to replication-coupled destruction follows a pattern of low abundance during S phase then rapid re-accumulation prior to mitosis (illustrated in **Figure A.1**). Importantly, CDT1, p21, and SET8 also function during mitosis, making their re-accumulation critical for normal mitotic progression (Varma et al. 2012; Kreis et al. 2013; Wu et al. 2010). Replication-coupled destruction is triggered by the ubiquitin E3 ligase, $CRL4^{CDT2}$. The mechanism of $CRL4^{CDT2}$ substrate recognition is unique in that the substrates must first interact with DNA-loaded PCNA ($PCNA^{DNA}$), and PCNA is DNA-loaded during both S phase and DNA repair (Arias and Walter 2007; Higa et al. 2003; Machida et al. 2005; Teer et al. 2006). Given the robust re-accumulation of $CRL4^{CDT2}$ substrates well in advance of mitosis, we sought to determine the relationship between PCNA *unloading* in late S phase and re-accumulation of $CRL4^{CDT2}$ substrates.

We have discovered that surprisingly, $CRL4^{CDT2}$ substrates accumulate *prior* to PCNA unloading and the completion of replication. Moreover, we demonstrate that activation of CDK1 inhibits degradation of $CRL4^{CDT2}$ substrates. We show here that CDK1 activity (either directly and/or indirectly) inhibits $CRL4^{CDT2}$ activity itself by preventing its accumulation on chromatin, an event necessary for $CRL4^{CDT2}$ activity. Activation of CDK1 as S phase completes is necessary for the normal re-accumulation of substrates such as CDT1 and SET8, and we show that, like CDT1, failure to re-accumulate SET8 *de novo* prior to mitosis leads to mitotic progression defects (Varma et al. 2012). The temporal control of $CRL4^{CDT2}$ activity ensures the accumulation of $CRL4^{CDT2}$ substrates during mitosis, thereby preventing chromosome instability. We propose that purposeful protection from replication-coupled destruction anticipates the end of S phase and primes efficient progression through mitosis.

Results

CRL4^{CDT2} substrate accumulation occurs in late S phase prior to PCNA unloading.

Previous work described replication-coupled destruction of CRL4^{CDT2} substrates and further documented their robust accumulation at later cell cycle stages illustrated in Figure 1A. Given that PCNA loading at replication and repair sites ("PCNA^{DNA}") is a prerequisite for CRL4^{CDT2} targeting, the normal substrate re-accumulation as S phase ends could simply be a consequence of PCNA unloading as replication completes. Nevertheless, replication can extend close to the time of mitosis, and this late replication has been implicated in the genome instability associated with common fragile sites (Debatisse et al. 2012). Since PCNA^{DNA} triggers CRL4^{CDT2}- mediated degradation, persistence of PCNA^{DNA} so late in S phase was not fully consistent with observations by us and others that CRL4^{CDT2} substrates re-accumulate well in advance of mitosis (Zhang et al. 2013; Abbas et al. 2010; Nishitani et al. 2008; Chandrasekaran et al. 2011). We therefore considered the possibility that substrates may be actively stabilized during the transition from S phase to mitosis. If so, then CRL4^{CDT2} substrates may in fact accumulate prior to PCNA^{DNA} unloading.

To test this idea we interrogated the timing of CRL4^{CDT2} substrate accumulation in individual cells relative to the dynamics of PCNA^{DNA} unloading as cells completed S phase. We synchronized cells in early S phase, released them to proceed to late S phase, and then extracted soluble proteins prior to fixation and immunostaining for endogenous PCNA^{DNA} and the CRL4^{CDT2} substrates CDT1, p21, and SET8. As expected, cells in early S phase had abundant PCNA^{DNA} in a characteristic early S phase pattern (Leonhardt et al. 2000) but had very little CDT1 (**Figure A.1B**, *top row*) and similarly low levels of p21 and SET8 (**Figures A.1C and D**, *top rows*). In late S phase (7 hours post release), PCNA was still DNA-loaded in some cells, and CDT1, p21, and SET8 were readily detectable in those same cells (**Figure A.1B**, *bottom row*, **A.1C, and D**). Late S phase cells are characterized by foci of

chromatin-bound PCNA at the nuclear periphery with more diffuse nuclear staining elsewhere as seen in **Figure A.1B and C** (Leonhardt et al. 2000). (Multiple mechanisms recruit these proteins to chromatin resulting in only partial co-localization with PCNA foci.) We counted the number of cells that retained $PCNA^{DNA}$ foci 7 hours into S phase (14%, n=150) and then scored those that also contained nuclear p21, SET8, or CDT1 using antibodies to the endogenous proteins. We found that 40-65% of $PCNA^{DNA}$-positive cells already had abundant $CRL4^{CDT2}$ substrates (**Figure A.1E**, we cannot distinguish differences among the individual substrate kinetics from differences in antibody avidity). Importantly, individual late S phase cells that retained $PCNA^{DNA}$ had nearly equivalent amounts of $PCNA^{DNA}$ relative to their early S phase counterparts (**Figure A.1F**). Thus, the accumulation of substrates was not accounted for by the amount of $PCNA^{DNA}$ declining in individual late S phase cells. The fact that cells with similar amounts of $PCNA^{DNA}$ showed dramatically different abilities to support replication-coupled destruction indicates a qualitative difference between early and late S phase cells with regard to $CRL4^{CDT2}$ activity. Moreover, the presence of CDT1, SET8, and p21 in late S phase nuclei with $PCNA^{DNA}$ suggested an active mechanism to inhibit $CRL4^{CDT2}$-mediated degradation.

$CRL4^{CDT2}$ substrates cannot be targeted during mitosis.

[It is worth noting that at 7 hours post-release (**Figure A.1**), not every cell contained both $PCNA^{DNA}$ and $CRL4^{CDT2}$ substrates consistent with the observation that even in synchronized cells, progression through S phase is not perfectly uniform. Our time courses indicate that the onset of $CRL4^{CDT2}$ substrate accumulation occurs during the final ~10-15% of S phase based on an average 7-8 hour S phase and mitotic entry at 8-9 hours (e.g. **Figure A.4A**). Since we could not arrest cells in very late S phase for biochemical analysis, we took advantage of the next available robust cell cycle block in prometaphase, which is

Figure A.1.

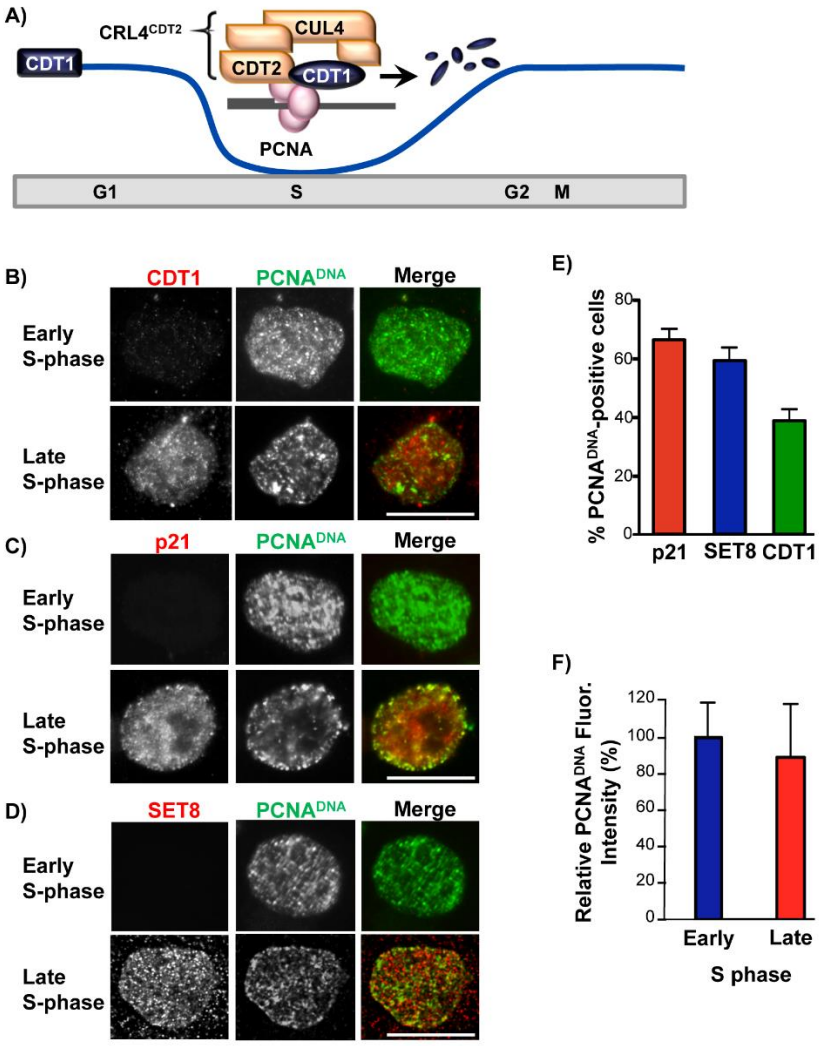

Figure A.1. Targets of replication-coupled destruction re-accumulate prior to the end of S phase. *A*, In early S phase PCNA is loaded onto DNA and is bound by $CRL4^{CDT2}$ substrates (e.g. CDT1). The interaction of substrates with $PCNA^{DNA}$ recruits the $CRL4^{CDT2}$ E3 ubiquitin ligase via the CDT2 substrate receptor subunit for replication-coupled destruction.
B, HCT116 cells were synchronized in early S phase by double-thymidine block. Soluble proteins were extracted, and bound proteins were fixed in early S phase (during the arrest) or in late S phase 7 h after release into fresh medium. Endogenous $PCNA^{DNA}$ and CDT1 were detected by immunostaining.
C and *D,* as in *B* except that p21 or SET8 were detected by immunostaining. Scale bars = 5 µm in B-D.
E, The percent of late S phase cells containing $PCNA^{DNA}$ that also contained SET8 (n = 60), p21 (n = 100), or CDT1 (n = 122) was quantified.
F, Total PCNA nuclear fluorescence was quantified for the early and late S phase samples in B (n = 15). A total of 60 cells were counted over three biological replicates ($\geq$15 cells were counted per replicate). Averages and standard deviations are indicated in both E and F.

1-2 hours later, to generate homogenous cell populations. To determine if $CRL4^{CDT2}$ substrates are actively protected from degradation late in the cell cycle, we deliberately stimulated synchronous replication-coupled destruction by UV-irradiating prometaphase cells. UV irradiation causes robust and simultaneous PCNA loading onto DNA during nucleotide excision repair, and thus UV treatment causes highly synchronous replication-coupled destruction of $CRL4^{CDT2}$ substrates by the same mechanism that operates during S phase (reviewed in (Abbas and Dutta 2011)). (Note that $CRL4^{CDT2}$-mediated degradation is stimulated by DNA synthesis *per se* and is not a component of the DNA damage checkpoint response (Higa et al. 2003)). We monitored the levels of CDT1 as well as three other $CRL4^{CDT2}$ substrates by immunoblotting lysates from the two conditions. As expected in asynchronous cells, CDT1, SET8, p21, and p12 were degraded following UV irradiation (**Figure A.2A and A.2B**, lanes 1 and 2). In stark contrast however, none of the four substrates were degraded in prometaphase cells (**Figure A.2A and B**, lanes 3 and 4).**]**

$CRL4^{CDT2}$ substrates are resistant to degradation in some quiescent cells because the substrate adapter subunit, CDT2, is itself degraded (Abbas et al. 2013b; Rossi et al. 2013). CDT2 was equally present in both asynchronous and prometaphase cells, so the substrate protection we observed could not be attributed to loss of CDT2 under these conditions (**Figure A.2B**, lanes 3 and 4). Importantly, releasing mitotic cells into the subsequent G1 fully restored sensitivity of SET8 and CDT1 to $CRL4^{CDT2}$-mediated degradation (**Figure A.2C**). SET8 is also an APC/C target (Wu et al. 2010), and we observed the expected low SET8 levels in untreated G1 cells relative to mitotic cells. Taken together, we conclude that the substrates of $CRL4^{CDT2}$ are protected from degradation in a cell cycle-dependent manner.

Figure A.2.

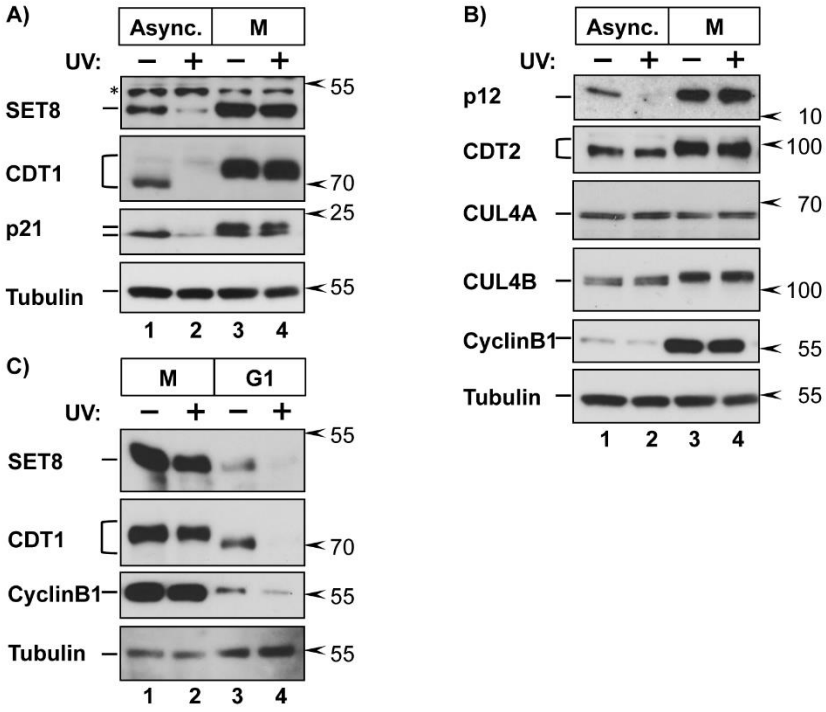

Figure A.2. CRL4^{CDT2} substrates are protected in mitosis.
[*A* and *B*, HCT116 cells were grown asynchronously ("Async.") or synchronized in prometaphase by release from a thymidine block into 100 nM nocodazole for 10 h ("M"). Cells were irradiated with 20 J/m^2 UV to induce PCNA^{DNA} loading (DNA repair synthesis) and harvested 2 h later or left untreated as indicated. Endogenous proteins were detected in whole cell lysates by immunoblotting (* in *A* denotes a nonspecific background band).**]**
C, HCT116 cells were synchronized in prometaphase as in *A* and released into fresh media for 2.5 h to proceed to G1. Cells were UV irradiated and harvested 90 min later followed by immunoblotting for the indicated proteins.

Mitotic kinase activity is required for protection from CRL4^{CDT2}-mediated degradation.

Our observation that CRL4^{CDT2} substrates are stable from late S phase through mitosis but susceptible to replication-coupled destruction during G1 suggested that a mitotic activity, such as one or more mitotic protein kinases, confers protection from CRL4^{CDT2}-mediated degradation. To test that possibility, we employed pharmacological inhibition of candidate kinases: cyclin-dependent kinases (CDKs) and the stress-activated mitogen-activated protein kinases (MAPK) p38 and JNK, which we previously showed could stabilize CRL4^{CDT2} substrates (Chandrasekaran et al. 2011). We briefly treated prometaphase cells with kinase inhibitors prior to UV irradiation then tested for reversal of mitotic stability by immunoblotting (**Figure A.3A and B**). In control cells as before, CRL4^{CDT2} substrates were stable in mitotic cells, but strikingly, treatment with the CDK1-specific inhibitor RO-3306 effectively reversed the protection (**Figure A.3A**, compare lanes 4 and 6; **Figure A.3B**, compare lanes 4 and 5). In contrast, treatment with the p38 or JNK inhibitors had little-to-no effect on substrate protection (**Figure A.3B**, lanes 6 and 7). Note that both p38 and JNK are active not only in mitosis but are also induced by UV (Yujiri et al. 1999; Takenaka et al. 1998); the JNK and p38 inhibitors were effective for inhibiting their respective kinases at these concentrations as measured by phosphorylation of representative substrates (**Figure A.3B** bottom panels). CDK1 inhibition also caused Cyclin B1 degradation (**Figure A.3B**, lanes 5 and 8), which is consistent with prior studies showing that inhibiting CDK1 in mitotic cells activates APC^{Cdc20} (Pesin and Orr-Weaver 2008; Yu 2007). (SET8 is also an APC^{Cdc20} target, but SET8 phosphorylation during mitosis blocks APC^{Cdc20} binding so SET8 was not degraded in cells treated with the CDK1 inhibitor alone (Wu et al. 2010)). Importantly, only CDK1 inhibition re-sensitized CRL4^{CDT2} substrates in mitosis (**Figure A.3B** compare lane 4 with lanes 5, 6, and 7). Even simultaneous inhibition of p38 and JNK could not substitute for CDK1 inhibition (data not shown). Furthermore, increasing concentrations of the CDK1 inhibitor resulted in progressive loss of CRL4^{CDT2} substrate protection (**Figure A.3C**).

We confirmed that re-acquisition of UV-induced degradation in CDK1-inhibited cells was still CUL4-dependent by co-treatment with the neddylation inhibitor, MLN4924 (**Figure A.3D**, compare lanes 6 and 8). Together, these data indicate that CDK1 activity is required for the protection of CRL^{CDT2} substrates from replication-coupled destruction.

CDK1 activity is required for substrate $CRL4^{CDT2}$ re-accumulation in late S phase.

[To understand the relationship of CDK1 activity in late S phase cells to the kinetics of $CRL4^{CDT2}$ substrate re-accumulation, we treated synchronized cells in mid-S phase (5 hours post thymidine release) with the CDK1 inhibitor. We then monitored both cell cycle progression and the anticipated re-accumulation of CDT1 and SET8 as S phase completed (**Figures A.4A and B**). Treatment with the CDK1 inhibitor, RO-3306, in asynchronous cells results in a G2 arrest (Vassilev 2006), and as expected it blocked cells released from early S synchronization, but CDK1 inhibition did not prevent S phase completion (**Figure A.4A**). However, CDK1 inhibition strongly and reproducibly dampened the normal late S and G2 increase in both SET8 and CDT1 protein levels **(Figure A.4B)**, compare lanes 5-8 to lanes 10-13). The levels of Cyclin A and Cyclin B1 at the 7 and 8 hour time points corresponding to late S and G2 phases were unperturbed by the inhibitor, but at the normal time of mitosis (at 9 hours) CDK1 inhibition caused premature Cyclin B1 loss, consistent with results in nocodazole-arrested cells (**Figure A.3B**, lanes 9-11). Importantly, these effects on Cyclin B1 levels happened 2 hours after the delay in CDT1 and SET8 re-accumulation.**]**

We once again examined individual late S phase cells (7 hours post-release) for the presence of both $PCNA^{DNA}$ and SET8 or CDT1. In a substantial proportion of control $PCNA^{DNA}$-positive cells SET8 and CDT1 had already re-accumulated, similar to **Figure A.1E** (**Figure A.4C**). When CDK1 was inhibited starting at 5 hours post S phase release however, the percent of double positive cell decreased nearly two-fold (**Figure A.4C**). Since the effects of CDK1 inhibition on $CRL4^{CDT2}$ substrate accumulation occurred well in advance of

Figure A.3.

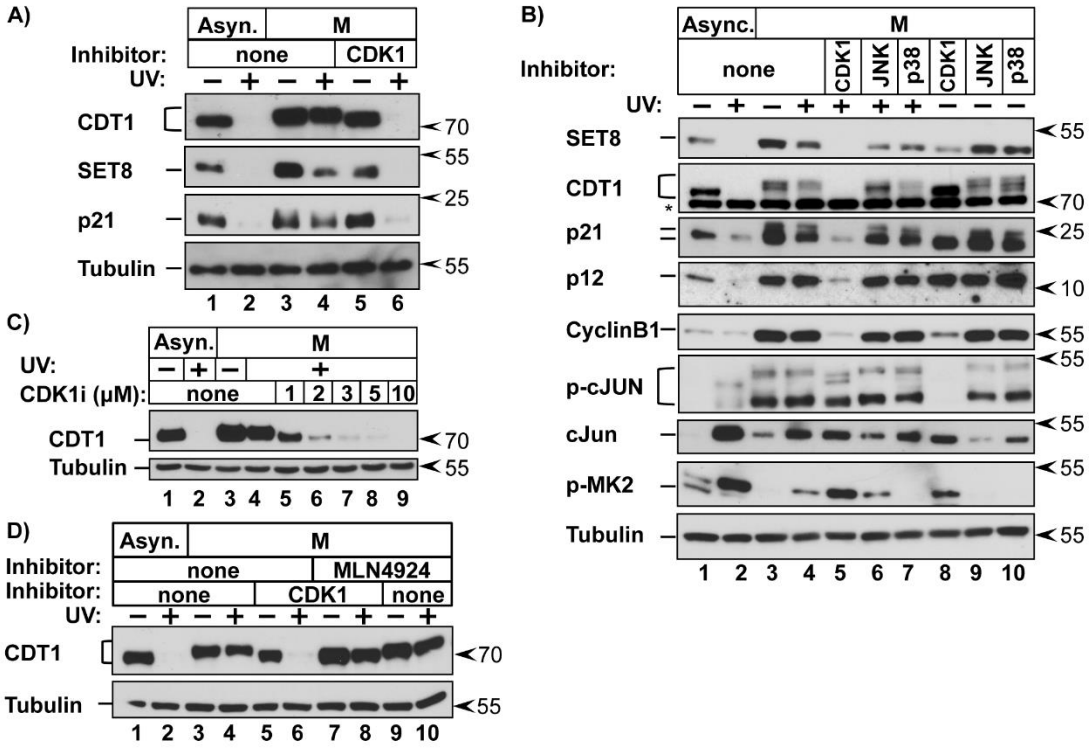

Figure A.3. CDK1 activity is required for CRL4^{CDT2} substrate protection.
A, Asynchronous or prometaphase HCT116 cells were treated with the CDK1 inhibitor RO-3306 as indicated 30 min prior to PCNA^{DNA} induction by UV and harvested 2 h later.
B, Top panel: Asynchronous or prometaphase cells were treated with the indicated kinase inhibitors or DMSO ("none") for 30 min prior to PCNA^{DNA} induction by UV irradiation. Endogenous proteins were detected by immunoblotting of whole cell lysates Bottom panels: Asynchronous cells were treated with the inhibitor JNK VIII or SB203580 (p38 inhibitor) 30 min prior to treatment with 250 mM NaCl and/or UV irradiation as indicated. (Hyperphosphorylated c-JUN migrates significantly slower than the partially phosphorylated form).
C, Asynchronous or prometaphase HCT116 cells were treated with indicated concentrations of RO-3306 for 30 min prior to UV irradiation and harvested 1 h later.
D, Asynchronous or prometaphase cells were untreated (-) or treated with UV (+) to induce PCNA^{DNA} and harvested 1 h after treatment. The CDK1 inhibitor RO-3306 and/or the CUL4 neddylation inhibitor MLN4924 (5 μM) were added 30 min prior to UV irradiation as indicated.

mitosis, CDK1 activity inhibits $CRL4^{CDT2}$ not only in prometaphase-arrested cells, but also during the transition from S phase into G2 and mitosis.

$CRL4^{CDT2}$ activity is itself inhibited.

[Our prior work provided evidence for stabilization of CDT1 by direct phosphorylation as cells transit from S phase to M phase (Chandrasekaran et al. 2011; Varma et al. 2012). Furthermore, our study and that of Kim et. al. (Kim et al. 2002) suggested that a similar direct p21 phosphorylation mechanism could control p21 stability. To determine if protection from $CRL4^{CDT2}$-mediated degradation during late cell cycle stages is solely the consequence of direct substrate phosphorylation, we expressed epitope-tagged WT p21 (HA-p21-WT) or p21 harboring alanine substitutions at the two phosphorylation sites that were reported to stabilize p21, T57 and S130 (HA-p21-AA) (Kim et al. 2002). In synchronized cells, both HA-p21-WT and HA-p21-AA (as well as endogenous p21) migrated slower by SDS-PAGE compared to asynchronous cells, and this mobility shift was reversed by phosphatase treatment (**Figure A.5A**, lanes 5 and 10). The HA-p21-AA mutant migrated faster than WT HA-p21 in lysates of mitotic cells but was just as stable as both ectopic and endogenous WT p21 (**Figure A.5A**, compare lanes 4 and 8). Residual sites of p21 phosphorylation affect p21 gel mobility, but have not been shown to affect p21 stability ((Hodeify et al. 2011) and reviewed in and reviewed in (Child and Mann 2006)). Nevertheless, mitotic phosphorylation of p21 at T57 and S130 is not the principal reason p21 is stable in mitotic cells.**]**

We similarly expressed epitope-tagged versions of WT CDT1 and CDT1 harboring 5 alanine substitutions (CDT1-5A) at the mitotic phosphorylation sites we had previously shown to stabilize CDT1. Specifically, we had shown that CDT1-5A is not protected from $CRL4^{CDT2}$ by stress MAP kinase activation (Chandrasekaran et al. 2011). These cells were then subjected to UV irradiation during asynchronous culture or after synchronization in prometaphase. Both endogenous CDT1 and epitope-tagged WT CDT1 were protected in

Figure A.4.

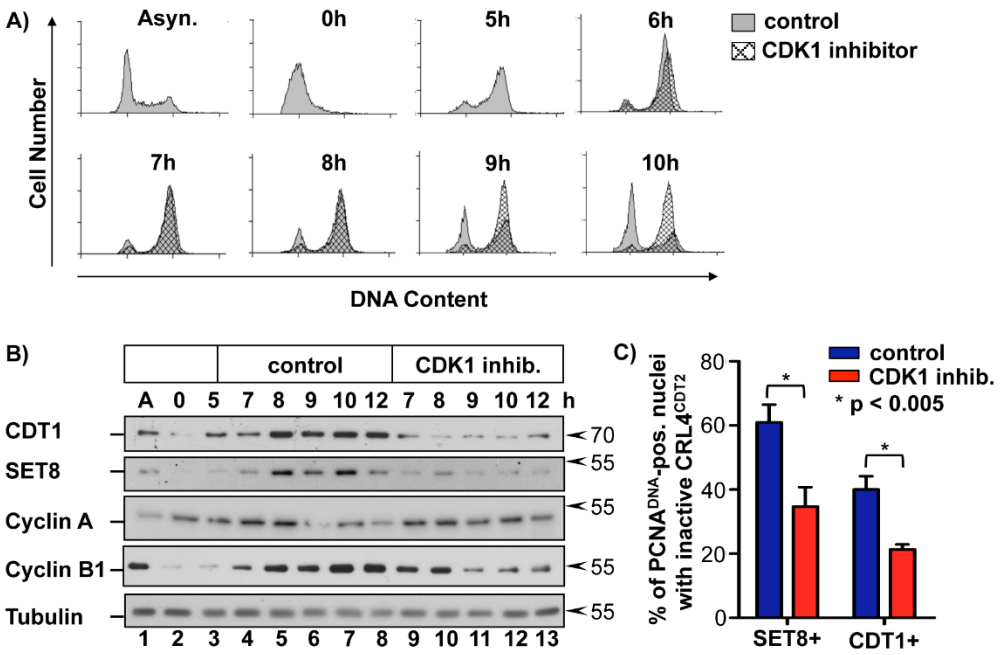

Figure A.4. CDK1 activity is required for substrate re-accumulation in late S phase. [*A*, HCT116 cells were synchronized in early S phase via double thymidine block and 5 h after release were treated with RO-3306 or DMSO (control). Cells were harvested at the indicated time points and analyzed for DNA content by flow cytometry.
B, HCT116 cells were treated as in *A* harvested at the indicated time points and analyzed via immunoblotting**.]**
C, HCT116 cells were treated as in *A*. Soluble proteins were extracted, and bound proteins were fixed in early S phase (during the arrest) or in late S phase 7 h after release into fresh medium. Endogenous $PCNA^{DNA}$, SET8, and CDT1 were detected by immunostaining as in Figure 1. Late S phase cells containing $PCNA^{DNA}$ were scored for the presence of SET8 or CDT1 as an indicator of inactive $CRL4^{CDT2}$ ($n \geq 75$ for each sample).

synchronized cells (**Figure A.5B**, compare lanes 6 and 8), and as expected, both WT proteins migrated slower by SDS-PAGE compared to asynchronous cells. CDT1-5A migrated slightly faster than WT CDT1 from lysates of mitotic cells, consistent with our prior analysis of this mutant. The clear residual mitotic shift of this mutant is consistent with additional phosphorylation sites in CDT1 that may or may not affect its stability (Miotto and Struhl 2011; Liu et al. 2004; Sugimoto et al. 2004). Like the p21-AA mutant, CDT1-5A was just as stable as both ectopic and endogenous CDT1 in prometaphase cells indicating that phosphorylation at these sites previously shown to stabilize CDT1 is not solely responsible for CDT1 mitotic stability (**Figure A.5B**, lanes 9-12). Together, these observations indicate that protection from $CRL4^{CDT2}$ likely involves more than phosphorylation of the substrates themselves. Moreover, the fact that all four of the tested $CRL4^{CDT2}$ substrates were resistant to degradation suggests that $CRL4^{CDT2}$ is globally suppressed during progression from late S phase into mitosis.

To probe the activity of $CRL4^{CDT2}$ itself in mitosis, we designed two reporter constructs for stable expression in which the N-terminal 28 amino acids of CDT1 were fused to either red fluorescent protein (RFP) or the SNAP-tag (Keppler et al. 2003). The N-terminal 28 amino acids contain CDT1's PIP degron and was previously shown to confer CUL4-dependent degradation to a heterologous protein (Senga et al. 2006). Importantly, neither reporter construct contains canonical CDK or MAPK phosphorylation sites. In asynchronously growing cells, the SNAP reporter fusion was degraded following UV irradiation (**Figure A.5C**, lanes 1 and 2); however, in prometaphase cells the reporter was stable (**Figure A.5C**, lanes 3 and 4). Furthermore, CDK1 inhibition re-sensitized the SNAP reporter to degradation (**Figure A.5C**, lanes 5 and 6) indicating that regulation of this reporter is similar to endogenous $CRL4^{CDT2}$ substrates. We observed nearly identical CDK1-dependent stabilization of the RFP reporter (**Figure A.5D**). These findings indicate that the ability of $CRL4^{CDT2}$ to target substrates is generally inhibited via a CDK1-dependent event

independently of any additional phosphorylation-mediated mechanisms of direct substrate stabilization.

CDK1 activity prevents chromatin association of CDT2.

[During productive $CRL4^{CDT2}$ targeting, PCNA is first loaded onto DNA for replication (S phase) or repair (e.g. post-UV). Proteins containing PIP degrons bind to $PCNA^{DNA}$, and the resulting complex is then recognized by the substrate receptor, CDT2 (Havens and Walter 2009). We postulated that one or more of these steps is inhibited by CDK1. We first tested if PCNA can be successfully loaded onto mitotic chromatin by UV-irradiating nocodazole-synchronized cells then analyzing chromatin fractions. We detected PCNA in chromatin fractions from untreated asynchronous cells (reflecting the S phase fraction; **Figure A.6A,** lane 7), and $PCNA^{DNA}$ was further induced by UV irradiation, which stimulates PCNA loading in all cell cycle phases (**Figure A.6A, lane 8**). As previously reported, CUL4A is also recruited to chromatin following UV irradiation (Groisman et al. 2003; Guerrero-Santoro et al. 2008; Kapetanaki et al. 2006), and as expected, a resident chromatin protein, ORC2, is unaffected **(Figure A.6A)**. In otherwise untreated mitotic cells, PCNA was not DNA-associated (as expected), but was loaded following UV irradiation (**Figure A.6A, lane 10**). Thus, mitotic chromatin is not *intrinsically* resistant to PCNA loading. In addition, PCNA from extracts of mitotic and asynchronous cells showed similar binding to recombinant p21 (but not a p21 PIP box mutant) *in vitro* (**Figure A.6B**). In stark contrast to PCNA, CDT2 could not be inducibly recruited to mitotic chromatin though it was readily recruited to chromatin in asynchronously growing cells (**Figure A.6A**, compare lanes 8 and 10). Finally, CDK1 inhibition restored CDT2 chromatin recruitment in mitotic cells (**Figure A.6A**, compare lanes 10 and 12). Thus, the CDK1-dependent inhibition of $CRL4^{CDT2}$- mediated degradation operates by interfering with chromatin recruitment of the CDT2 substrate receptor. Consistent with this finding, we noted that CDT2 is lost from chromatin fractions in late S

Figure A.5.

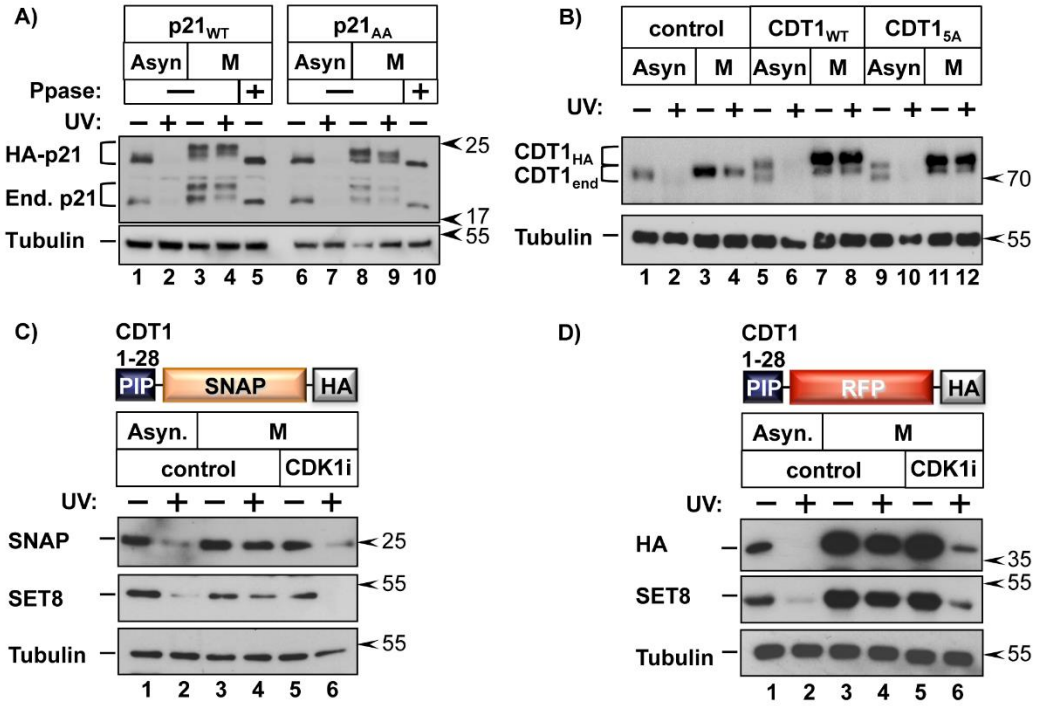

Figure A.5. **CDK1- dependent inhibition of CRL4^{CDT2} activity. [***A*, HCT116 cells stably expressing HA-tagged WT or p21-AA (T57A and S130A mutations) were grown asynchronously or arrested in prometaphase. Cells were harvested 2 h after PCNA^{DNA} induction by UV irradiation; cell lysates were treated with λ-phosphatase (Ppase) prior to SDS-PAGE as indicated.**]**
B, HeLa cells stably expressing HA-tagged WT or CDT1-5A (39) were grown asynchronously or arrested in prometaphase. Cells were harvested 1 h after PCNA^{DNA} induction by UV.
C, HeLa cells stably expressing the illustrated PIP degron-SNAP fusion were grown asynchronously or arrested in prometaphase and treated with the CDK1 inhibitor RO-3306 or control DMSO 30 min prior to PCNA^{DNA} induction by UV irradiation; cells were harvested 1hr after UV.
D, As in *C* except with HeLa cells stably expressing a PIP degron-RFP (mCherry) fusion.

phase earlier than PCNA itself (**Figure A.6C**, lanes 11-13) coincident with the normal re-accumulation time points for CDT1 and SET8 (e.g. **Figures A.1B, A.1D and A.4B**).**]**

De novo SET8 re-accumulation is essential for normal mitotic progression.

Having demonstrated active inhibition of $CRL4^{CDT2}$ targeting as cells progress from S phase to M phase, we next considered the possible biological significance of this mechanism. Replication-coupled destruction via $CRL4^{CDT2}$ during S phase ensures a single round of replication through the destruction of both CDT1 and SET8; their abnormal persistence in S phase leads to repeated rounds of origin relicensing and re-replication (Arias and Walter 2005; Tardat et al. 2010). On the basis of these facts alone, it should be detrimental to actively accumulate proteins like CDT1 and SET8 prior to the subsequent G1. However, CDT1 also has an essential function in mitosis that we recently documented (Varma et al. 2012), thus providing incentive for high levels of CDT1 before mitosis. In addition, sufficient levels of p21 are required in mitosis for normal mitotic progression (Kreis et al. 2013). Given that all $CRL4^{CDT2}$ substrates follow a similar pattern of mitotic stabilization, we postulated that CDT1 is not the only substrate needed in abundance and *de novo* at the end of S phase, and we turned our attention to SET8. Depleting SET8 from asynchronous cells leads to multiple defects including not only inefficient origin licensing in G1 but also impaired chromatin condensation in mitosis. Thus far, these phenotypes have all been attributed to the loss of SET8-deposited histone H4K20me1 (Tardat et al. 2010; Wu et al. 2010; Oda et al. 2010). However, it is not yet known if the mitotic defects from SET8 depletion are due to the absence of SET8 specifically during G2 and mitosis or if they arise *secondarily* from the absence of SET8 in a prior cell cycle phase such as G1. It is possible that SET8 activity deposits the essential methylations for chromosome condensation during G1 making SET8 dispensable during G2.

Figure A.6.

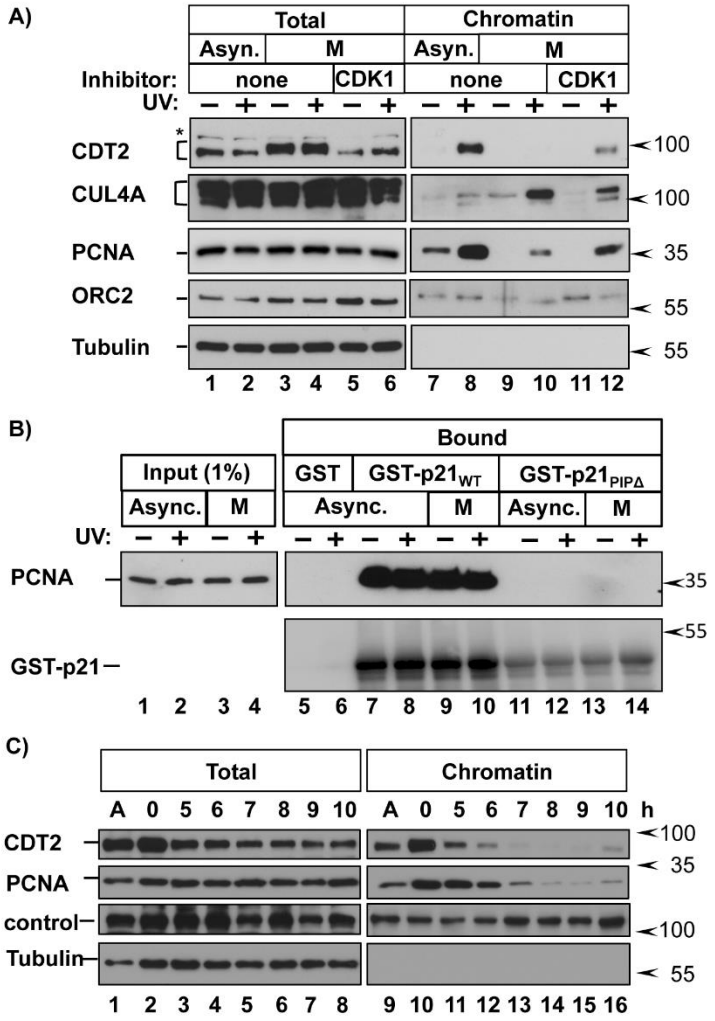

Figure A.6. CDK1 activity prevents CDT2 chromatin recruitment. [*A*, HCT116 cells were grown asynchronously or synchronized in prometaphase. Cells were treated with DMSO ("none") or the CDK1 inhibitor RO-3306 for 30 min prior to $PCNA^{DNA}$ induction by UV irradiation and harvested 90 min later. Endogenous proteins in whole cell extracts and chromatin-bound fractions were analyzed by immunoblotting.**]**

B, GST, GST-$p21_{WT}$, or GST-$p21\Delta_{PIP}$ were produced in *E. coli* and bound to glutathione beads. The protein-coated beads were then incubated with whole cell lysates from asynchronous or mitotic cells as described in (39). Endogenous PCNA and GST-tagged p21 were detected by immunoblotting.

[*C*, HCT116 cells were synchronized in early S phase via double thymidine block and released into fresh media. Cells were harvested at the indicated time points. Endogenous proteins in whole cell extracts and chromatin-bound fractions were analyzed by immunoblotting.**]**

To determine if SET8 is required specifically *during* transit from late S phase into mitosis, we employed a synchronization-knockdown procedure we developed during the investigation of CDT1's mitotic function. We synchronized cells in early S phase after the G1 function of SET8 had been fully completed and released them in the presence of either control or *SET8* siRNA to proceed otherwise unperturbed through S phase (**Figure A.7A**). *SET8* siRNA effectively prevented accumulation of both SET8 and monomethylation of histone H4K20 after S phase (**Figure A.7B**, compare lanes 2-7 to lanes 8-13). Of note, SET8 depletion also caused a reduction in H4K20me2 indicating that establishment of histone H4K20me1 during late S phase is required to maintain H4K20me2 levels during G2 and mitosis. H4K20me1 has recently been shown to be required for proper kinetochore assembly (Hori et al. 2014). Our data clearly support this finding and further indicate that this deposition occurs during G2/M as SET8 re-accumulates (**Figure A.7B**).

We examined mitotic chromosome morphology in the synchronized SET8-depleted cells by staining for DNA with DAPI and for the mitotic spindle with anti-tubulin. Control cells analyzed 10 hours after release from the early S phase block contained metaphase chromosomes that were fully condensed and properly aligned at the metaphase plate (**Figure A.7C**, top panel). In contrast, chromosomes in cells that had normal SET8 in G1, but contained little-to-no SET8 only in G2 were less dense and formed a "cloud" of DNA that failed to align properly in metaphase (**Figure A.7C**, bottom panels). We replicated both the failure to re-accumulate normal H4K20me1 and the mitotic chromosome condensation defects using a different *SET8* siRNA in synchronized cells (**Figure A.7D**). Furthermore, we quantified mitotic progression 10 hours after thymidine release: cells with normal SET8 in G1 but blocked from re-accumulating SET8 in late S/ G2 were significantly enriched in pre-anaphase states with a corresponding decrease in cells that had completed anaphase at 10

Figure A.7.

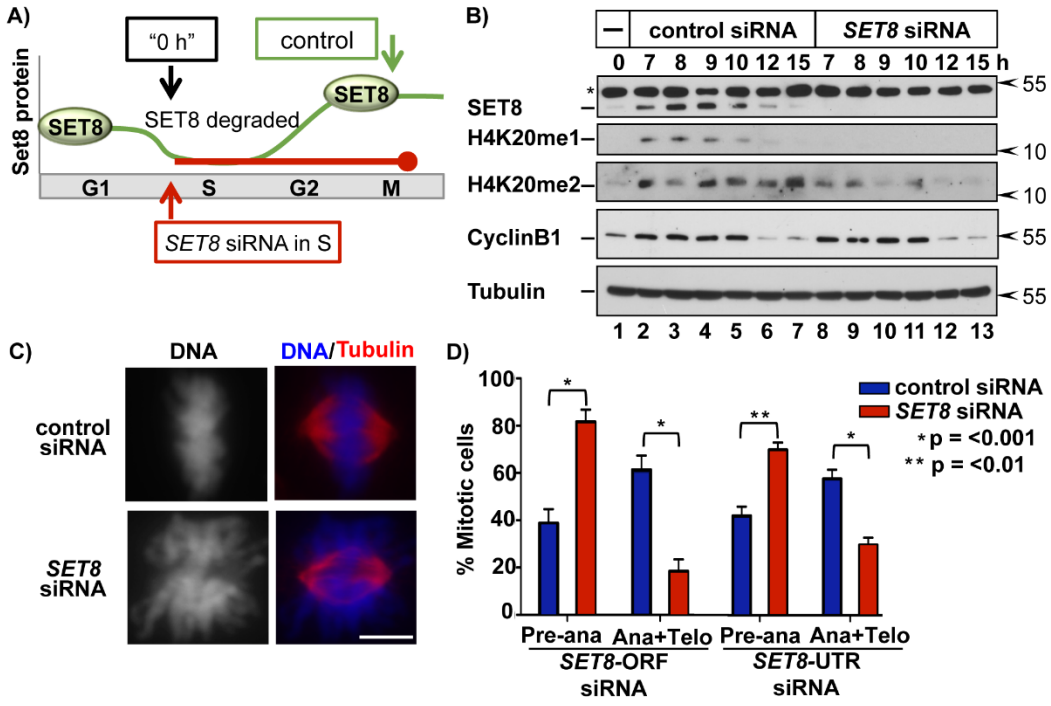

Figure A.7. *De novo* SET8 re-accumulation after S phase is necessary for normal mitotic progression. *A*, Illustration of the experimental approach to block SET8 re-accumulation only after S phase.
B, HCT116 cells were synchronized in early S phase via double-thymidine block. Cells were released into fresh medium containing control (luciferase) or *SET8*-ORF siRNA and harvested at the indicated time points for immunoblotting of the indicated endogenous proteins (* denotes a nonspecific background band).
C, Cells were synchronized as in *A* then released into siRNA-containing medium for 10 h prior to fixation and immunofluorescence staining for tubulin and DAPI staining for DNA. Scale bar = 5 µm.
D, The number of mitotic cells from *C* in pre-anaphase *vs.* anaphase/telophase was quantified in three biological replicates (n=300 for each replicate) using two different siRNAs as indicated.

hours (**Figure A.7D**). These data highlight the importance of SET8 re-accumulation, and by extension general $CRL4^{CDT2}$ inhibition, prior to mitosis for proper chromosome condensation and mitotic progression. Thus, CDK1 activity in late S phase and G2 phase is required for the normally robust rebound in the levels of $CRL4^{CDT2}$ substrates, and the re-accumulation (of CDT1 and SET8) is important for proper mitotic progression.

Discussion

At least three substrates (CDT1, p21, and SET8) have known roles in mitosis (Varma et al. 2012; Kreis et al. 2013; Wu et al. 2010; Centore et al. 2010), and it is possible that other $CRL4^{CDT2}$ substrates also have mitotic roles making general substrate stabilization important for mitosis. Independent of these mitotic roles, the known substrates of replication-coupled destruction via $CRL4^{CDT2}$ are proteins with clear roles in G1 or S phase. For example, the early step of origin licensing, minichromosome maintenance complex (MCM) recruitment to chromatin, begins in telophase (Nishitani and Lygerou 2002; Dimitrova et al. 2002). Thus, with respect to origin licensing, once the nuclear envelope reforms in telophase the daughter nuclei are G1-like nuclei in a shared cytoplasm. Since telophase occurs just 2-3 hours after the end of S phase in cultured somatic cells, active inhibition of replication-coupled destruction may also facilitate G1 events, a notion that has been suggested regarding CDT1 accumulation (Ballabeni et al. 2004, 2013; Tsunematsu et al. 2013). Based on our findings, this need for early accumulation may apply to the entire cohort of $CRL4^{CDT2}$ substrates.

$PCNA^{DNA}$ is an efficient and potent trigger for replication-coupled destruction. The bulk of CDT1 can be degraded within minutes of UV irradiation (Chandrasekaran et al. 2011) and occurs nearly simultaneously with S phase onset (Arias and Walter 2005, 2006; Nishitani et al. 2006). The potency of $PCNA^{DNA}$ then presents a challenge near the end of S phase because $CRL4^{CDT2}$ substrates are needed in abundance for mitosis and the

subsequent G1. (Though CDT1 can also be targeted by $CRL1^{SKP2}$ (Liu et al. 2004; Senga et al. 2006; Nishitani et al. 2006), we have noted in multiple cell lines that $CRL4^{CDT2}$ is the major regulator of CDT1 degradation in S phase (Chandrasekaran et al. 2011).) Replication of at least 1% of the genome occurs as late as 90 min prior to the onset of mitosis (Widrow et al. 1998), and this late replication requires the continued presence of $PCNA^{DNA}$. Instead of a long G2 phase following complete $PCNA^{DNA}$ unloading to allow buildup of essential mitotic proteins – including those that are actively degraded at the onset of S phase – G2 can be short because that buildup begins during late S phase. We detected significant amounts of $CRL4^{CDT2}$ substrates in the same cells that still contained nearly as much $PCNA^{DNA}$ as they did at the start of S phase. Our findings indicate that CDK1 itself or a CDK1-dependent activity overrides the ability of $PCNA^{DNA}$ to stimulate $CRL4^{CDT2}$ recruitment for replication-coupled destruction. The first active CDK1 complex that appears contains Cyclin A, and this form of CDK1 may be responsible for initiating $CRL4^{CDT2}$ inhibition; later inhibition would be accomplished via Cyclin B/CDK1. In keeping with this idea, pharmacological CDK1 inhibition blunted $CRL4^{CDT2}$ substrate re-accumulation at time points that coincide with the expected time of Cyclin A/CDK1 activity (**Figure A.4B**). Interestingly, depleting Cyclin A in early S phase-arrested embryonic stem cells prevented accumulation of CDT1 8 hours after release (Ballabeni et al. 2011).

It is clear that the ultimate target(s) of CDK1 (either direct or indirect) is neither $PCNA^{DNA}$ nor $PCNA^{DNA}$-substrate interactions, but rather the subsequent chromatin recruitment of CDT2 (illustrated in **Figure A.8**). This inhibition is distinct from the recently reported SCF-dependent CDT2 degradation and underscores the importance of regulating the CDT2 substrate receptor for cell cycle control (Abbas et al. 2013b; Rossi et al. 2013). In fact, phosphorylation of CDT2 during S phase promotes interaction with 14-3-3 proteins that protect CDT2 from this SCF-mediated degradation (Dar et al. 2014). We and others have

Figure A.8.

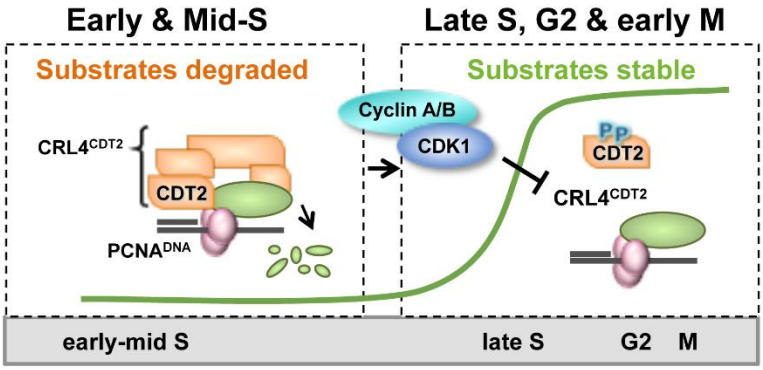

Figure A.8. Model. $CRL4^{CDT2}$ substrates are efficiently degraded in early S phase as a result of PCNA loading onto DNA ($PCNA^{DNA}$). Beginning in late S phase, active CDK1 blocks substrate-mediated chromatin recruitment of the CDT2 receptor allowing re-accumulation of the cohort of $CRL4^{CDT2}$ substrates that were subject to replication-coupled destruction. Many of these substrates are required for normal mitotic progression.

noted extensive mitotic phosphorylation of CDT2 in mitotic cells, and human CDT2 bears 19 conserved ser/thr-pro sites, but it is currently unknown if phosphorylation at these sites affects CDT2 substrate interactions. We have found however, that CDT2 binding to CRL4 is unaffected in mitosis (data not shown). Given the number of potential mitotic proline-directed kinases, the number of potential CDT2 phosphorylation sites, and observations that other members of the $CRL4^{CDT2}$ complex (CUL4A/B and Roc1) are phosphorylated in mitosis (Olsen et al. 2010; Dephoure et al. 2008), further studies are required to define the mechanism of $CRL4^{CDT2}$ inhibition. Since the details of how CDT2 contacts the substrate-$PCNA^{DNA}$ remain unknown, we cannot yet explain how a CDK1-dependent event blocks this interaction. Importantly however, CDT2 chromatin recruitment could conceivably be achieved by *any* PIP degron-PCNA complex in sufficient abundance, we infer that not only is the interaction between CDT2 and the substrates tested here inhibited, but the interaction between CDT2 and any as-yet undiscovered substrates is also inhibited. For example, two recent reports identified, thymine DNA glycosylase (TDG) as a target of $CRL4^{CDT2}$ in *Xenopus* and human cells (Shibata et al. 2014; Slenn et al. 2014). The behavior of our two reporter substrates and accumulated findings herein suggest that TDG is also protected via CDK1.

Substrates of replication-coupled destruction accumulate beginning in late S phase and are abundant in mitosis. In contrast, experimental manipulations that stabilize the substrates CDT1 or SET8 *throughout* S phase cause severe genome damage from origin re-licensing and re-firing (Arias and Walter 2005; Tardat et al. 2010; Abbas et al. 2010; Arias and Walter 2006; Li and Blow 2005; Jin et al. 2006; Dorn et al. 2009). If the continued presence of either CDT1 or SET8 during S phase is toxic, how then do G2 cells tolerate the high levels of both CDT1 and SET8 prior to mitosis? In other words, why do the high levels of CDT1 and SET8 not trigger re-replication in late S/G2/M? Replication-coupled destruction

is only one of many mechanisms that prevent re-replication, but interestingly many of the other mechanisms are not fully in place until late in S phase. For example, the CDT1 inhibitor, geminin, is induced in S phase but its levels are substantially lower in early S phase than in late S phase (Wohlschlegel et al. 2000; McGarry and Kirschner 1998). Other mechanisms such as the degradation of the largest subunit of the origin recognition complex, Orc1, and the nuclear export of the CDC6 licensing protein are also most evident in mid-to-late S phase (reviewed in (Arias and Walter 2007)). Further, Cyclin A/CDK2 (mid-to-late S phase) is a better inhibitor of origin licensing than Cyclin E/CDK2 (early-to mid S phase) (Wheeler et al. 2008). In addition, we recently provided evidence that the mitotic phosphorylation of CDT1 not only stabilizes CDT1 but also inhibits its licensing activity (Chandrasekaran et al. 2011). Of note, these additional mechanisms impacting $CRL4^{CDT2}$ substrate targeting likely fine-tune the kinetics of individual substrate degradation and re-accumulation. Therefore, in early S phase while both geminin and Cyclin A are low, we postulate that replication-coupled destruction of CDT1 and SET8 is most critical, but by late S phase, it is “safe” for CDT1 and SET8 to accumulate to high levels because the many other mechanisms that block origin re-licensing are by then fully established.

The anticipatory accumulation of proteins and activities prior to the cell cycle phase in which they are needed is well established. For example, a series of mid-G1 events including CDC6 accumulation results in replication origin licensing during late G1 that is in turn essential for S phase execution (Mailand and Diffley 2005). Likewise, Cyclin B1 accumulation in G2 occurs in advance of M phase. Moreover, the concept of a checkpoint that prevents a cell cycle transition until the preceding one is complete is also well known. We have explored here a variation on these themes in which an essential regulatory mechanism (replication-coupled destruction) is actively inhibited immediately before and during the next cell cycle phase (prior to and during M phase). In contrast to a checkpoint

that blocks the transition to the next phase, this mechanism blocks regulation of the current phase so the next phase can be launched efficiently. Re-accumulation of $CRL4^{CDT2}$ targets to their maximal levels in anticipation of their requirement primes cells for subsequent cell cycle events. As such, our discovery of CDK1-mediated inhibition of $CRL4^{CDT2}$ adds a new dimension to a general cell cycle theme: proactive preparation for cell cycle phase launch.

Materials and Methods

Cell culture and manipulations

HCT116, 293T, and HeLa cells were cultured in Dulbecco's modified Eagle medium (DMEM) (Difco) supplemented with 10% fetal calf serum (Sigma). HCT116 and HeLa cells were synchronized in early S phase by double thymidine block (2 mM thymidine for 17 hours, release into fresh media for 9 hours, 2 mM thymidine 15 hours) or in prometaphase by treatment with 2 mM thymidine for 18 hours followed by release into 100 nM nocodazole for 10 hours as previously described (Whitfield et al. 2002; Grant et al. 2013). Kinase inhibitors were used at the following concentrations: c-Jun N-terminal kinase (JNK) inhibitor VIII at 10 μM (EMD Millipore), p38 inhibitor SB203580 at 30 μM (LC Laboratories), and the CDK1 inhibitor RO-3306 (Sigma) at 10 μM or as indicated. DNA damage was induced by a single treatment of 20 J/m^2 UV. Small interfering RNA (siRNA) transfections were performed with 400 nM of each siRNA duplex using Dharmafect 1 reagent (Dharmacon) according to the manufacturer's guidelines. This high concentration of siRNA was required for efficient knockdown given the brief siRNA treatment time. Synthetic duplexed RNA oligonucleotides were synthesized by Life Technologies; Luciferase (5'- CUUACGCUGAGUACUUCGA-3'); SET8-ORF (5'-GATGCAACTAGAGAGACA-3') (Tardat et al. 2010); SET8-UTR (5'-AAGCAUACAAGCCGAACGUU-3') (Pesavento et al. 2008).

Antibodies

Antibodies were purchased from the following sources: MAPKAP kinase 2, phospho-MAPKAP kinase 2 (p-MK2), phospho-cJUN (Ser63), and SET8 from Cell Signaling Technologies; hemagglutinin (HA) from Roche; alpha tubulin (DM1A) from Sigma; PCNA (PC-10), p21, Cyclin A, Cyclin B1, and Orc2 from Santa Cruz; H4K20me1 from EMD Millipore (cat.#04-735); H4K20me2 from Active Motif (cat.#39174); CDT2 and p12 antibodies were a gift from A. Dutta. Cul4B and Cul4A antibodies were a gift from Y. Xiong. Antibodies to human CDT1 have been previously described (Cook et al. 2004). AlexaFluor 488 and Rhodamine Red-X-labeled donkey secondary antibodies for immunofluorescence microscopy were obtained from Jackson ImmunoResearch Laboratories**.**

Plasmids and protein lysate preparation

HA-tagged mutant CDT1 and p21 were generated via PCR and cloned into pLX302 (Addgene plasmid 25896) (Yang et al. 2011) or pBABE (Addgene plasmid 51070) (Greulich et al. 2012) expression vectors, respectively, as were the tagged wild type constructs. Plasmids expressing glutathione-S-transferase (GST)-$p21_{WT}$ and GST-$p21_{PIP}$ fusions were generated by recombinational cloning between pENTR-p21 derivatives and pDEST15 for N-terminal GST fusion (Gateway LR clonase; Life Technologies) and expressed in BL21 cells. The PIP box was inactivated by site-directed mutagenesis to generate the $p21_{PIP}$ mutant (MTDFY to AAAA). Whole-cell lysates were prepared either by direct lysis of equal cell numbers in 2X Laemmli sample buffer with 10% β-mercaptoethanol or in CSK buffer (supplemented with 0.1% TritonX-100 and protease and phosphatase inhibitors) (Todorov et al. 1995). Chromatin-enriched fractions were isolated as previously described (Cook et al. 2002) by the addition of micrococcal nuclease and $CaCl_2$ to Triton-insoluble pellets to release DNA-bound material into the soluble pool and clarified by centrifugation. Alternatively, sonication was used to solubilize the chromatin-bound proteins.

Protein-protein interaction assays

Recombinant GST fusion proteins GST-p21$_{WT}$ or GST-p21$_{PIP}$ (mutated PIP box) were immobilized on glutathione-Sepharose 4B beads (GE Healthcare). Whole cell extracts (from HCT116 cells) were prepared in CSK buffer (supplemented with 0.1% Triton X-100 and protease and phosphatase inhibitors) and 1 mg of cell lysate was incubated with the bound GST-p21 derivatives for 3 hours at 4°C. The bound complexes were washed three times in complete CSK buffer, resuspended in 50 μL of 2X SDS sample buffer, and boiled for 5 minutes to elute bound proteins.

Immunofluorescence microscopy

Cells were rinsed briefly in 1X phosphate-buffered saline (PBS, pH 7.4) prior to fixation. Cells were typically pre-fixed with 4% paraformaldehyde for 60 seconds, permeabilized with 0.5% Triton X-100 for 5 minutes and then fixed for 15 minutes using 4% paraformaldehyde. For all immunostaining procedures involving PCNA, the cells were first pre-fixed in 2% paraformaldehyde for 60 seconds, then permeabilized with 0.5% Triton X-100 for 5 minutes and then fixed with 2% paraformaldehyde for 15 minutes followed by -20°C methanol for 4 minutes. Blocking steps, antibody incubations, and washes were all performed in 1X PBS buffer plus 0.1% BSA. All antibody incubations were for 1 hour at 37ºC and washes were for 10 minutes at room temperature. DAPI staining (0.1 μg/ml) was performed for 10 minutes, and cells were mounted using either Prolong Antifade (Life Technologies/Molecular Probes) or VECTASHIELD mounting media (Vector Laboratories, Inc.).

For indirect immunofluorescence microscopy of interphase nuclei, images were acquired using Metamorph Software and a 60X/1.4NA (PlanApo) DIC oil immersion objective (Nikon) mounted on a Nikon TE300 inverted microscope equipped with a Yokogawa CSU10 spinning disk and a Hamamatsu Orca ER cooled CCD camera. For

fluorescence intensity measurements, the average values for integrated nuclear PCNA fluorescence from control and experimental cell samples were subjected to background subtraction to obtain the specific nuclear fluorescence levels. For indirect immunofluorescence microscopy of mitotic cells, images were acquired using Metamorph Software and a 100X/1.4NA (PlanApo) DIC oil immersion objective mounted on a Leica DMIRB inverted microscope equipped with a Photometric HQ2 cooled CCD camera. Scale bars = 5 μm in all figures.

Flow cytometry

Prior to flow cytometry analysis, cells were trypsinized, fixed in 70% ethanol, and treated with propidium iodide/RNase solution according to standard methods. Flow cytometry analysis was performed using a Cyan FACScan (DakoCytomation) and Summit v4.3 software (DakoCytomation) as described previously (Hall et al. 2008).

REFERENCES

Abbas T, Dutta A. 2011. CRL4Cdt2: Master coordinator of cell cycle progression and genome stability. *Cell Cycle* **10**: 241–249.

Abbas T, Keaton M, Dutta A. 2013a. Regulation of TGF- β signaling, exit from the cell cycle, and cellular migration through cullin cross-regulation. 2175–2182.

Abbas T, Mueller AC, Shibata E, Keaton M, Rossi M, Dutta A. 2013b. CRL1-FBXO11 Promotes Cdt2 Ubiquitylation and Degradation and Regulates Pr-Set7/Set8-Mediated Cellular Migration. *Mol Cell* **21**: 1–12.

Abbas T, Shibata E, Park J, Jha S, Karnani N, Dutta A. 2010. CRL4(Cdt2) regulates cell proliferation and histone gene expression by targeting PR-Set7/Set8 for degradation. *Mol Cell* **40**: 9–21.

Abbas T, Sivaprasad U, Terai K, Amador V, Pagano M, Dutta A. 2008. PCNA-dependent regulation of p21 ubiquitylation and degradation via the CRL4Cdt2 ubiquitin ligase complex. *Genes Dev* **22**: 2496–506.

Amador V, Ge S, Santamaría PG, Guardavaccaro D, Pagano M. 2007. APC/C(Cdc20) controls the ubiquitin-mediated degradation of p21 in prometaphase. *Mol Cell* **27**: 462–73.

Aparicio OM. 2013. Location , location , location : it ’ s all in the timing for replication origins. 117–128.

Arentson E, Faloon P, Seo J, Moon E, Studts JM, Fremont DH, Choi K. 2002. Oncogenic potential of the DNA replication licensing protein CDT1. 1150–1158.

Arias EE, Walter JC. 2006. PCNA functions as a molecular platform to trigger Cdt1 destruction and prevent re-replication. *Nat Cell Biol* **8**: 84–90.

Arias EE, Walter JC. 2005. Replication-dependent destruction of Cdt1 limits DNA replication to a single round per cell cycle in Xenopus egg extracts. *Genes Dev* **19**: 114–26.

Arias EE, Walter JC. 2007. Strength in numbers: preventing rereplication via multiple mechanisms in eukaryotic cells. *Genes Dev* **21**: 497–518.

Ballabeni a., Park I-H, Zhao R, Wang W, Lerou PH, Daley GQ, Kirschner MW. 2011. Cell cycle adaptations of embryonic stem cells. *Proc Natl Acad Sci* **108**: 19252–19257.

Ballabeni A, Melixetian M, Zamponi R, Masiero L, Marinoni F, Helin K. 2004. Human geminin promotes pre-RC formation and DNA replication by stabilizing CDT1 in mitosis. *EMBO J* **23**: 3122–3132.

Ballabeni A, Zamponi R, Moore JK, Helin K, Kirschner MW. 2013. Geminin deploys multiple mechanisms to regulate Cdt1 before cell division thus ensuring the proper execution of DNA replication. *Proc Natl Acad Sci U S A* **110**: E2848–53.

Bell SP, Dutta A. 2002. DNA replication in eukaryotic cells. *Annu Rev Biochem* **71**: 333–74.

Bendjennat M, Boulaire J, Jascur T, Brickner H, Barbier V, Sarasin A, Fotedar A, Fotedar R. 2003. UV irradiation triggers ubiquitin-dependent degradation of p21(WAF1) to promote DNA repair. *Cell* **114**: 599–610.

Bennett EJ, Rush J, Gygi SP, Harper JW. 2010. Dynamics of cullin-RING ubiquitin ligase network revealed by systematic quantitative proteomics. *Cell* **143**: 951–965.

Bienko M, Green CM, Sabbioneda S, Crosetto N, Matic I, Hibbert RG, Begovic T, Niimi A, Mann M, Lehmann AR, et al. 2010. Regulation of Translesion Synthesis DNA Polymerase η by Monoubiquitination. *Mol Cell* **37**: 396–407.

Blow JJ, Dutta A. 2005. Preventing re-replication of chromosomal DNA. *Nat Rev Mol Cell Biol* **6**: 476–86.

Bornstein G, Bloom J, Sitry-Shevah D, Nakayama K, Pagano M, Hershko A. 2003. Role of the SCFSkp2 ubiquitin ligase in the degradation of p21Cip1 in S phase. *J Biol Chem* **278**: 25752–7.

Bowers JL, Randell JCW, Chen S, Bell SP. 2004. ATP hydrolysis by ORC catalyzes reiterative Mcm2-7 assembly at a defined origin of replication. *Mol Cell* **16**: 967–978.

Burke TW, Cook JG, Asano M, Nevins JR. 2001. Replication factors MCM2 and ORC1 interact with the histone acetyltransferase HBO1. *J Biol Chem* **276**: 15397–408.

Campeau E, Ruhl VE, Rodier F, Smith CL, Rahmberg BL, Fuss JO, Campisi J, Yaswen P, Cooper PK, Kaufman PD. 2009. A versatile viral system for expression and depletion of proteins in mammalian cells. *PLoS One* **4**.

Centore RC, Havens CG, Manning AL, Li J-M, Flynn RL, Tse A, Jin J, Dyson NJ, Walter JC, Zou L. 2010. CRL4Cdt2-Mediated Destruction of the Histone Methyltransferase Set8 Prevents Premature Chromatin Compaction in S Phase. *Mol Cell* **40**: 22–33.

Chandrasekaran S, Tan TX, Hall JR, Cook JG. 2011. Stress-activated MAP kinases, p38 and JNK, control the stability and activity of the Cdt1 DNA replication licensing factor. *Mol Cell Biol*.

Chawla G, Lin C-H, Han A, Shiue L, Ares M, Black DL. 2009. Sam68 regulates a set of alternatively spliced exons during neurogenesis. *Mol Cell Biol* **29**: 201–13.

Child ES, Mann DJ. 2006. The intricacies of p21 phosphorylation: Protein/protein interactions, subcellular localization and stability. *Cell Cycle* **5**: 1313–1319.

Choi H, Larsen B, Lin Z-Y, Breitkreutz A, Mellacheruvu D, Fermin D, Qin ZS, Tyers M, Gingras A-C, Nesvizhskii AI. 2011. SAINT: probabilistic scoring of affinity purification-mass spectrometry data. *Nat Methods* **8**: 70–3.

Choudhuri T, Murakami M, Kaul R, Sahu SK, Mohanty S, Verma SC, Kumar P, Robertson ES. 2010. Nm23-H1 can induce cell cycle arrest and apoptosis in B cells. *Cancer Biol Ther* **9**: 1065–1078.

Cook JG, Chasse D a D, Nevins JR. 2004. The regulated association of Cdt1 with minichromosome maintenance proteins and Cdc6 in mammalian cells. *J Biol Chem* **279**: 9625–33.

Cook JG, Park C-H, Burke TW, Leone G, DeGregori J, Engel A, Nevins JR. 2002. Analysis of Cdc6 function in the assembly of mammalian prereplication complexes. *Proc Natl Acad Sci U S A* **99**: 1347–52.

Cope GA, Suh GSB, Aravind L, Schwarz SE, Zipursky SL, Koonin E V, Deshaies RJ. 2002. Role of Predicted Metalloprotease Motif of Jab1/Csn5 in Cleavage of Nedd8 from Cul1. *Science* **298**: 608–611.

Craney A, Rape M. 2013. Dynamic regulation of ubiquitin-dependent cell cycle control. *Curr Opin Cell Biol* **25**: 704–710.

Dar A, Wu D, Lee N, Shibata E, Dutta A. 2014. 14-3-3 proteins play a role in the cell cycle by shielding Cdt2 from ubiquitin-mediated degradation. *Mol Cell Biol*.

Davidson IF, Li A, Blow JJ. 2006. Deregulated replication licensing causes DNA fragmentation consistent with head-to-tail fork collision. *Mol Cell* **24**: 433–43.

Debatisse M, Le Tallec B, Letessier A, Dutrillaux B, Brison O. 2012. Common fragile sites: Mechanisms of instability revisited. *Trends Genet* **28**: 22–32.

Dephoure N, Zhou C, Villén J, Beausoleil S a, Bakalarski CE, Elledge SJ, Gygi SP. 2008. A quantitative atlas of mitotic phosphorylation. *Proc Natl Acad Sci U S A* **105**: 10762–10767.

Deshaies RJ, Joazeiro C a P. 2009. RING domain E3 ubiquitin ligases. *Annu Rev Biochem* **78**: 399–434.

Dimitrova DS, Prokhorova T a, Blow JJ, Todorov IT, Gilbert DM. 2002. Mammalian nuclei become licensed for DNA replication during late telophase. *J Cell Sci* **115**: 51–9.

Donovan S, Harwood J, Drury LS, Diffley JF. 1997. Cdc6p-dependent loading of Mcm proteins onto pre-replicative chromatin in budding yeast. *Proc Natl Acad Sci U S A* **94**: 5611–5616.

Dorn ES, Chastain PD, Hall JR, Cook JG. 2009. Analysis of re-replication from deregulated origin licensing by DNA fiber spreading. *Nucleic Acids Res* **37**: 60–9.

Ducoux M, Urbach S, Baldacci G, Hübscher U, Koundrioukoff S, Christensen J, Hughes P. 2001. Mediation of proliferating cell nuclear antigen (PCNA)-dependent DNA replication through a conserved p21(Cip1)-like PCNA-binding motif present in the third subunit of human DNA polymerase delta. *J Biol Chem* **276**: 49258–49266.

Duda DM, Borg L a., Scott DC, Hunt HW, Hammel M, Schulman B a. 2008. Structural Insights into NEDD8 Activation of Cullin-RING Ligases: Conformational Control of Conjugation. *Cell* **134**: 995–1006.

Edwards MC, Tutter A V, Cvetic C, Gilbert CH, Prokhorova T a, Walter JC. 2002. MCM2-7 complexes bind chromatin in a distributed pattern surrounding the origin recognition complex in Xenopus egg extracts. *J Biol Chem* **277**: 33049–57.

Elzen N Den, Pines J. 2001. Cyclin A Is Destroyed in Prometaphase and Can Delay Chromosome Alignment and Anaphase 7. 121–135.

Evrin C, Clarke P, Zech J, Lurz R, Sun J, Uhle S, Li H, Stillman B, Speck C. 2009. A double-hexameric MCM2-7 complex is loaded onto origin DNA during licensing of eukaryotic DNA replication. *Proc Natl Acad Sci U S A* **106**: 20240–5.

Faust D, Dolado I, Cuadrado A, Oesch F, Weiss C, Nebreda AR, Dietrich C. 2005. p38alpha MAPK is required for contact inhibition. *Oncogene* **24**: 7941–5.

Franz A, Orth M, Pirson P a, Sonneville R, Blow JJ, Gartner A, Stemmann O, Hoppe T. 2011. CDC-48/p97 Coordinates CDT-1 Degradation with GINS Chromatin Dissociation to Ensure Faithful DNA Replication. *Mol Cell* **44**: 85–96.

Ge XQ, Jackson D a., Blow JJ. 2007. Dormant origins licensed by excess Mcm2-7 are required for human cells to survive replicative stress. *Genes Dev* **21**: 3331–3341.

Gibson DG, Aparicio JG, Hu F, Aparicio OM. 2004. Diminished S-phase cyclin-dependent kinase function elicits vital Rad53-dependent checkpoint responses in Saccharomyces cerevisiae. *Mol Cell Biol* **24**: 10208–10222.

Girard F, Strausfeld U, Fernandez a, Lamb NJ. 1991. Cyclin A is required for the onset of DNA replication in mammalian fibroblasts. *Cell* **67**: 1169–1179.

Gottifredi V, McKinney K, Poyurovsky M V., Prives C. 2004. Decreased p21 Levels Are Required for Efficient Restart of DNA Synthesis after S Phase Block. *J Biol Chem* **279**: 5802–5810.

Grant GD, Brooks L, Zhang X, Mahoney JM, Martyanov V, Wood T a, Sherlock G, Cheng C, Whitfield ML. 2013. Identification of cell cycle-regulated genes periodically expressed in U2OS cells and their regulation by FOXM1 and E2F transcription factors. *Mol Biol Cell* **24**: 3634–50.

Greulich H, Kaplan B, Mertins P, Chen T, Tanaka KE, Yun C. 2012. Functional analysis of receptor tyrosine kinase mutations in lung cancer identi fi es oncogenic extracellular domain mutations of ERBB2. *Pnas*.

Groisman R, Polanowska J, Kuraoka I, Sawada JI, Saijo M, Drapkin R, Kisselev AF, Tanaka K, Nakatani Y. 2003. The ubiquitin ligase activity in the DDB2 and CSA complexes is differentially regulated by the COP9 signalosome in response to DNA damage. *Cell* **113**: 357–367.

Groth A, Corpet A, Cook AJL, Roche D, Bartek J, Lukas J, Almouzni G. 2007. Regulation of replication fork progression through histone supply and demand. *Science* **318**: 1928–1931.

Guerrero-Santoro J, Kapetanaki MG, Hsieh CL, Gorbachinsky I, Levine AS, Rapić-Otrin V. 2008. The cullin 4B-Based UV-damaged DNA-binding protein ligase binds to UV-damaged chromatin and ubiquitinates histone H2A. *Cancer Res* **68**: 5014–5022.

Gulbis JM, Kelman Z, Hurwitz J, Donnell MO, Kuriyan J. 1996. Structure of the C-Terminal Region Complexed with Human PCNA. **87**: 297–306.

Hagting A, Den Elzen N, Vodermaier HC, Waizenegger IC, Peters J-M, Pines J. 2002. Human securin proteolysis is controlled by the spindle checkpoint and reveals when the APC/C switches from activation by Cdc20 to Cdh1. *J Cell Biol* **157**: 1125–37.

Hall JR, Lee HO, Bunker BD, Dorn ES, Rogers GC, Duronio RJ, Gowen J, Hill C, Carolina N. 2008. Cdt1 and Cdc6 are destabilized by rereplication-induced DNA damage. *J Biol Chem* **283**: 25356–63.

Han C, Wani G, Zhao R, Qian J, Sharma N, He J, Zhu Q, Wang Q-E, Wani A a. 2014. Cdt2-mediated XPG degradation promotes gap-filling DNA synthesis in nucleotide excision repair. *Cell Cycle* 37–41.

Havens CG, Shobnam N, Guarino E, Centore RC, Zou L, Kearsey SE, Walter JC. 2012. Direct role for proliferating cell nuclear antigen in substrate recognition by the E3 ubiquitin ligase CRL4Cdt2. *J Biol Chem* **287**: 11410–21.

Havens CG, Walter JC. 2009. Docking of a specialized PIP Box onto chromatin-bound PCNA creates a degron for the ubiquitin ligase CRL4Cdt2. *Mol Cell* **35**: 93–104.

Havens CG, Walter JC. 2011. Mechanism of CRL4(Cdt2), a PCNA-dependent E3 ubiquitin ligase. *Genes Dev* **25**: 1568–82.

Herzog F. 2009. Mitotic Checkpoint Complex. *Science (80-)* **1985**: 1477–1481.

Higa LA a, Mihaylov IS, Banks DP, Zheng J, Zhang H. 2003. Radiation-mediated proteolysis of CDT1 by CUL4-ROC1 and CSN complexes constitutes a new checkpoint. *Nat Cell Biol* **5**: 1008–1015.

Hodeify R, Tarcsafalvi A, Megyesi J, Safirstein RL, Price PM. 2011. Cdk2-dependent phosphorylation of p21 regulates the role of Cdk2 in cisplatin cytotoxicity. *Am J Physiol Renal Physiol* **300**: F1171–F1179.

Holmberg C, Fleck O, Hansen H a, Liu C, Slaaby R, Carr AM, Nielsen O. 2005. Ddb1 controls genome stability and meiosis in fission yeast Ddb1 controls genome stability and meiosis in fission yeast. **7**: 853–862.

Hori T, Shang WH, Toyoda A, Misu S, Monma N, Ikeo K, Molina O, Vargiu G, Fujiyama A, Kimura H, et al. 2014. Histone H4 Lys 20 Monomethylation of the CENP-A Nucleosome Is Essential for Kinetochore Assembly. *Dev Cell* **29**: 740–749.

Houston SI, McManus KJ, Adams MM, Sims JK, Carpenter PB, Hendzel MJ, Rice JC. 2008. Catalytic function of the PR-Set7 histone H4 lysine 20 monomethyltransferase is essential for mitotic entry and genomic stability. *J Biol Chem* **283**: 19478–19488.

Hu J, Xiong Y. 2006. An evolutionarily conserved function of proliferating cell nuclear antigen for Cdt1 degradation by the Cul4-Ddb1 ubiquitin ligase in response to DNA damage. *J Biol Chem* **281**: 3753–6.

Hua XH, Yan H, Newport J. 1997. A role for Cdk2 kinase in negatively regulating DNA replication during S phase of the cell cycle. *J Cell Biol* **137**: 183–192.

Ibarra A, Schwob E, Méndez J. 2008. Excess MCM proteins protect human cells from replicative stress by licensing backup origins of replication. *Proc Natl Acad Sci U S A* **105**: 8956–61.

Ishii T, Shiomi Y, Takami T, Murakami Y, Ohnishi N, Nishitani H. 2010. Proliferating cell nuclear antigen-dependent rapid recruitment of Cdt1 and CRL4Cdt2 at DNA-damaged sites after UV irradiation in HeLa cells. *J Biol Chem* **285**: 41993–2000.

Ivan M, Kondo K, Yang H, Kim W, Valiando J, Ohh M, Salic a, Asara JM, Lane WS, Kaelin WG. 2001. HIFalpha targeted for VHL-mediated destruction by proline hydroxylation: implications for O2 sensing. *Science* **292**: 464–468.

Izawa D, Pines J. 2011. How APC/C-Cdc20 changes its substrate specificity in mitosis. *Nat Cell Biol* **13**: 223–33.

Jiang W, Wells NJ, Hunter T. 1999. Multistep regulation of DNA replication by Cdk phosphorylation of HsCdc6. *Proc Natl Acad Sci U S A* **96**: 6193–8.

Jin J, Arias EE, Chen J, Harper JW, Walter JC. 2006. A family of diverse Cul4-Ddb1-interacting proteins includes Cdt2, which is required for S phase destruction of the replication factor Cdt1. *Mol Cell* **23**: 709–21.

Jin J, Cardozo T, Lovering RC, Elledge SJ, Pagano M, Harper JW. 2004. Systematic analysis and nomenclature of mammalian F-box proteins. *Genes Dev* **18**: 2573–2580.

Jørgensen S, Eskildsen M, Fugger K, Hansen L, Larsen MSY, Kousholt AN, Syljuåsen RG, Trelle MB, Jensen ON, Helin K, et al. 2011. SET8 is degraded via PCNA-coupled CRL4(CDT2) ubiquitylation in S phase and after UV irradiation. *J Cell Biol* **192**: 43–54.

Kapetanaki MG, Guerrero-Santoro J, Bisi DC, Hsieh CL, Rapić-Otrin V, Levine AS. 2006. The DDB1-CUL4ADDB2 ubiquitin ligase is deficient in xeroderma pigmentosum group E and targets histone H2A at UV-damaged DNA sites. *Proc Natl Acad Sci U S A* **103**: 2588–2593.

Karachentsev D, Sarma K, Reinberg D, Steward R. 2005. PR-Set7-dependent methylation of histone H4 Lys 20 functions in repression of gene expression and is essential for mitosis service PR-Set7-dependent methylation of histone H4 Lys 20 functions in repression of gene expression and is essential for mitosis. **31**: 431–435.

Keppler A, Gendreizig S, Gronemeyer T, Pick H, Vogel H, Johnsson K. 2003. A general method for the covalent labeling of fusion proteins with small molecules in vivo. *Nat Biotechnol* **21**: 86–89.

Kerns SL, Torke SJ, Benjamin JM, McGarry TJ. 2007. Geminin prevents rereplication during Xenopus development. *J Biol Chem* **282**: 5514–5521.

Kim G-Y, Mercer SE, Ewton DZ, Yan Z, Jin K, Friedman E. 2002. The stress-activated protein kinases p38 alpha and JNK1 stabilize p21(Cip1) by phosphorylation. *J Biol Chem* **277**: 29792–802.

Kim J, Feng H, Kipreos ET. 2007. C. elegans CUL-4 Prevents Rereplication by Promoting the Nuclear Export of CDC-6 via a CKI-1-Dependent Pathway. *Curr Biol* **17**: 966–972.

Kim JH, Lee SR, Li LH, Park HJ, Park JH, Lee KY, Kim MK, Shin BA, Choi SY. 2011. High cleavage efficiency of a 2A peptide derived from porcine teschovirus-1 in human cell lines, zebrafish and mice. *PLoS One* **6**: 1–8.

Kim SH, Michael WM. 2008. Regulated Proteolysis of DNA Polymerase ?? during the DNA-Damage Response in C. elegans. *Mol Cell* **32**: 757–766.

Kim Y, Starostina NG, Kipreos ET. 2008. The CRL4Cdt2 ubiquitin ligase targets the degradation of p21Cip1 to control replication licensing. *Genes Dev* **22**: 2507–19.

Komander D, Rape M. 2012. The ubiquitin code. *Annu Rev Biochem* **81**: 203–29.

Kreis N-N, Sanhaji M, Rieger M a, Louwen F, Yuan J. 2013. p21Waf1/Cip1 deficiency causes multiple mitotic defects in tumor cells. *Oncogene* 1–13.

Labib K. 2010. How do Cdc7 and cyclin-dependent kinases trigger the initiation of chromosome replication in eukaryotic cells? *Genes Dev* **24**: 1208–19.

Lee C, Hong B, Choi JM, Kim Y. 2004. Structural basis for inhibition of the replication licensing factor Cdt1 by geminin. *Nature* **430**: 913–917.

Lee J, Zhou P. 2010. Cullins and Cancer. *Genes Cancer* **1**: 690–699.

Leonhardt H, Rahn HP, Weinzierl P, Sporbert a, Cremer T, Zink D, Cardoso MC. 2000. Dynamics of DNA replication factories in living cells. *J Cell Biol* **149**: 271–80.

Li A, Blow JJ. 2005. Cdt1 downregulation by proteolysis and geminin inhibition prevents DNA re-replication in Xenopus. *EMBO J* **24**: 395–404.

Li C, Vassilev A, Depamphilis ML. 2004. Role for Cdk1 (Cdc2)/ Cyclin A in Preventing the Mammalian Origin Recognition Complex ' s Largest Subunit (Orc1) from Binding to Chromatin during Mitosis Role for Cdk1 (Cdc2)/ Cyclin A in Preventing the Mammalian Origin Recognition Complex ' s Large. *Mol Cell Biol* **24**: 5875–5888.

Li C-J, DePamphilis ML. 2002. Mammalian Orc1 protein is selectively released from chromatin and ubiquitinated during the S-to-M transition in the cell division cycle. *Mol Cell Biol* **22**: 105–116.

Lin JJ, Milhollen M a., Smith PG, Narayanan U, Dutta A. 2010. NEDD8-targeting drug MLN4924 elicits DNA rereplication by stabilizing Cdt1 in S phase, triggering checkpoint activation, apoptosis, and senescence in cancer cells. *Cancer Res* **70**: 10310–10320.

Lindon C, Pines J. 2004. Ordered proteolysis in anaphase inactivates Plk1 to contribute to proper mitotic exit in human cells. *J Cell Biol* **164**: 233–241.

Liu C, Poitelea M, Watson A, Yoshida S, Shimoda C, Holmberg C, Nielsen O, Carr AM. 2005. Transactivation of Schizosaccharomyces pombe cdt2+ stimulates a Pcu4-Ddb1-CSN ubiquitin ligase. *EMBO J* **24**: 3940–3951.

Liu C, Yu I, Pan H, Lin S, Hsu H. 2007. L2dtl Is Essential for Cell Survival and Nuclear Division in Early Mouse Embryonic Development *. **282**: 1109–1118.

Liu E, Li X, Yan F, Zhao Q, Wu X. 2004. Cyclin-dependent Kinases Phosphorylate Human Cdt1 and Induce Its Degradation. *J Biol Chem* **279**: 17283–17288.

Liu J, Furukawa M, Matsumoto T, Xiong Y. 2002. NEDD8 modification of CUL1 dissociates p120CAND1, an inhibitor of CUL1-SKP1 binding and SCF ligases. *Mol Cell* **10**: 1511–1518.

Liu L, Lee S, Zhang J, Peters SB, Hannah J, Zhang Y, Yin Y, Koff A, Ma L, Zhou P. 2009. CUL4A Abrogation Augments DNA Damage Response and Protection against Skin Carcinogenesis. *Mol Cell* **34**: 451–460.

Lovejoy C a, Lock K, Yenamandra A, Cortez D. 2006. DDB1 maintains genome integrity through regulation of Cdt1. *Mol Cell Biol* **26**: 7977–7990.

Lu D, Hsiao JY, Davey NE, Van Voorhis V a., Foster S a., Tang C, Morgan DO. 2014. Multiple mechanisms determine the order of APC/C substrate degradation in mitosis. *J Cell Biol*.

Lutzmann M, Maiorano D, Méchali M. 2006. A Cdt1-geminin complex licenses chromatin for DNA replication and prevents rereplication during S phase in Xenopus. *EMBO J* **25**: 5764–5774.

Lyapina S, Cope G, Shevchenko a, Serino G, Tsuge T, Zhou C, Wolf D a, Wei N, Shevchenko a, Deshaies RJ. 2001. Promotion of NEDD-CUL1 conjugate cleavage by COP9 signalosome. *Science* **292**: 1382–1385.

Machida YJ, Hamlin JL, Dutta A. 2005. Right place, right time, and only once: replication initiation in metazoans. *Cell* **123**: 13–24.

Maga G, Hubscher U. 2003. Proliferating cell nuclear antigen (PCNA): a dancer with many partners. *J Cell Sci* **116**: 3051–60.

Mahbubani HM, Paull T, Elder JK, Blow JJ. 1992. DNA replication initiates at multiple sites on plasmid DNA in Xenopus egg extracts. *Nucleic Acids Res* **20**: 1457–1462.

Mailand N, Diffley JFX. 2005. CDKs promote DNA replication origin licensing in human cells by protecting Cdc6 from APC/C-dependent proteolysis. *Cell* **122**: 915–26.

Maiorano D, Moreau J, Méchali M. 2000. XCDT1 is required for the assembly of pre-replicative complexes in Xenopus laevis. *Nature* **404**: 622–625.

Malecki MJ, Sanchez-Irizarry C, Mitchell JL, Histen G, Xu ML, Aster JC, Blacklow SC. 2006. Leukemia-associated mutations within the NOTCH1 heterodimerization domain fall into at least two distinct mechanistic classes. *Mol Cell Biol* **26**: 4642–4651.

Malumbres M, Barbacid M. 2001. To cycle or not to cycle: a critical decision in cancer. *Nat Rev Cancer* **1**: 222–31.

Mansilla SF, Soria G, Vallerga MB, Habif M, Martínez-López W, Prives C, Gottifredi V. 2013. UV-triggered p21 degradation facilitates damaged-DNA replication and preserves genomic stability. *Nucleic Acids Res* **41**: 6942–51.

Mantiero D, Mackenzie A, Donaldson A, Zegerman P. 2011. Limiting replication initiation factors execute the temporal programme of origin firing in budding yeast. *EMBO J* **30**: 4805–4814.

Maurier F. 1997. A Role for Sam68 in Cell Cycle Progression Antagonized by a Spliced Variant within the KH Domain. *J Biol Chem* **272**: 3129–3132.

McGarry TJ, Kirschner MW. 1998. Geminin, an inhibitor of DNA replication, is degraded during mitosis. *Cell* **93**: 1043–1053.

Mellacheruvu D, Wright Z, Couzens AL, Lambert J-P, St-Denis N a, Li T, Miteva Y V, Hauri S, Sardiu ME, Low TY, et al. 2013. The CRAPome: a contaminant repository for affinity purification-mass spectrometry data. *Nat Methods* **10**: 730–6.

Méndez J, Stillman B. 2000. Chromatin association of human origin recognition complex, cdc6, and minichromosome maintenance proteins during the cell cycle: assembly of prereplication complexes in late mitosis. *Mol Cell Biol* **20**: 8602–8612.

Meng X, Zhou Y, Lee EYC, Lee MYWT, Frick DN. 2010. The p12 subunit of human polymerase ?? modulates the rate and fidelity of DNA synthesis. *Biochemistry* **49**: 3545–3554.

Michishita M, Morimoto A, Ishii T, Komori H, Shiomi Y, Higuchi Y, Nishitani H. 2011. Positively charged residues located downstream of PIP box, together with TD amino acids within PIP box, are important for CRL4(Cdt2) -mediated proteolysis. *Genes Cells* **16**: 12–22.

Miotto B, Struhl K. 2011. JNK1 Phosphorylation of Cdt1 Inhibits Recruitment of HBO1 Histone Acetylase and Blocks Replication Licensing in Response to Stress. *Mol Cell* 1–10.

Morgan D. 1997. Cyclin-dependent kinases : Engines , clocks , and microprocessors. *Annu Rev Cell Dev Biol* **13**: 261–291.

Musacchio A, Salmon ED. 2007. The spindle-assembly checkpoint in space and time. *Nat Rev Mol Cell Biol* **8**: 379–393.

Nakayama K, Nagahama H, Minamishima Y a, Matsumoto M, Nakamichi I, Kitagawa K, Shirane M, Tsunematsu R, Tsukiyama T, Ishida N, et al. 2000. Targeted disruption of Skp2 results in accumulation of cyclin E and p27(Kip1), polyploidy and centrosome overduplication. *EMBO J* **19**: 2069–2081.

Nakayama KI, Nakayama K. 2006. Ubiquitin ligases: cell-cycle control and cancer. *Nat Rev Cancer* **6**: 369–81.

Nevis KR, Cordeiro-Stone M, Cook JG. 2009. Origin licensing and p53 status regulate Cdk2 activity during G(1). *Cell Cycle* **8**: 1952–63.

Nishitani H, Lygerou Z. 2002. Control of DNA replication licensing in a cell cycle. *Genes Cells* **7**: 523–34.

Nishitani H, Lygerou Z, Nishimoto T. 2004. Proteolysis of DNA replication licensing factor Cdt1 in S-phase is performed independently of Geminin through its N-terminal region. *J Biol Chem* **279**: 30807–30816.

Nishitani H, Lygerou Z, Nishimoto T, Nurse P. 2000. The Cdt1 protein is required to license DNA for replication in fission yeast. *Nature* **404**: 625–628.

Nishitani H, Shiomi Y, Iida H, Michishita M, Takami T, Tsurimoto T. 2008. CDK inhibitor p21 is degraded by a proliferating cell nuclear antigen-coupled Cul4-DDB1Cdt2 pathway during S phase and after UV irradiation. *J Biol Chem* **283**: 29045–52.

Nishitani H, Sugimoto N, Roukos V, Nakanishi Y, Saijo M, Obuse C, Tsurimoto T, Nakayama KI, Nakayama K, Fujita M, et al. 2006. Two E3 ubiquitin ligases, SCF-Skp2 and DDB1-Cul4, target human Cdt1 for proteolysis. *EMBO J* **25**: 1126–36.

O'Connell BC, Adamson B, Lydeard JR, Sowa ME, Ciccia A, Bredemeyer AL, Schlabach M, Gygi SP, Elledge SJ, Harper JW. 2010. A genome-wide camptothecin sensitivity screen identifies a mammalian MMS22L-NFKBIL2 complex required for genomic stability. *Mol Cell* **40**: 645–57.

Oda H, Hübner MR, Beck DB, Vermeulen M, Hurwitz J, Spector DL, Reinberg D. 2010. Regulation of the histone H4 monomethylase PR-Set7 by CRL4(Cdt2)-mediated PCNA-dependent degradation during DNA damage. *Mol Cell* **40**: 364–76.

Olsen J V, Vermeulen M, Santamaria A, Kumar C, Miller ML, Jensen LJ, Gnad F, Cox J, Jensen TS, Nigg E a, et al. 2010. Quantitative phosphoproteomics reveals widespread full phosphorylation site occupancy during mitosis. *Sci Signal* **3**: ra3.

Osaka F, Saeki M, Katayama S, Aida N, Toh-E a, Kominami K, Toda T, Suzuki T, Chiba T, Tanaka K, et al. 2000. Covalent modifier NEDD8 is essential for SCF ubiquitin-ligase in fission yeast. *EMBO J* **19**: 3475–3484.

Pagano M, Theodoras AM, Tam SW, Draetta GF. 1994. Cyclin D 1-mediated inhibition of repair and replicative DNA synthesis in human fibrob | asts. 1627–1639.

Paoletti AC, Parmely TJ, Tomomori-Sato C, Sato S, Zhu D, Conaway RC, Conaway JW, Florens L, Washburn MP. 2006. Quantitative proteomic analysis of distinct mammalian Mediator complexes using normalized spectral abundance factors. *Proc Natl Acad Sci U S A* **103**: 18928–33.

Paolinelli R, Mendoza-Maldonado R, Cereseto A, Giacca M. 2009. Acetylation by GCN5 regulates CDC6 phosphorylation in the S phase of the cell cycle. *Nat Struct Mol Biol* **16**: 412–420.

Pardee a B. 1974. A restriction point for control of normal animal cell proliferation. *Proc Natl Acad Sci U S A* **71**: 1286–90.

Perdiguero E, Ruiz-Bonilla V, Gresh L, Hui L, Ballestar E, Sousa-Victor P, Baeza-Raja B, Jardí M, Bosch-Comas A, Esteller M, et al. 2007. Genetic analysis of p38 MAP kinases in myogenesis: fundamental role of p38alpha in abrogating myoblast proliferation. *EMBO J* **26**: 1245–56.

Perry JJP, Tainer J a., Boddy MN. 2008. A SIM-ultaneous role for SUMO and ubiquitin. *Trends Biochem Sci* **33**: 201–208.

Pesavento JJ, Yang H, Kelleher NL, Mizzen C a. 2008. Certain and progressive methylation of histone H4 at lysine 20 during the cell cycle. *Mol Cell Biol* **28**: 468–486.

Pesin J a, Orr-Weaver TL. 2008. Regulation of APC/C activators in mitosis and meiosis. *Annu Rev Cell Dev Biol* **24**: 475–499.

Petersen BO. 2000. Cell cycle- and cell growth-regulated proteolysis of mammalian CDC6 is dependent on APC-CDH1. *Genes Dev* **14**: 2330–2343.

Petersen BO, Lukas J, Sørensen CS, Bartek J, Helin K. 1999. Phosphorylation of mammalian CDC6 by cyclin A/CDK2 regulates its subcellular localization. *EMBO J* **18**: 396–410.

Petroski MD, Deshaies RJ. 2005. Function and regulation of cullin-RING ubiquitin ligases. *Nat Rev Mol Cell Biol* **6**: 9–20.

Pierce NW, Lee JE, Liu X, Sweredoski MJ, Graham RLJ, Larimore E a., Rome M, Zheng N, Clurman BE, Hess S, et al. 2013. Cand1 promotes assembly of new SCF complexes through dynamic exchange of F box proteins. *Cell* **153**: 206–215.

Ralph E, Boye E, Kearsey SE. 2006. DNA damage induces Cdt1 proteolysis in fission yeast through a pathway dependent on Cdt2 and Ddb1. *EMBO Rep* **7**: 1134–1139.

Raman M, Havens CG, Walter JC, Harper JW. 2011. A genome-wide screen identifies p97 as an essential regulator of DNA damage-dependent CDT1 destruction. *Mol Cell* **44**: 72–84.

Randell JCW, Bowers JL, Rodríguez HK, Bell SP. 2006. Sequential ATP hydrolysis by Cdc6 and ORC directs loading of the Mcm2-7 helicase. *Mol Cell* **21**: 29–39.

Rape M, Reddy SK, Kirschner MW. 2006. The processivity of multiubiquitination by the APC determines the order of substrate degradation. *Cell* **124**: 89–103.

Remus D, Beuron F, Tolun G, Griffith JD, Morris EP, Diffley JFX. 2009. Concerted loading of Mcm2-7 double hexamers around DNA during DNA replication origin licensing. *Cell* **139**: 719–30.

Rizzardi LF, Coleman KE, Varma D, Matson JP, Oh S, Cook JG. 2014. Cyclin-dependent Kinase 1 (CDK1)-dependent Inhibition of the E3 Ubiquitin Ligase, CRL4CDT2, Ensures Robust Transition from S Phase to Mitosis. *J Biol Chem* **290**: 556–567.

Rosenblatt J, Gu Y, Morgan DO. 1992. Human cyclin-dependent kinase 2 is activated during the S and G2 phases of the cell cycle and associates with cyclin A. *Proc Natl Acad Sci U S A* **89**: 2824–2828.

Rossi M, Duan S, Jeong Y-T, Horn M, Saraf A, Florens L, Washburn MP, Antebi A, Pagano M. 2013. Regulation of the CRL4Cdt2 Ubiquitin Ligase and Cell-Cycle Exit by the SCFFbxo11 Ubiquitin Ligase. *Mol Cell* 1–8.

Roux KJ, Kim DI, Raida M, Burke B. 2012. A promiscuous biotin ligase fusion protein identifies proximal and interacting proteins in mammalian cells. *J Cell Biol* **196**: 801–810.

Rowles a, Chong JPJ, Brown L, Howell M, Evan GI, Blow JJ. 1996. Interaction between the origin recognition complex and the replication licencing system in Xenopus. *Cell* **87**: 287–296.

Rowles a, Tada S, Blow JJ. 1999. Changes in association of the Xenopus origin recognition complex with chromatin on licensing of replication origins. *J Cell Sci* **112 (Pt 1**: 2011–8.

Sakata E, Yamaguchi Y, Miyauchi Y, Iwai K, Chiba T, Saeki Y, Matsuda N, Tanaka K, Kato K. 2007. Direct interactions between NEDD8 and ubiquitin E2 conjugating enzymes upregulate cullin-based E3 ligase activity. *Nat Struct Mol Biol* **14**: 167–168.

Sansam CL, Shepard JL, Lai K, Ianari A, Danielian PS, Amsterdam A, Hopkins N, Lees J a. 2006. DTL/CDT2 is essential for both CDT1 regulation and the early G2/M checkpoint. *Genes Dev* **20**: 3117–29.

Scarr RB, Smith MR, Beddall M, Sharp PA. 2000. A Novel 50-Kilodalton Fragment of Host A Novel 50-Kilodalton Fragment of Host Cell Factor 1 (C1) in G0 Cells. **1**.

Schafer K. 1998. The Cell Cycle: A Review. *Vet Pathol* **35**: 461–478.

Sclafani R a, Holzen TM. 2007. Cell cycle regulation of DNA replication. *Annu Rev Genet* **41**: 237–80.

Senga T, Sivaprasad U, Zhu W, Park JH, Arias EE, Walter JC, Dutta A. 2006. PCNA is a cofactor for Cdt1 degradation by CUL4/DDB1-mediated N-terminal ubiquitination. *J Biol Chem* **281**: 6246–52.

Sheaff R and RJ. 1996. End of the line: proteolytic degradation of cyclin-dependent kinase inhibitors. *Chem Biol* **3**: 869–873.

Sherr CJ, Roberts JM. 1999. CDK inhibitors: positive and negative regulators of G1-phase progression. *Genes Dev* **13**: 1501–1512.

Shibata E, Abbas T, Huang X, Wohlschlegel J a, Dutta A. 2011. Selective ubiquitylation of p21 and Cdt1 by UBCH8 and UBE2G ubiquitin-conjugating enzymes via the CRL4Cdt2 ubiquitin ligase complex. *Mol Cell Biol* **31**: 3136–45.

Shibata E, Dar A, Dutta A. 2014. CRL4Cdt2 E3 Ubiquitin Ligase and PCNA Cooperate to Degrade Thymine DNA Glycosylase in S-phase. *J Biol Chem*.

Shibutani ST, de la Cruz AF a, Tran V, Turbyfill WJ, Reis T, Edgar B a, Duronio RJ. 2008. Intrinsic negative cell cycle regulation provided by PIP box- and Cul4Cdt2-mediated destruction of E2f1 during S phase. *Dev Cell* **15**: 890–900.

Shin JH, Grabowski B, Kasiviswanathan R, Bell SD, Kelman Z. 2003. Regulation of minichromosome maintenance helicase activity by Cdc6. *J Biol Chem* **278**: 38059–38067.

Shreeram S, Sparks A, Lane DP, Blow JJ. 2002. Cell type-specific responses of human cells to inhibition of replication licensing. *Oncogene* **21**: 6624–32.

Slenn TJ, Morris B, Havens CG, Freeman RM, Takahashi TS, Walter JC. 2014. Thymine DNA glycosylase is a CRL4Cdt2 substrate. *J Biol Chem* **289**: 23043–23055.

Soria G, Speroni J, Podhajcer OL, Prives C, Gottifredi V. 2008. p21 differentially regulates DNA replication and DNA-repair-associated processes after UV irradiation. *J Cell Sci* **121**: 3271–82.

Soucy T a, Smith PG, Milhollen M a, Berger AJ, Gavin JM, Adhikari S, Brownell JE, Burke KE, Cardin DP, Critchley S, et al. 2009. An inhibitor of NEDD8-activating enzyme as a new approach to treat cancer. *Nature* **458**: 732–736.

Sugimoto N, Tatsumi Y, Tsurumi T, Matsukage A, Kiyono T, Nishitani H, Fujita M. 2004. Cdt1 Phosphorylation by Cyclin A-dependent Kinases Negatively Regulates Its Function without Affecting Geminin Binding. *J Biol Chem* **279**: 19691–19697.

Takeda DY, Parvin JD, Dutta A. 2005. Degradation of Cdt1 during S phase is Skp2-independent and is required for efficient progression of mammalian cells through S phase. *J Biol Chem* **280**: 23416–23.

Takenaka K, Moriguchi T, Nishida E. 1998. Activation of the protein kinase p38 in the spindle assembly checkpoint and mitotic arrest. **280**: 599–602.

Tardat M, Brustel J, Kirsh O, Lefevbre C, Callanan M, Sardet C, Julien E. 2010. The histone H4 Lys 20 methyltransferase PR-Set7 regulates replication origins in mammalian cells. *Nat Cell Biol* **12**: 1086–1093.

Tatsumi Y, Sugimoto N, Yugawa T, Narisawa-Saito M, Kiyono T, Fujita M. 2006. Deregulation of Cdt1 induces chromosomal damage without rereplication and leads to chromosomal instability. *J Cell Sci* **119**: 3128–40.

Teer JK, Machida YJ, Labit H, Novac O, Hyrien O, Marheineke K, Zannis-Hadjopoulos M, Dutta A. 2006. Proliferating human cells hypomorphic for origin recognition complex 2 and pre-replicative complex formation have a defect in p53 activation and Cdk2 kinase activation. *J Biol Chem* **281**: 6253–60.

Teixeira LK, Reed SI. 2013. Ubiquitin ligases and cell cycle control. *Annu Rev Biochem* **82**: 387–414.

Terai K, Abbas T, Jazaeri A a, Dutta A. 2010. CRL4(Cdt2) E3 ubiquitin ligase monoubiquitinates PCNA to promote translesion DNA synthesis. *Mol Cell* **37**: 143–9.

Terai K, Shibata E, Abbas T, Dutta A. 2013. Degradation of p12 subunit by CRL4Cdt2 E3 ligase inhibits fork progression after DNA damage. *J Biol Chem* **288**: 30509–30514.

Thornton TM, Rincon M. 2009. Non-Classical P38 Map Kinase Functions : Cell Cycle Checkpoints and Sur- vival. *Cell* **5**.

Tian W, Li B, Warrington R, Tomchick DR, Yu H, Luo X. 2012. Structural analysis of human Cdc20 supports multisite degron recognition by APC/C. *Proc Natl Acad Sci* **109**: 18419–18424.

Todorov IT, Attaran A, Kearsey SE. 1995. BM28, a human member of the MCM2-3-5 family, is displaced from chromatin during DNA replication. *J Cell Biol* **129**: 1433–1445.

Tognetti S, Riera A, Speck C. 2014. Switch on the engine: how the eukaryotic replicative helicase MCM2–7 becomes activated. *Chromosoma* **124**: 13–26.

Tsunematsu T, Takihara Y, Ishimaru N, Pagano M, Takata T, Kudo Y. 2013. Aurora-A controls pre-replicative complex assembly and DNA replication by stabilizing geminin in mitosis. *Nat Commun* **4**: 1885.

Ueki T, Nishidate T, Park JH, Lin ML, Shimo a, Hirata K, Nakamura Y, Katagiri T. 2008. Involvement of elevated expression of multiple cell-cycle regulator, DTL/RAMP (denticleless/RA-regulated nuclear matrix associated protein), in the growth of breast cancer cells. *Oncogene* **27**: 5672–5683.

Varma D, Chandrasekaran S, Sundin LJR, Reidy KT, Wan X, Chasse D a D, Nevis KR, Deluca JG, Salmon ED, Cook JG. 2012. Recruitment of the human Cdt1 replication licensing protein by the loop domain of Hec1 is required for stable kinetochore-microtubule attachment. *Nat Cell Biol* **14**: 1–12.

Vassilev LT. 2006. Cell cycle synchronization at the G2/M phase border by reversible inhibition of CDK1. *Cell Cycle* **5**: 2555–2556.

Vaziri C, Saxena S, Jeon Y, Lee C, Murata K, Machida Y, Wagle N, Hwang DS, Dutta A. 2003. A p53-dependent checkpoint pathway prevents rereplication. *Mol Cell* **11**: 997–1008.

Vejrup-Hansen R, Fleck O, Landvad K, Fahnøe U, Broendum SS, Schreurs A-S, Kragelund BB, Carr AM, Holmberg C, Nielsen O. 2014. Spd2 assists Spd1 in the modulation of ribonucleotide reductase architecture but does not regulate deoxynucleotide pools. *J Cell Sci* **127**: 2460–70.

Waga S, Hannon GJ BD& SB. 1994. The p21 inhibitor of cyclin-dependent kinases controls DNA replication by interaction with PCNA. *Nature* **369**: 574–578.

Wagner EF, Nebreda AR. 2009. Signal integration by JNK and p38 MAPK pathways in cancer development. *Nat Rev Cancer* **9**: 537–49.

Warbrick E, Lane DP, Glover DM, Cox LS. 1997. Homologous regions of Fen1 and p21Cip1 compete for binding to the same site on PCNA: a potential mechanism to co-ordinate DNA replication and repair. *Oncogene* **14**: 2313–2321.

Watanabe K, Tateishi S, Kawasuji M, Tsurimoto T, Inoue H, Yamaizumi M. 2004. Rad18 guides poleta to replication stalling sites through physical interaction and PCNA monoubiquitination. *EMBO J* **23**: 3886–3896.

Wheeler LW, Lents NH, Baldassare JJ. 2008. Cyclin A-CDK activity during G1 phase impairs MCM chromatin loading and inhibits DNA synthesis in mammalian cells. *Cell Cycle* **7**: 2179–2188.

Whitfield ML, Sherlock G, Saldanha AJ, Murray JI, Ball CA, Alexander KE, Matese JC, Perou CM, Hurt MM, Brown PO, et al. 2002. Identification of genes periodically expressed in the human cell cycle and their expression in tumors. **13**: 1977–2000.

Widrow RJ, Hansen RS, Kawame H, Gartler SM, Laird CD. 1998. Very late DNA replication in the human cell cycle. *Proc Natl Acad Sci U S A* **95**: 11246–11250.

Wohlschlegel J a, Dwyer BT, Dhar SK, Cvetic C, Walter JC, Dutta a. 2000. Inhibition of eukaryotic DNA replication by geminin binding to Cdt1. *Science* **290**: 2309–12.

Woodward AM, Göhler T, Luciani MG, Oehlmann M, Ge X, Gartner A, Jackson D a., Blow JJ. 2006. Excess Mcm2-7 license dormant origins of replication that can be used under conditions of replicative stress. *J Cell Biol* **173**: 673–683.

Wu H, Zhang Y. 2014. Reversing DNA methylation: Mechanisms, genomics, and biological functions. *Cell* **156**: 45–68.

Wu S, Wang W, Kong X, Congdon LM, Yokomori K, Kirschner MW, Rice JC. 2010. Dynamic regulation of the PR-Set7 histone methyltransferase is required for normal cell cycle progression. *Genes Dev* **24**: 2531–42.

Wu S, Zhu W, Nhan T, Toth JI, Petroski MD, Wolf D a. 2013. CAND1 controls in vivo dynamics of the cullin 1-RING ubiquitin ligase repertoire. *Nat Commun* **4**: 1642.

Xouri G, Lygerou Z, Nishitani H, Pachnis V, Nurse P, Taraviras S. 2004. Cdt1 and geminin are down-regulated upon cell cycle exit and are over-expressed in cancer-derived cell lines. *Eur J Biochem* **271**: 3368–78.

Yang X, Boehm JS, Yang X, Salehi-Ashtiani K, Hao T, Shen Y, Lubonja R, Thomas SR, Alkan O, Bhimdi T, et al. 2011. A public genome-scale lentiviral expression library of human ORFs. *Nat Methods* **8**: 659–661.

Yin L, Yu VC, Zhu G, Chang DC. 2008. SET8 plays a role in controlling G1/S transition by blocking lysine acetylation in histone through binding to H4 N-terminal tail. *Cell Cycle* **7**: 1423–1432.

Yoshida K, Takisawa H, Kubota Y. 2005. Intrinsic nuclear import acitivity of geminin is essential to prevent re-initiation of DNA replication in Xenopus eggs. *Genes to Cells* **10**: 63–73.

Yu H. 2007. Cdc20: A WD40 Activator for a Cell Cycle Degradation Machine. *Mol Cell* **27**: 3–16.

Yujiri T, Fanger GR, Garrington TP, Schlesinger TK, Gibson S, Johnson GL. 1999. Kinase Activation in Response to Changes in the Microtubule Cytoskeleton *. **274**: 12605–12610.

Zhang L, Mei Y, Fu N-Y, Guan L, Xie W, Liu H-H, Yu C-D, Yin Z, Yu VC, You H. 2012. TRIM39 regulates cell cycle progression and DNA damage responses via stabilizing p21. *Proc Natl Acad Sci U S A*.

Zhang S, Zhao H, Darzynkiewicz Z, Zhou P, Zhang Z, Lee EYC, Lee MYWT. 2013. A novel function of CRL4(Cdt2): regulation of the subunit structure of DNA polymerase δ in response to DNA damage and during the S phase. *J Biol Chem* **288**: 29550–61.

Zhao H, Zhang S, Xu D, Lee MY, Zhang Z, Lee EY, Darzynkiewicz Z. 2014. Expression of the p12 subunit of human DNA polymerase δ (Pol δ), CDK inhibitor p21(WAF1), Cdt1, cyclin A, PCNA and Ki-67 in relation to DNA replication in individual cells. *Cell Cycle* **13**: 3529–3540.